

DTIC FILE COPY

2

# NAVAL POSTGRADUATE SCHOOL Monterey, California

AD-A200 970



## THESIS

A STUDY OF SECOND AND THIRD ORDER  
MODELS FOR THE TRACKING  
SUBSYSTEM OF A RADAR GUIDED MISSILE

by

John W. Williams

June 1988

Thesis Advisor:

H. A. Titus

Approved for public release; distribution is unlimited

DTIC  
ELECTE  
DEC 07 1988  
S H D

88 12

6 1988

# REPORT DOCUMENTATION PAGE

1a. REPORT SECURITY CLASSIFICATION <b>UNCLASSIFIED</b>			1b. RESTRICTIVE MARKINGS		
2a. SECURITY CLASSIFICATION AUTHORITY			3. DISTRIBUTION/AVAILABILITY OF REPORT Approved for public release; distribution is unlimited		
2b. DECLASSIFICATION/DOWNGRADING SCHEDULE					
4. PERFORMING ORGANIZATION REPORT NUMBER(S)			5. MONITORING ORGANIZATION REPORT NUMBER(S)		
6a. NAME OF PERFORMING ORGANIZATION <b>Naval Postgraduate School</b>		6b. OFFICE SYMBOL (If applicable) <b>62</b>	7a. NAME OF MONITORING ORGANIZATION <b>Naval Postgraduate School</b>		
6c. ADDRESS (City, State, and ZIP Code) <b>Monterey, California 93943-5000</b>			7b. ADDRESS (City, State, and ZIP Code) <b>Monterey, California 93943-5000</b>		
8a. NAME OF FUNDING / SPONSORING ORGANIZATION		8b. OFFICE SYMBOL (If applicable)	9. PROCUREMENT INSTRUMENT IDENTIFICATION NUMBER		
8c. ADDRESS (City, State, and ZIP Code)			10. SOURCE OF FUNDING NUMBERS		
			PROGRAM ELEMENT NO.	PROJECT NO.	TASK NO.
			WORK UNIT ACCESSION NO.		
11. TITLE (Include Security Classification) <b>A STUDY OF SECOND AND THIRD ORDER MODELS FOR THE TRACKING SUBSYSTEM OF A RADAR GUIDED MISSILE</b>					
12. PERSONAL AUTHOR(S) <b>WILLIAMS, John W.</b>					
13a. TYPE OF REPORT <b>Master's Thesis</b>		13b. TIME COVERED FROM _____ TO _____	14. DATE OF REPORT (Year, Month, Day) <b>1988 June</b>		15. PAGE COUNT <b>139</b>
16. SUPPLEMENTARY NOTATION The views expressed in this thesis are those of the author and do not reflect the official policy or position of the Department of Defense of the U.S. Government.					
17. COSATI CODES			18. SUBJECT TERMS (Continue on reverse if necessary and identify by block number)		
FIELD	GROUP	SUB-GROUP	radar guided missile, tracking, missile modeling, coriolis equation, Kalman filter, aircraft modeling		
19. ABSTRACT (Continue on reverse if necessary and identify by block number) This thesis is a study of missile and target parameters used in second and third order modeling of the tracking subsystem used in radar guided missiles. Guidance methods are analyzed to determine which method is optimum in a search for an "ideal" missile. Target parameters which have an effect on the missile tracking system are analyzed and a target acceleration probability model is discussed. A two dimensional third order tracking model is simulated utilizing a Kalman filter for target parameter estimation and prediction. Linear second and third order tracking models are simulated and compared with the third order Kalman filter tracker. This thesis concludes that a proportional navigation guidance method, with a non linear third order tracking Kalman filter, is the better model. Benefits of using a non linear third order Kalman filter may not override the cost and complexity of implementation of the model.					
20. DISTRIBUTION/AVAILABILITY OF ABSTRACT <input checked="" type="checkbox"/> UNCLASSIFIED/UNLIMITED <input type="checkbox"/> SAME AS RPT <input type="checkbox"/> DTIC USERS			21. ABSTRACT SECURITY CLASSIFICATION <b>UNCLASSIFIED</b>		
22a. (NAME OF RESPONSIBLE INDIVIDUAL) <b>Harold A. Titus</b>			22b. TELEPHONE (Include Area Code) <b>408-646-2560</b>		22c. OFFICE SYMBOL <b>62Ts</b>

Approved for public release; distribution is unlimited

A STUDY OF SECOND AND THIRD ORDER MODELS FOR THE  
TRACKING SUBSYSTEM OF A RADAR GUIDED MISSILE

by

John Walter Williams  
Captain, United States Marine Corps  
B.S., United States Naval Academy, 1978

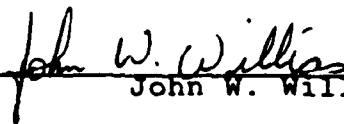
Submitted in partial fulfillment of the  
requirements for the degree of

MASTER OF SCIENCE IN ELECTRICAL ENGINEERING

from the

NAVAL POSTGRADUATE SCHOOL  
June 1988

Author:

  
John W. Williams

Approved by:

  
H. A. Titus, Thesis Advisor

  
Michael A. Morgan, Second Reader

  
John P. Powers, Chairman, Department of  
Electrical and Computer Engineering

  
Gordon E. Schacher, Dean of  
Science and Engineering

# ABSTRACT

This thesis is a study of missile and target parameters used in second and third order modeling of the tracking subsystem used in radar guided missiles. Guidance methods are analyzed to determine which method is optimum in a search for an "ideal" missile. Target parameters which have an effect on the missile tracking system are analyzed and a target acceleration probability model is discussed. A two dimensional third order tracking model is simulated utilizing a Kalman filter for target parameter estimation and prediction. Linear second and third order tracking models are simulated and compared with the third order Kalman filter tracker. This thesis concludes that a proportional navigation guidance method, with a non linear third order tracking Kalman filter, is the better model. Benefits of using a non linear third order Kalman filter may not override the cost and complexity of implementation of the model. (C) (FR)



Accession For	
NTIS GRA&I	<input checked="" type="checkbox"/>
DTIC TAB	<input type="checkbox"/>
Unannounced	<input type="checkbox"/>
Justification	
By	
Distribution/	
Availability Codes	
Avail and/or	
Dist	Special
A-1	

## TABLE OF CONTENTS

I.	INTRODUCTION . . . . .	1
II.	THE IDEAL MISSILE . . . . .	3
	A. HEAD-ON ASPECT . . . . .	6
	1. 0G Target Acceleration . . . . .	43
	2. 3G Target Acceleration . . . . .	44
	3. 6G Target Acceleration . . . . .	45
	B. TAIL ASPECT . . . . .	45
	1. 0G Target Acceleration . . . . .	45
	2. 3G Target Acceleration . . . . .	46
	3. 6G Target Acceleration . . . . .	46
	C. BEAM ASPECT . . . . .	47
	1. 0G Target Acceleration . . . . .	47
	2. 3G Target Acceleration . . . . .	48
	3. 6G Target Acceleration . . . . .	48
	D. CONCLUSIONS . . . . .	48
III.	TARGET MODEL . . . . .	50
	A. TACTICS FOR MISSILE DEFENSE . . . . .	53
IV.	SYSTEM MODEL . . . . .	56
	A. COORDINATE SYSTEM . . . . .	56
	B. EQUATIONS OF MOTION . . . . .	57
	C. SECOND ORDER MODEL . . . . .	60
	D. THIRD ORDER MODEL . . . . .	62
V.	KALMAN FILTER . . . . .	64
VI.	SIMULATION . . . . .	70
	A. ASSUMPTIONS . . . . .	70
	B. INITIALIZATION . . . . .	71
	C. SECOND ORDER MODEL . . . . .	71
	D. THIRD ORDER MODEL . . . . .	71
	1. Time Invariant, Constant Phi Model . . . . .	72
	2. Time Variant, Variable Phi Model . . . . .	72
	E. RESULTS . . . . .	75
	1. Gains . . . . .	75

2.	Head-on Aspect . . . . .	107
a.	0G Target Acceleration . . . . .	107
b.	3G Target Acceleration . . . . .	107
c.	6G Target Acceleration . . . . .	108
3.	Tail Aspect . . . . .	108
a.	0G Target Acceleration . . . . .	108
b.	3G Target Acceleration . . . . .	108
c.	6G Target Acceleration . . . . .	109
4.	Beam Aspect . . . . .	109
a.	0G Target Acceleration . . . . .	109
b.	3G Target Acceleration . . . . .	109
c.	6G Target Acceleration . . . . .	110
VII.	CONCLUSIONS . . . . .	111
	REFERENCES . . . . .	112
	APPENDIX A. IDEAL MISSILE PROGRAM LISTING . . . . .	113
	APPENDIX B. THIRD ORDER SIMULATION PROGRAM LISTING. . . . .	117
	INITIAL DISTRIBUTION LIST . . . . .	130

# TABLE OF VARIABLES

AT	acceleration of target (g)
AM	acceleration of missile (g)
B	antenna angle
B0	initial antenna angle (rad)
BD0	initial antenna angular rate (rad/sec)
BDOT	antenna angular rate
BDDOT	antenna commanded angular acceleration
D2R	conversion factor degrees to radians
DELR	matrix of state space range errors
DXT	X coordinate, impact point for Direct Path missile
DYT	Y coordinate, impact point for Direct Path missile
G	force of gravity, 32.2 ft/sec/sec
GAMMA	antenna angle (rad)
G0	initial antenna angle (rad)
GD0	initial antenna angular rate (rad/sec)
GDOT	antenna angle rate (rad/sec)
GDDOT	antenna commanded angular acceleration
GR	matrix of gains, range channel for Kalman filter
GS	matrix of gains, bearing channel for Kalman filter
H	observation vector, used in comment lines
K2F	conversion factor knots to feet/sec
LOS	line of sight angle (rad)
LOSD	line of sight rate (rad/sec)
LPHDG	lead pursuit missile heading (rad)
LPHDGO	initial lead pursuit missile heading (rad)
LPLOS	line of sight for lead pursuit missile (rad)
LPLOSD	line of sight rate for lead pursuit missile
LPR	range for lead pursuit missile to target (ft)
LPRD	range rate for lead pursuit missile (ft/sec)
LPXM	lead pursuit missile position X coordinate
LPYM	lead pursuit missile position Y coordinate
MISSX0	initial missile location X parameter (ft)

MISSY0	initial missile location Y parameter (ft)
P	prediction covariance matrix,
PHDG	initial proportional navigation missile heading
PHI	discrete model state space matrix
PNAM	prop nav missile commanded acceleration
PNHDG	prop nav missile heading (rad)
PNLOS	line of sight angle for prop nav missile (rad)
PNLOSD	line of sight rate for prop nav missile (rad/sec)
PNR	range for prop nav missile to target (ft)
PNRD	range rate for prop nav missile (ft/sec)
PPHDG	pure pursuit missile heading (rad)
PPLOS	line of sight angle for pure pursuit missile (rad)
PPLOSD	line of sight rate for pure pursuit missile
PPR	range for pure pursuit missile to target (ft)
PPRD	range rate for pure pursuit missile (ft/sec)
PPXM	pure pursuit missile position X coordinate
PPYM	pure pursuit missile position Y coordinate
PR	error covariance matrix for range channel
PROP NAV	proportional navigation
PS	error covariance matrix for bearing channel
PXM	prop nav missile position X coordinate
PYM	prop nav missile position Y coordinate
QR	maneuvering covariance matrix range channel
QS	maneuvering covariance matrix bearing channel
R0	initial range missile to target (ft)
R,RM	measured range from missile to target (ft)
RD	range rate from missile to target (ft/sec)
RDDK	estimate of range acceleration at time k
RDDKP1	prediction of range acceleration for time k+1
RDK	estimate of range rate at time k
RDOTM	measured range rate
RKP1	prediction of range rate for time k+1
RK	estimate of range at time k
RKP1	prediction of range at time k+1
RMCOV	measurement covariance matrix for range channel



RNG	matrix of range state space values
RPHI	PHI matrix for range channel
S	Sigma, estimate of line of sight
S	matrix of state space sigma values
SDEL	matrix of error values
SG	gain matrix for bearing channel for Kalman filter
SMCOV	measurement covariance matrix, bearing channel
SOHDG	missile heading of second order simulation (rad)
SOLOS	line of sight for second order simulation (rad)
SOR	range for second order simulation (ft)
SOU	commanded acceleration for second order simulation
SOXM	missile position X coordinate for second order
SOYM	missile position Y coordinate for second order
TEMP1	temporary matrix for storing values
TEMP2	temporary matrix for storing values
TEMP3	temporary matrix for storing values
TGTA	acceleration of target (ft/sec/sec)
TGTAX	target acceleration in X direction
TGTAY	target acceleration in Y direction
TGTHDG	target heading (rad)
TGTV	velocity of target, 667 ft/sec
TGTVX0	initial velocity of target X parameter (ft/sec)
TGTVY0	initial velocity of target Y parameter (ft/sec)
THDG	initial target heading (rad)
TK	sample interval (sec)
TK	square of the sample interval
TTGO	initial time to go (sec)
TTG	time to go until impact (sec)
TVELX	target velocity in X direction (ft/sec)
TVELY	target velocity in Y direction (ft/sec)
U	commanded missile acceleration
VM	velocity of missile, 2500 ft/sec
VT	velocity of target (kts)
XT	target position X coordinate
YT	target position Y coordinate

## I. INTRODUCTION

Aviation plays an extensive role in current combat scenarios. An aircraft, because of its capability to carry missiles, is a very formidable weapon platform. Missiles provide offensive killing power which change tactics in battle scenarios. In order to have the edge in the air to air arena, an aircraft must possess the best defensive and offensive capabilities. One of the main weapons in the aircraft arsenal is the radar guided missile.

Radar guided missiles are all weather capable, can be launched outside of visual range and are less susceptible to countermeasures, compared with other missile types. Improvement of the missile is a constant necessity to maintain air superiority.

Improvements in aircraft maneuverability dictate the need for missiles to increase performance and capabilities. A rule of thumb for design is that the missile must have a 4:1 acceleration advantage over the target. With modern aircraft able to sustain lateral accelerations of ten times the force of gravity (G) the missile must be capable of 40G.

Guidance methods are chosen which optimize the missile capabilities to destroy the target. The guidance method selected has a large impact on the design of other missile subsystems. For any missile to guide to the target, the sensor subsystem must track the target. To optimize the guidance and tracking of radar guided missiles a predicting filter can be used.

One of the simplest missile guidance techniques is a second order system which compensates for bearing error and bearing rate error. This thesis will look at third order models to help optimize the missile sensor subsystem to provide better guidance command inputs. A major impetus for

finding an optimum predicting guidance method is to improve missile performance in the final guidance stages.

There is a region at the end of the missile flight path, where the time to intercept is so short that inputs to the missile control surfaces will not be effective. If the missile has an exact solution of target parameters, it can predict the future target position, through the time where no inputs will be effective. The missile is flying to the projected position of the target, compensating for the time delay of control effectiveness.

Section II will look at some guidance methods and target parameters to aid in finding the optimum missile guidance. Section III looks at target models and how to implement them in the computer simulation. Section IV derives the second and third order models. A Kalman Predicting Filter is discussed in Section V. Computer simulation and implementation of two dimensional third order models with the Kalman Filter is given in Section VI. Section VII contains conclusions and recommendations. Program listings of the computer simulation are in Appendix A and Appendix B.

## II. THE IDEAL MISSILE

Definition of an ideal missile is very difficult. Cost or performance functions can be generated to account for miss distance, fuel expended, control inputs, flight path and numerous other parameters. To the operator the ideal missile is one that destroys the target. The designer must try to account for a variety of scenarios and targets to design the optimum missile. Tradeoffs of performance and costs will dictate what the final sub-optimum missile will be.

In an attempt to find an ideal missile insight may be gained by looking at the various flight paths and parameters for different guidance methods. Three methods to look at are pure pursuit, lead pursuit and proportional navigation. Pure pursuit would entail a missile always flying directly at the target. Lead pursuit would be the case of a missile always flying to a point slightly ahead of the target. The magnitude of the lead may vary from one time constant, to the total missile flight time, ahead of the target. The latter would produce a lead collision intercept. Proportional navigation utilizes line of sight rate to guide the turn of the missile, to zero any further line of sight rate. The commanded acceleration to the missile is given by the equation:

$$AM = k \dot{\beta} V_c \quad (1)$$

where  $AM$  = missile acceleration  
 $k$  = constant of proportionality  
 $\dot{\beta}$  = antenna angle rate  
 $V_c$  = closing velocity

The constant of proportionality is determined by the designer. Observing the effects of the proportionality

constant on the line of sight rate shown in Figure II-1, any constant above 3 is an appropriate value. For  $k$  less than 3 the line of sight rate has its largest slope at the end of the intercept. For  $k$  greater than 3 the line of sight rate will be very small prior to the impact point.

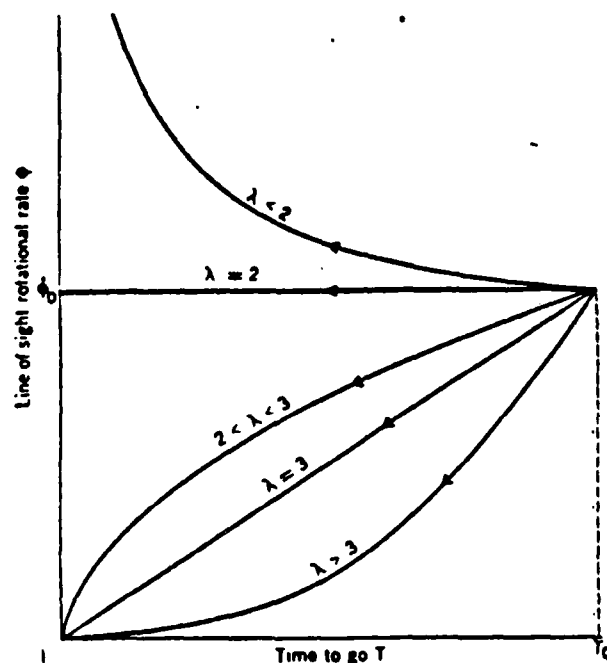


Figure II-1. Prop Nav Proportionality Constant [Ref. 1]

Three guidance methods are analyzed to compare flight paths, heading changes, line of sight angle and line of sight rate. A fourth missile is simulated and plotted, identified by "direct".

The direct path missile is programmed using "a posteriori" knowledge of the target flight path. The direct path missile goes to the point of impact, in a straight line, from the point of launch.

If the "ideal missile" is defined such that there is no missile maneuvering, burns minimal fuel, has the greatest launch distance, minimum intercept time and accounts for all target maneuver, it will be a direct path missile.

Two programs were written using Dynamic Simulation Language, DSL, to analyze the guidance methods and produce plots. The programs are included in Appendix A.

Three scenarios are used to compare the guidance methods:

- head-on aspect
- tail aspect
- beam aspect

Three target accelerations are used to determine the effect of the target maneuver on the parameters. The selected target accelerations are:

- 0 g's
- 3 g's
- 6 g's

A second order proportional navigation missile with a proportional navigation guidance constant of four, where the line of sight angle and angle rate is estimated by the antenna parameters of angular position and angular rate. The governing equations for tracking in bearing are:

$$\beta = \int_0^T \dot{\beta} dt + \beta_0 \quad (2)$$

$$\dot{\beta} = \int_0^T \ddot{\beta} dt + \dot{\beta}_0 \quad (3)$$

$$\ddot{\beta} = -20 \cdot \dot{\beta} + 100 \cdot (\text{LOS} - \beta) \quad (4)$$

where  $\beta$  = antenna position angle  
 $\dot{\beta}$  = antenna angle rate  
 $\ddot{\beta}$  = antenna angular acceleration  
LOS = actual target bearing

Pure pursuit and lead pursuit guidance missiles are initialized heading directly at the target. Pure pursuit guidance maintains heading directly at the target by

calculating the heading at each step of the discrete simulation. The equation for pure pursuit heading is:

$$\text{PPHDG} = \text{atan}((y_t - y_m) / (x_t - x_m)) \quad (5)$$

where  $y_t$  = current target Y coordinate  
 $x_t$  = current target X coordinate  
 $y_m$  = current missile Y coordinate  
 $x_m$  = current missile X coordinate

Lead pursuit maintains a heading in front of the target, with a variable lead, calculated using half the time to go, given by:

$$\text{LPHDG} = \text{atan}((y_t + t_{\text{vely}} * .5 * t_{\text{tg}}) / (x_t + t_{\text{velx}} * .5 * t_{\text{tg}})) \quad (6)$$

where  $y_t$  = current target Y coordinate  
 $x_t$  = current target X coordinate  
 $t_{\text{vely}}$  = target velocity in Y direction  
 $t_{\text{velx}}$  = target velocity in X direction  
 $t_{\text{tg}}$  = time to go in the intercept

The results of the comparisons are given in graph form in Figure II-2 through Figure II-37.

#### A. HEAD-ON ASPECT

Figures II-2 through II-13 are the results of missile guidance comparisons for head-on aspect initial condition with 0G, 3G and 6G constant target acceleration. The missile begins at the origin of the graph. The target initial position is at  $x = 10000$  ft,  $y = 500$  ft. Applied lateral target acceleration is away from the missile.

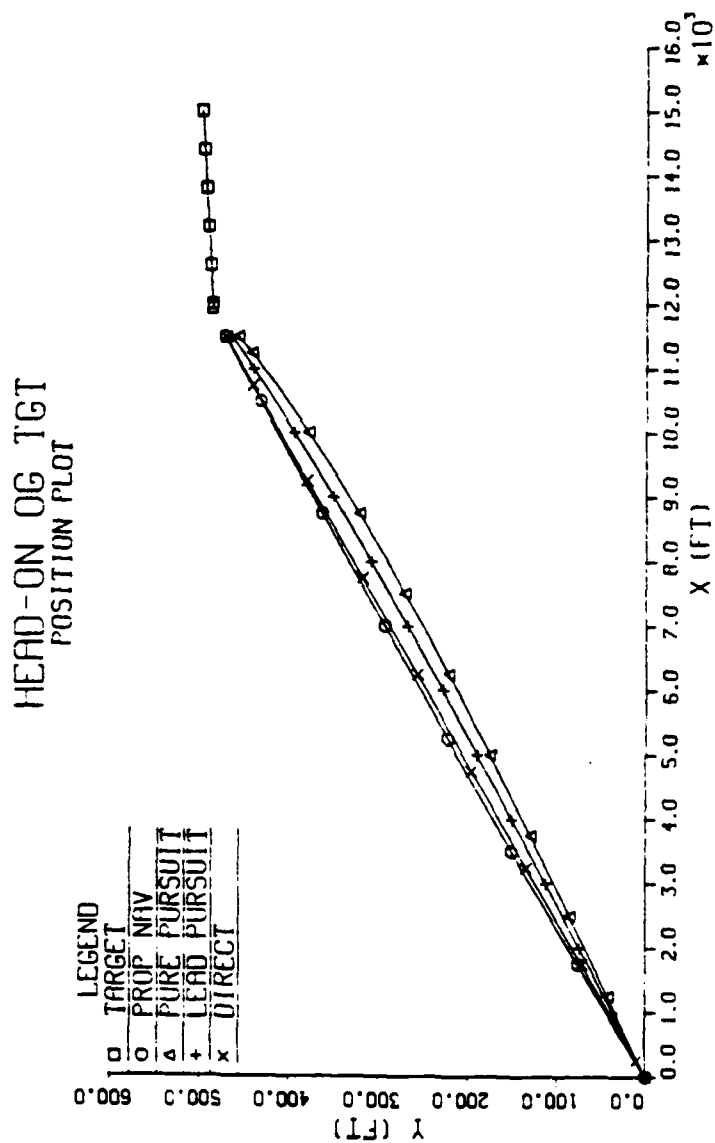


Figure II-2 Position Plot for Head-on  
Aspect No Target Turn



# HEAD-ON OG TGT MISSILE HEADINGS

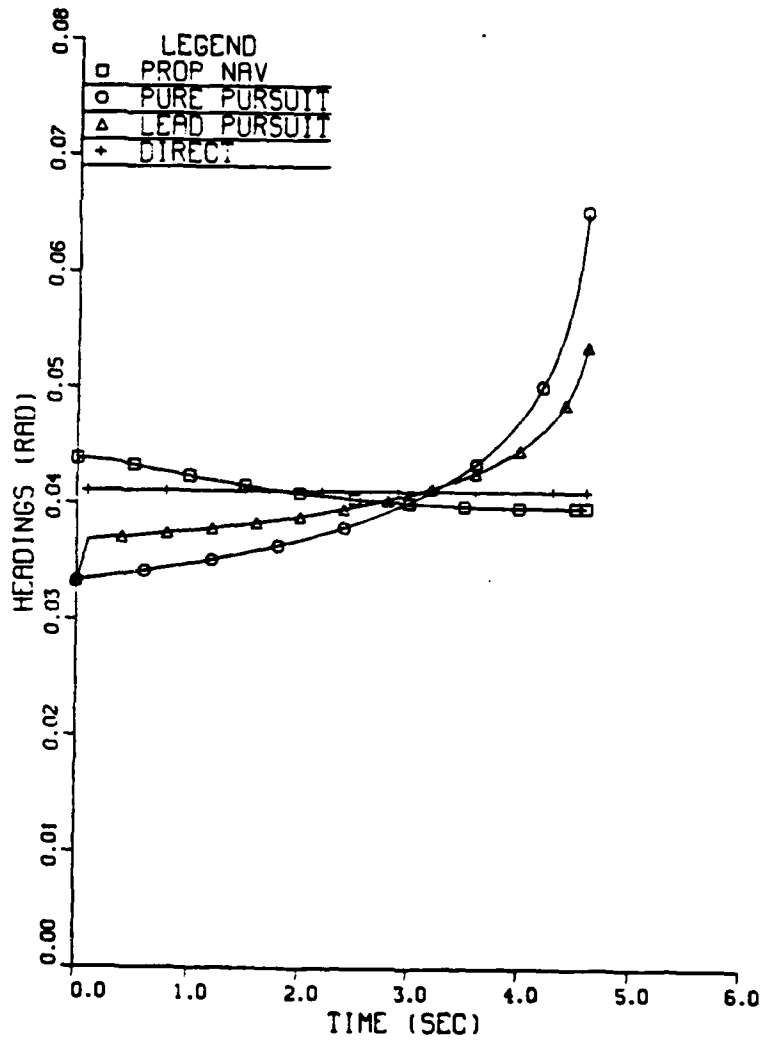


Figure II-3 Missile Heading Plot for Head-on Aspect No Target Turn

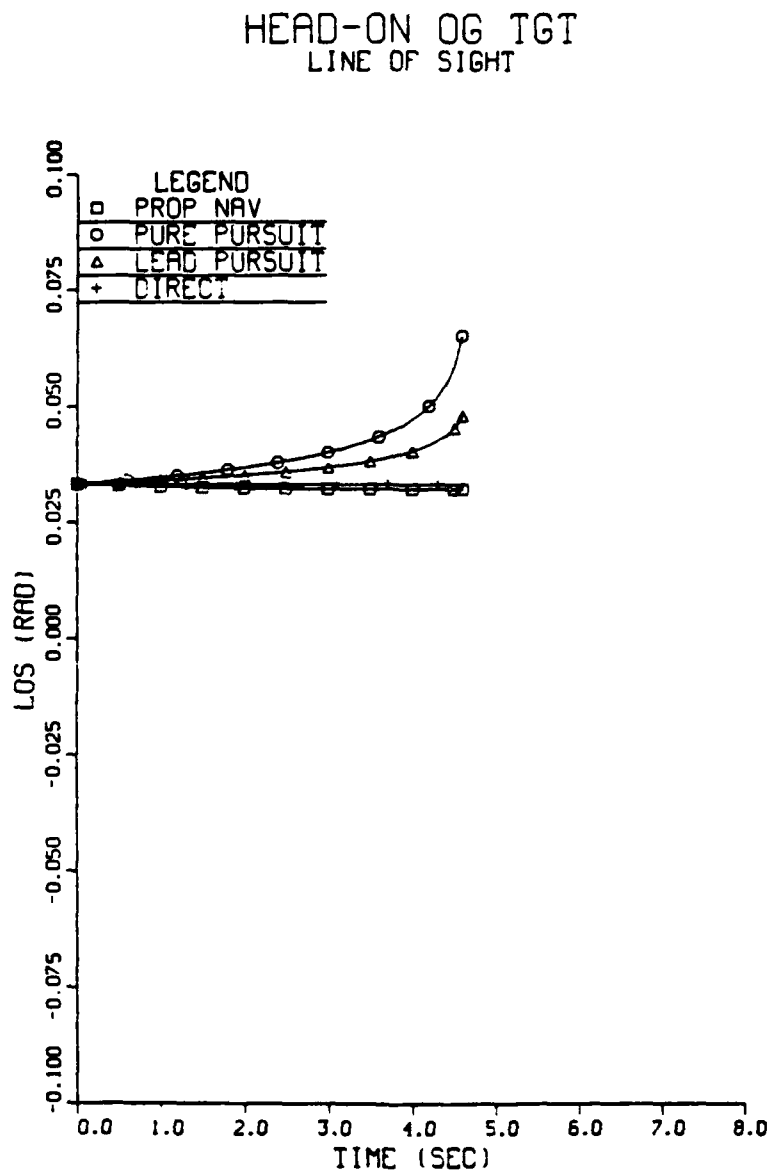


Figure II-4 Line of Sight Angle Plot for Head-on Aspect No Target Turn

# HEAD-ON OG TGT LOS RATE

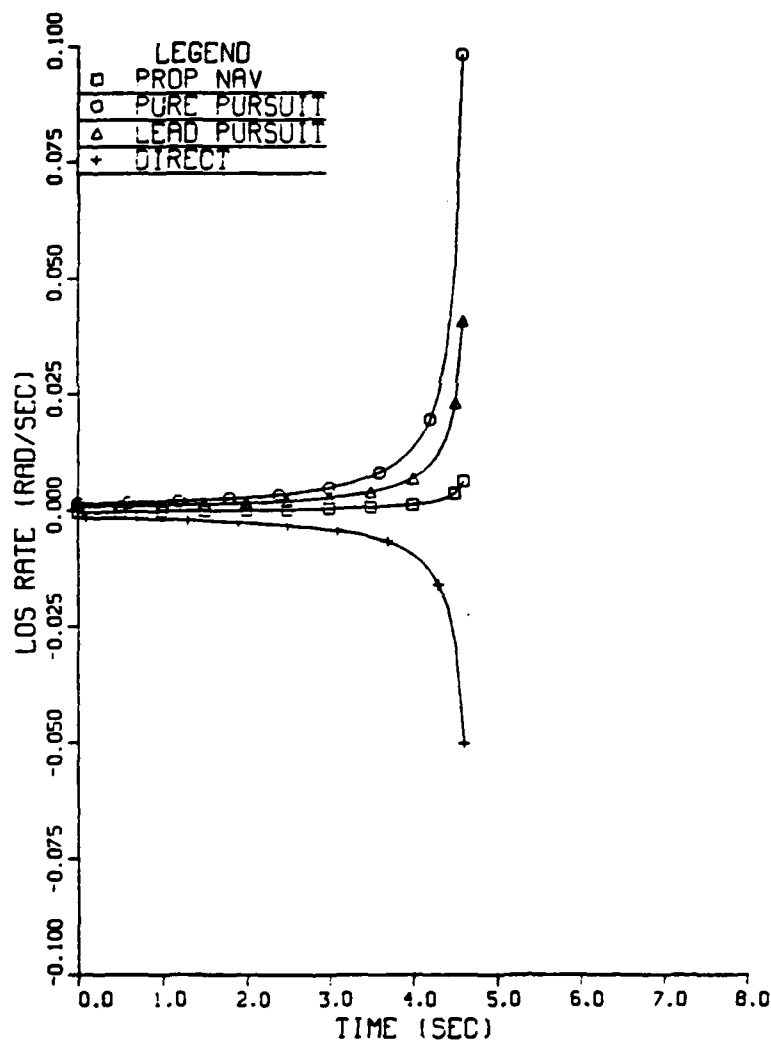


Figure II-5 Line of Sight Rate Plot for Head-on Aspect No Target Turn

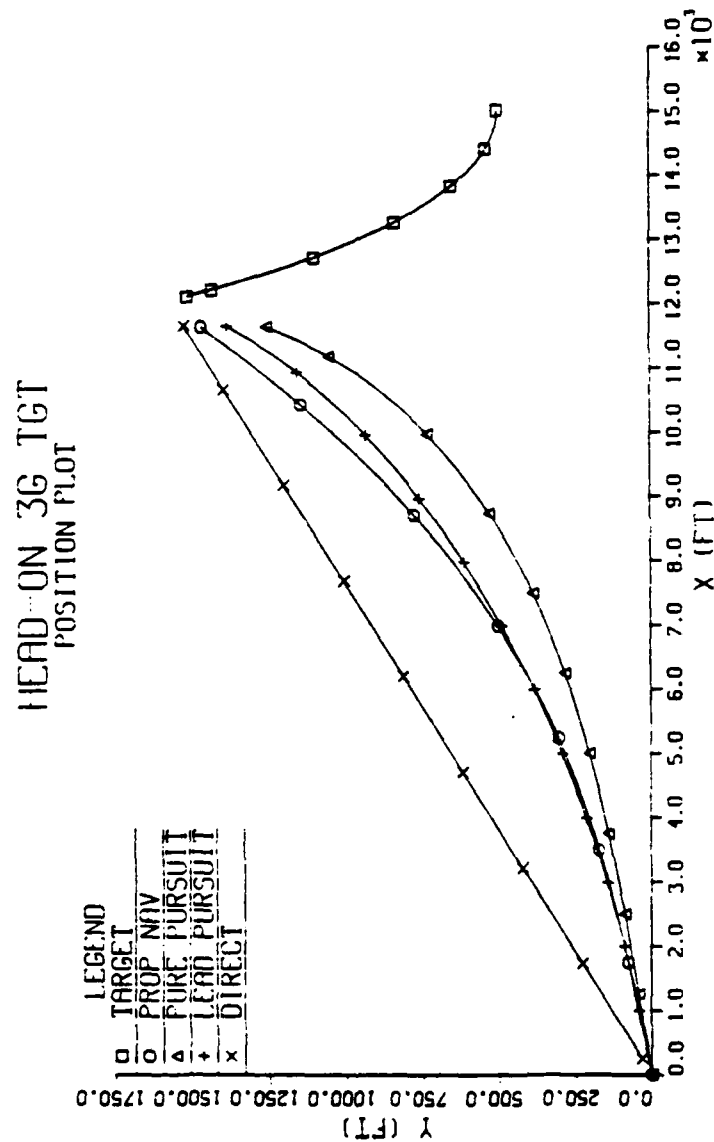


Figure II-6 Position Plot for Head-on  
Aspect Constant 3G Target Turn

# HEAD-ON 3G TGT MISSILE HEADINGS

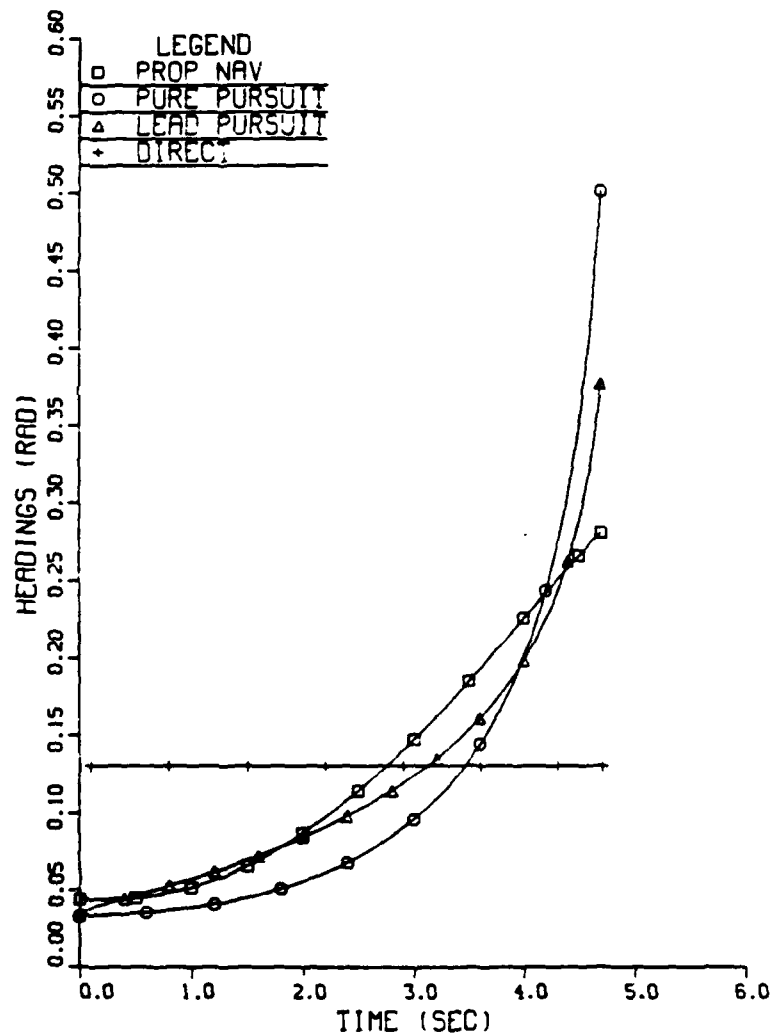


Figure II-7 Missile Heading Plot for Head-on  
Aspect Constant 3G Target Turn

# HEAD-ON 3G TGT LINE OF SIGHT

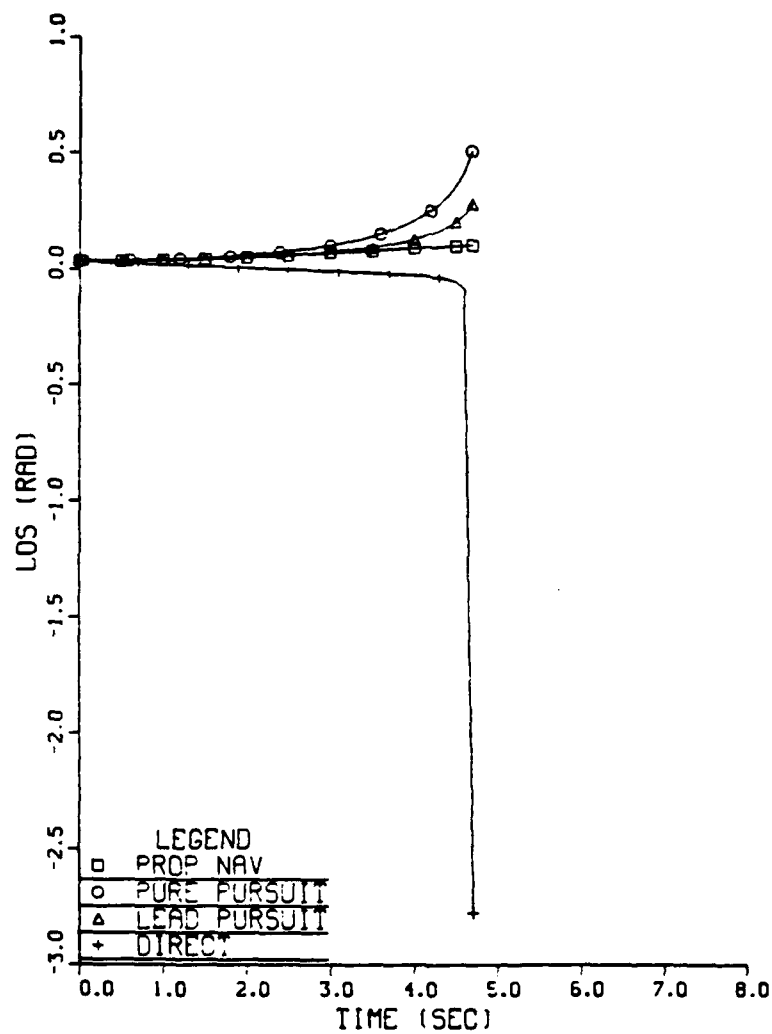


Figure II-2 Line of Sight Angle Plot for Head-on  
Aspect Constant 3G Target Turn

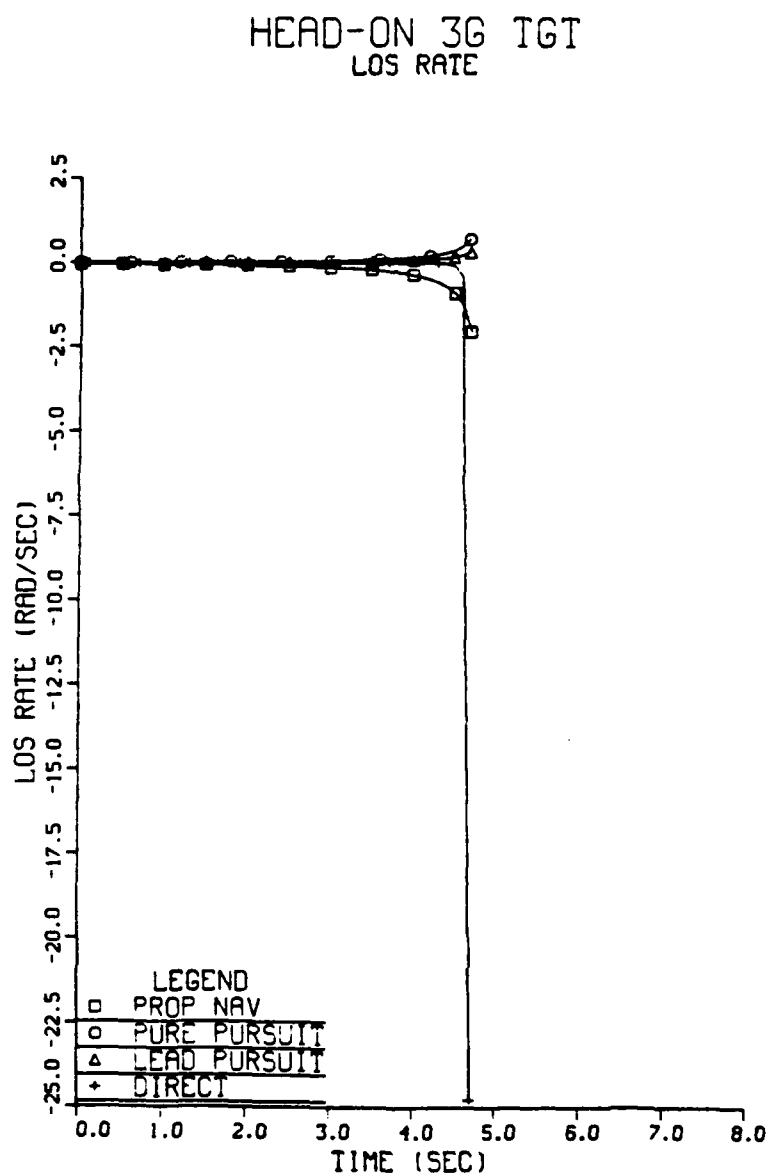


Figure II-9 Line of Sight Rate Plot for Head-on Aspect Constant 3G Target Turn

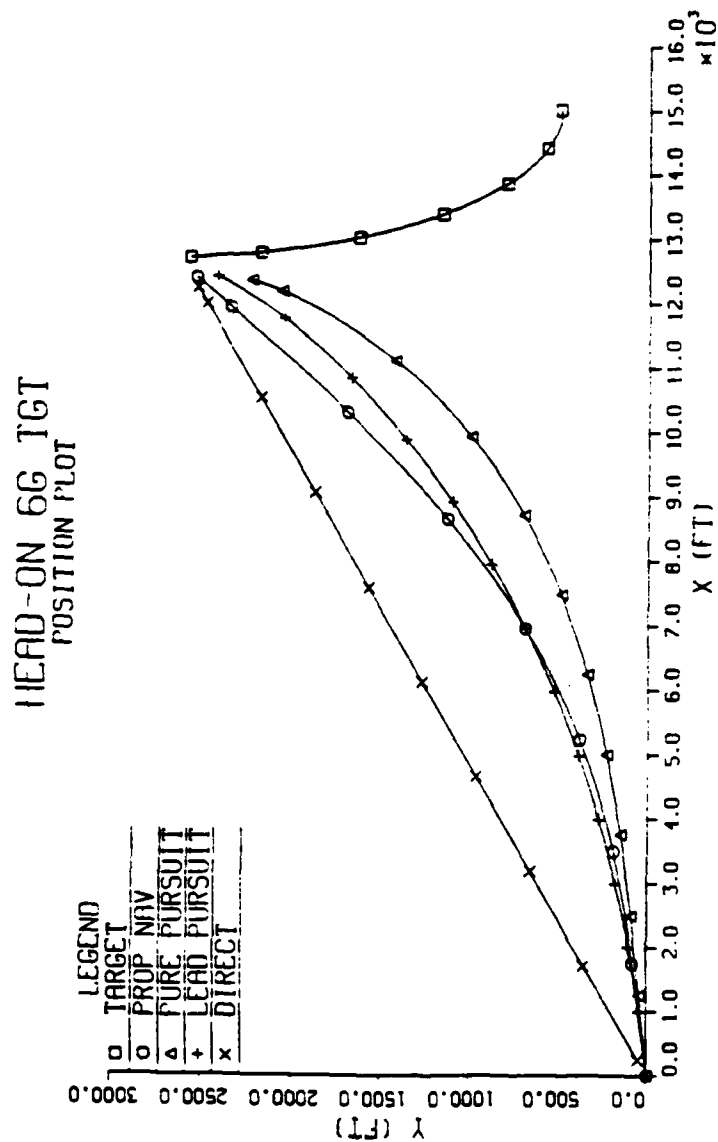


Figure II-10 Position Plot for Head-on  
Aspect Constant 6G Target Turn



REPRODUCED AT GOVERNMENT EXPENSE

# HEAD-ON 6G TGT MISSILE HEADINGS

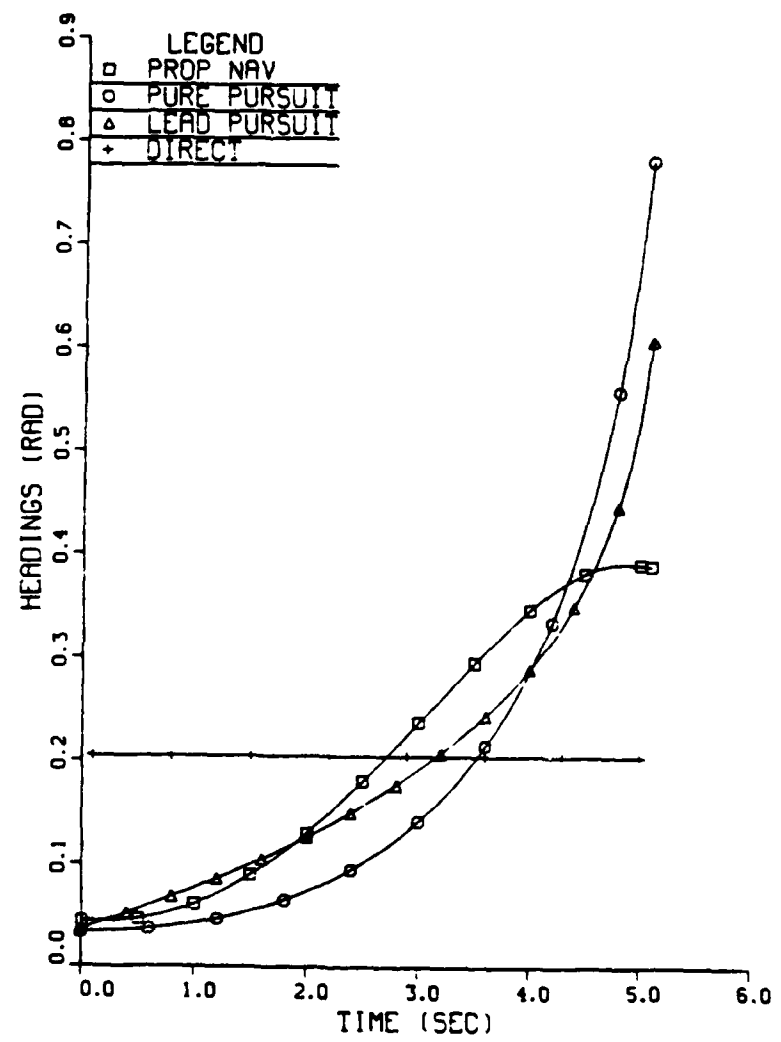


Figure II-11 Missile Headings Plot for Head-on  
Aspect Constant 6G Target Turn

# HEAD-ON 6G TGT LINE OF SIGHT

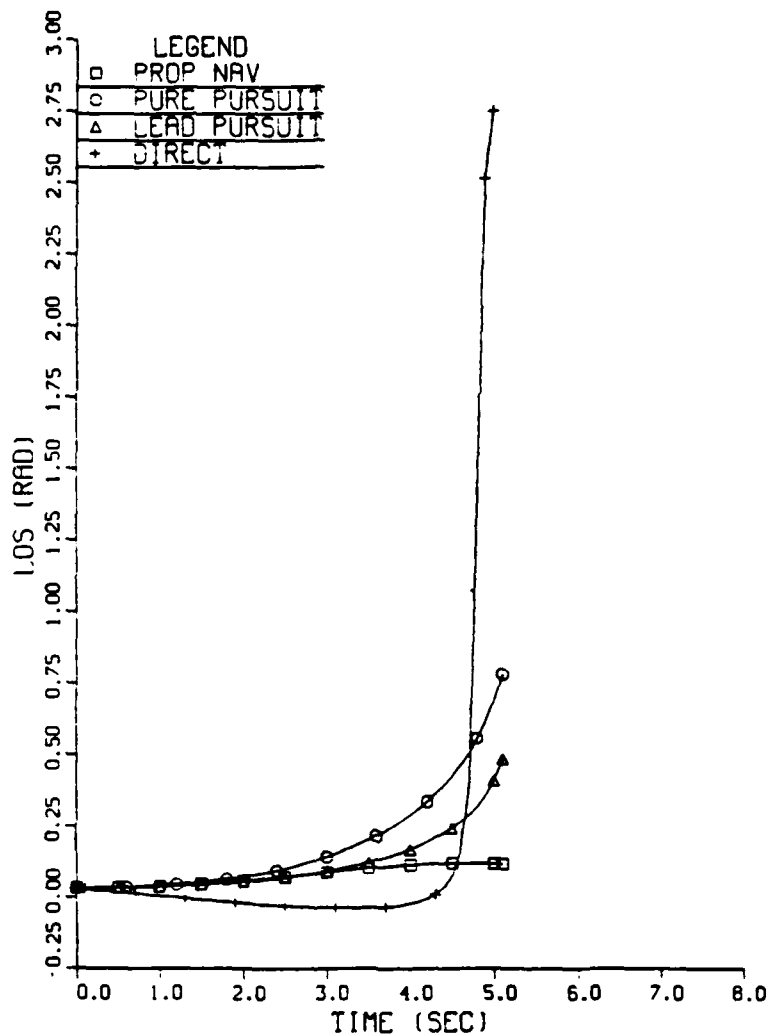


Figure II-12 Line of Sight Angle Plot for Head-on Aspect Constant 6G Target Turn

REPRODUCED AT GOVERNMENT EXPENSE

# HEAD-ON 6G TGT LOS RATE

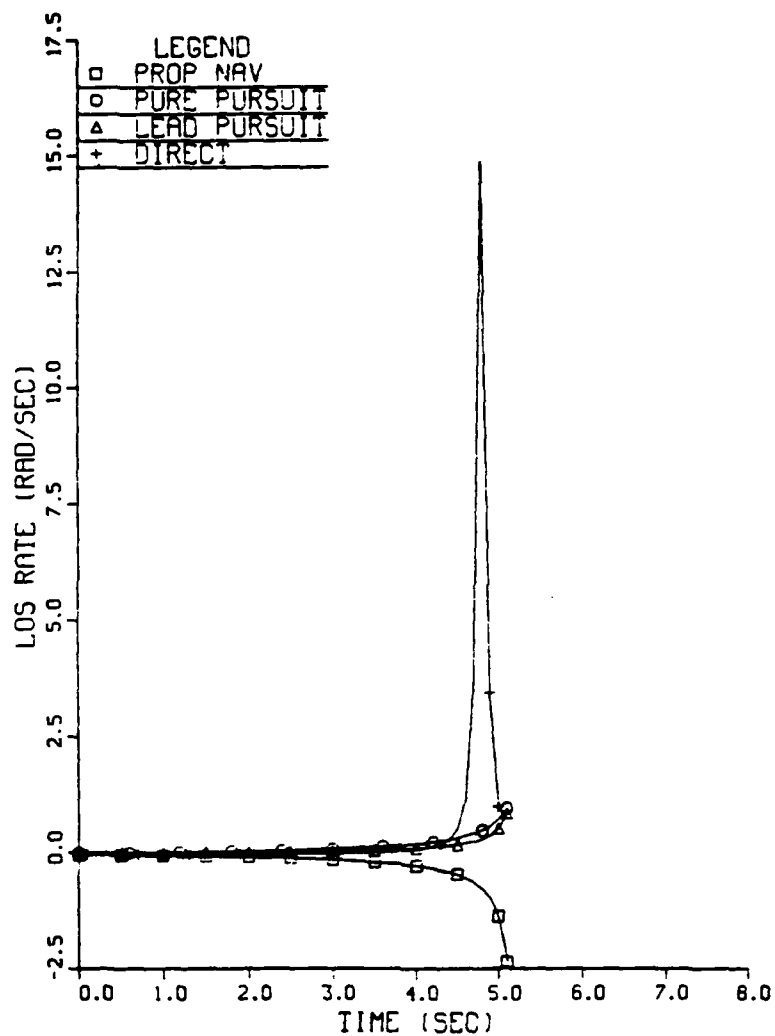


Figure II-13 Line of Sight Rate Plot for Head-on Aspect Constant 6G Target Turn

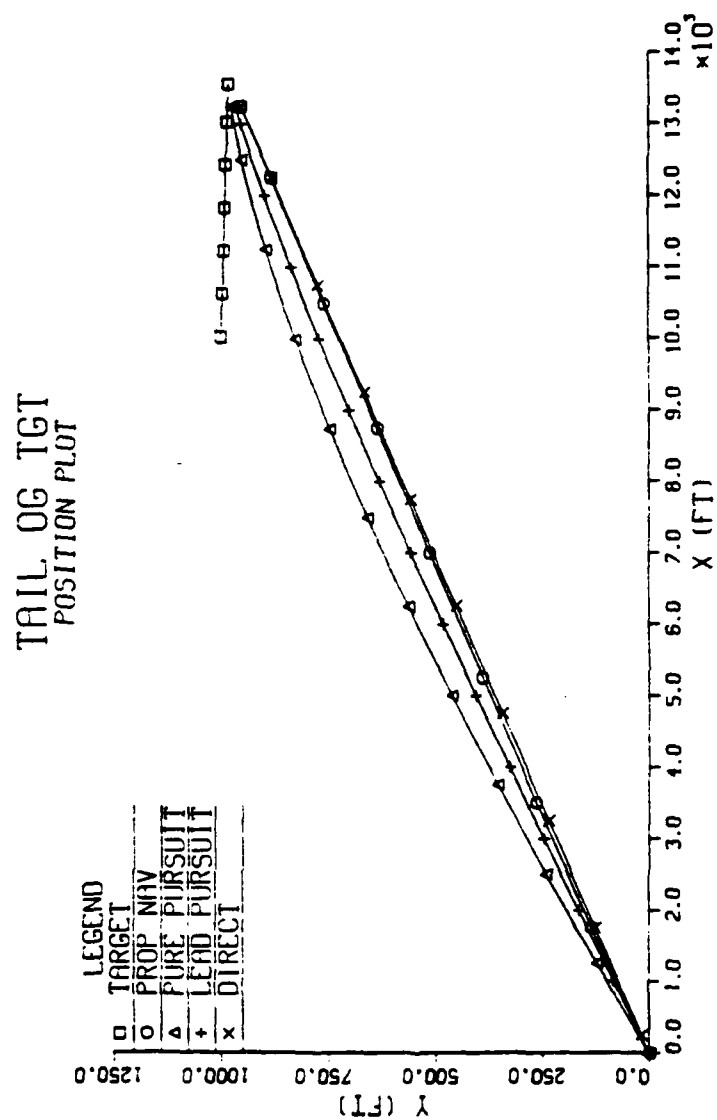


Figure II-14 Position Plot for Tail Aspect Constant No Target Turn

# TAIL OG TGT MISSILE HEADINGS

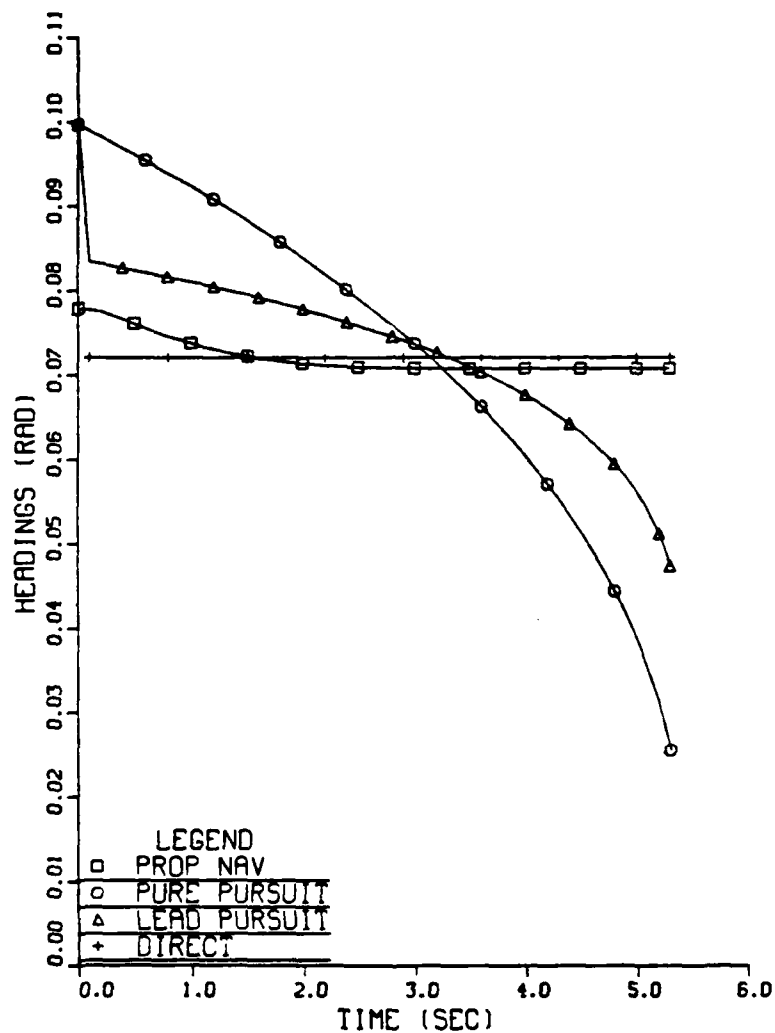


Figure II-15 Missile Heading Plot Tail Aspect Constant No Target Turn

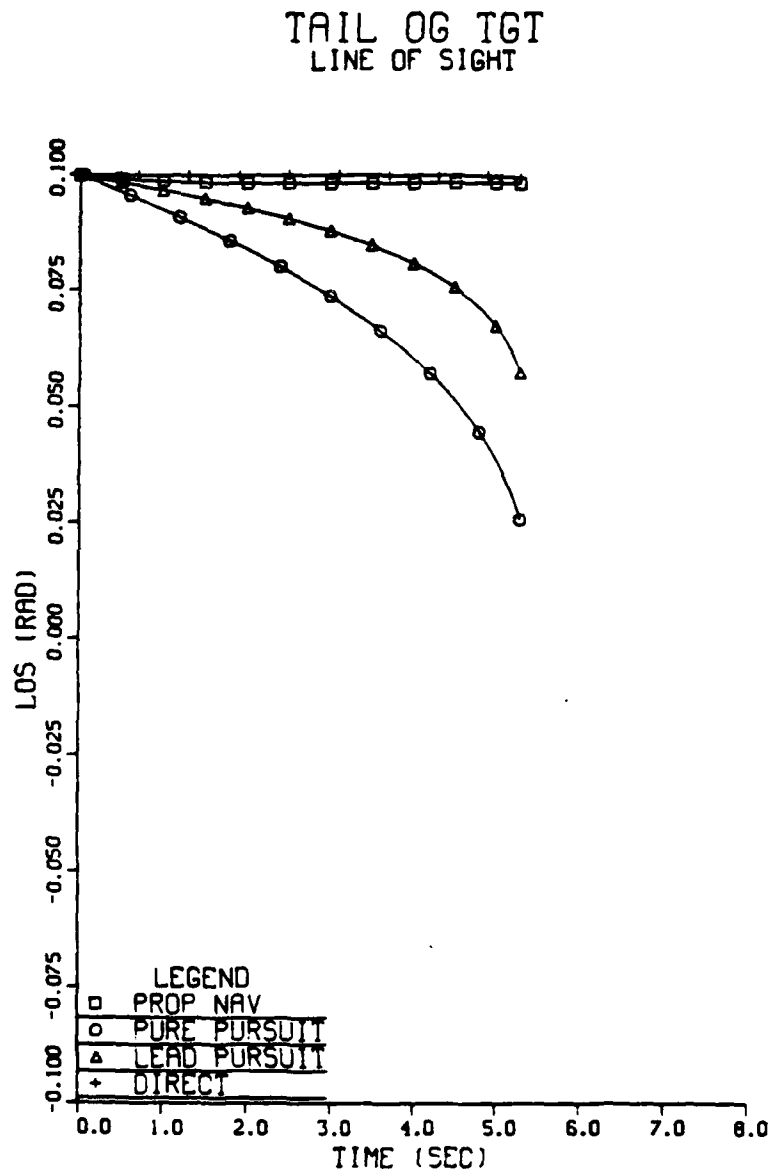


Figure II-16 Line of Sight Angle Plot Tail  
Aspect Constant No Target Turn

# TAIL OG TGT LOS RATE

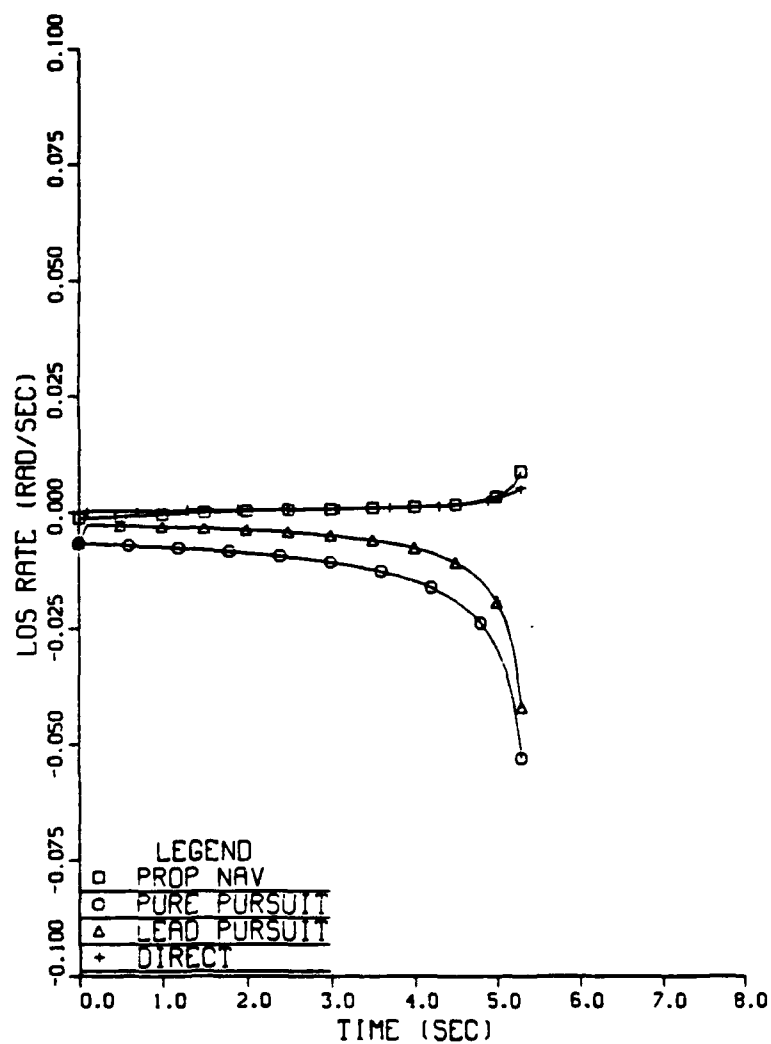


Figure II-17 Line of Sight Rate Plot Tail Aspect Constant No Target Turn

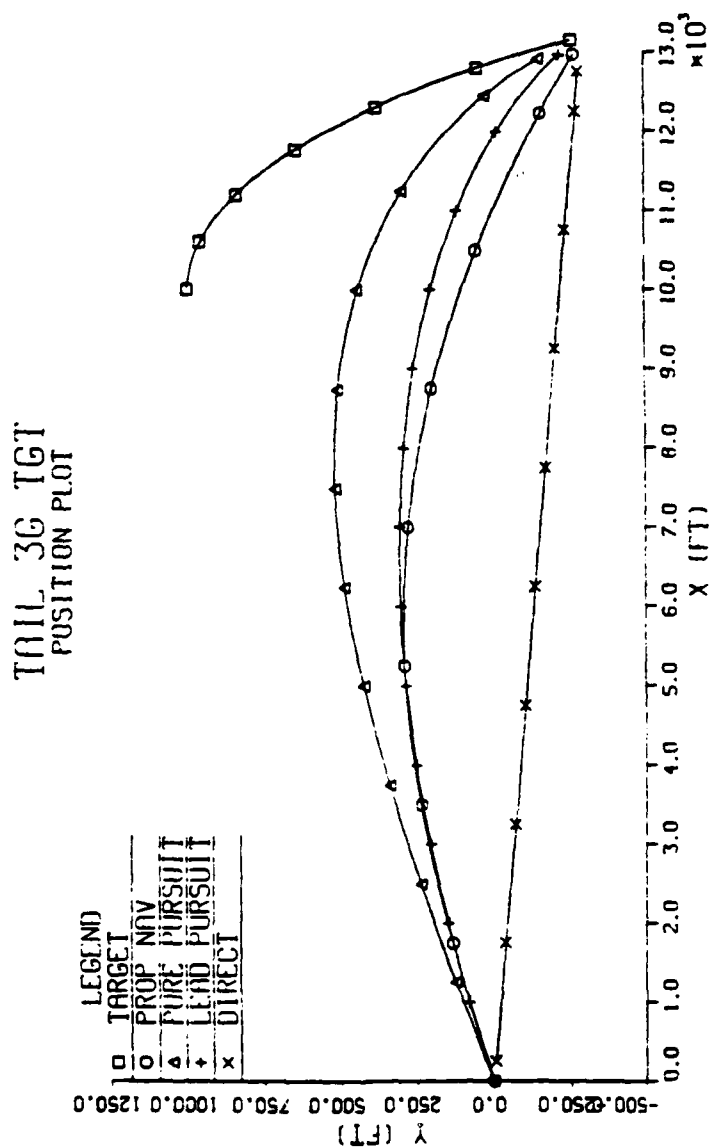


Figure II-18 Position Plot Tail  
Aspect Constant 3G Target Turn



# TAIL 3G TGT MISSILE HEADINGS

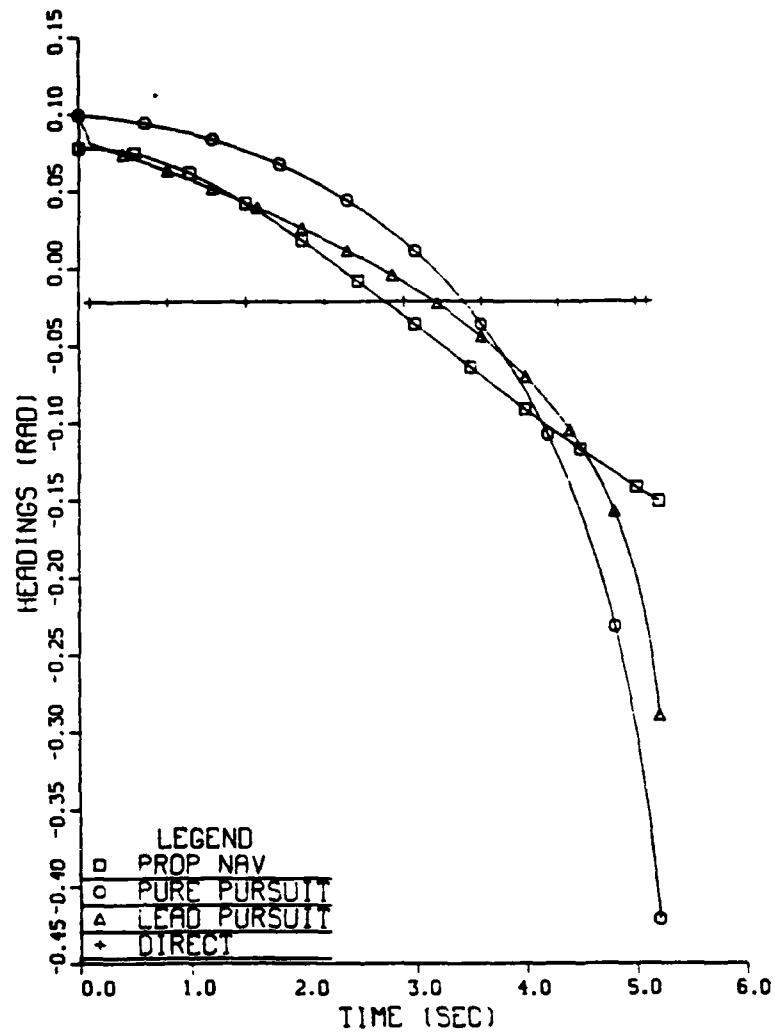


Figure II-19 Missile Heading Plot Tail  
Aspect Constant 3G Target Turn

# TAIL 3G TGT LINE OF SIGHT

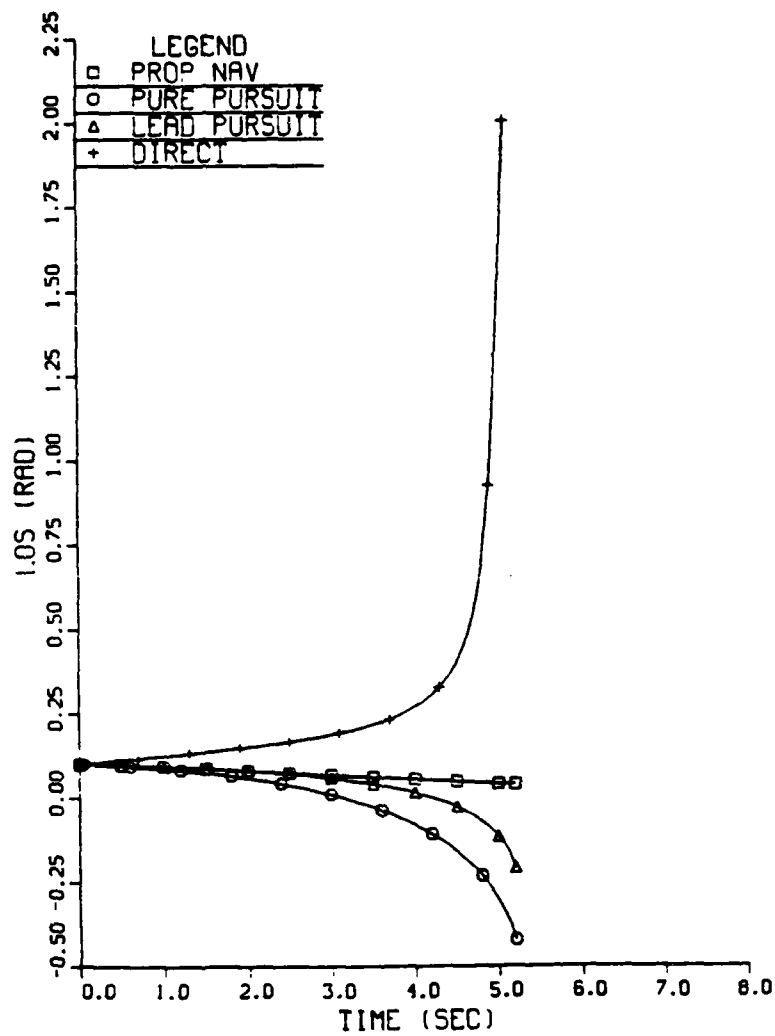


Figure II-20 Line of Sight Angle Plot Tail  
Aspect Constant 3G Target Turn

# TAIL 3G TGT LOS RATE

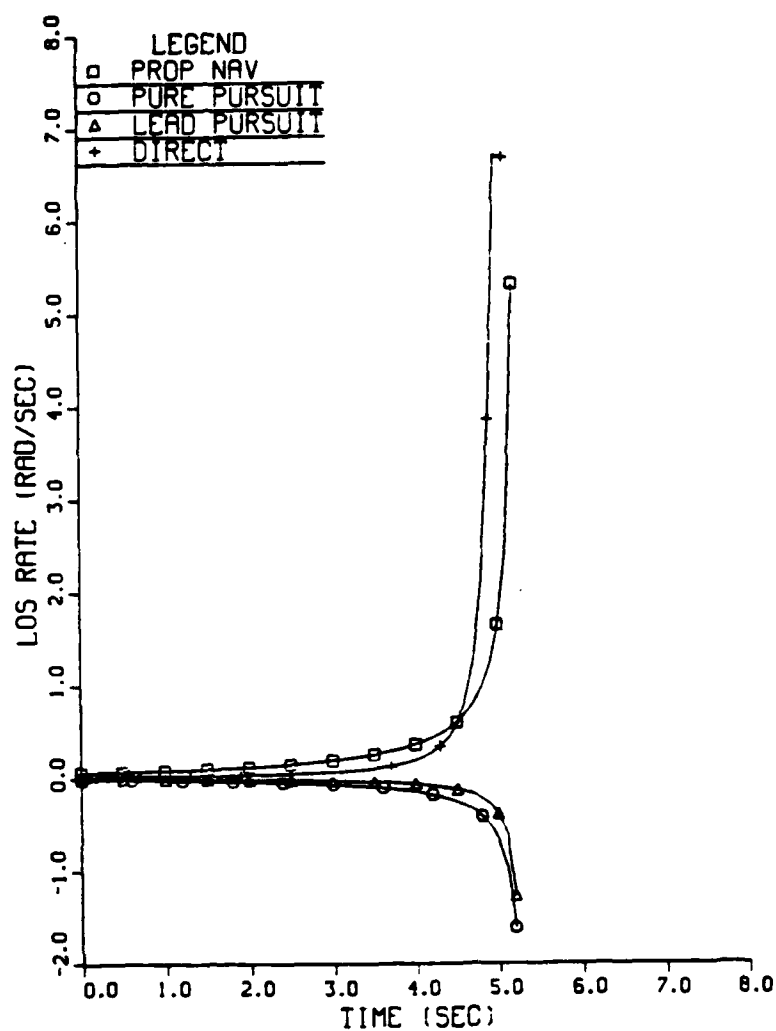


Figure II-21 Line of Sight Rate Plot Tail  
Aspect Constant 3G Target Turn

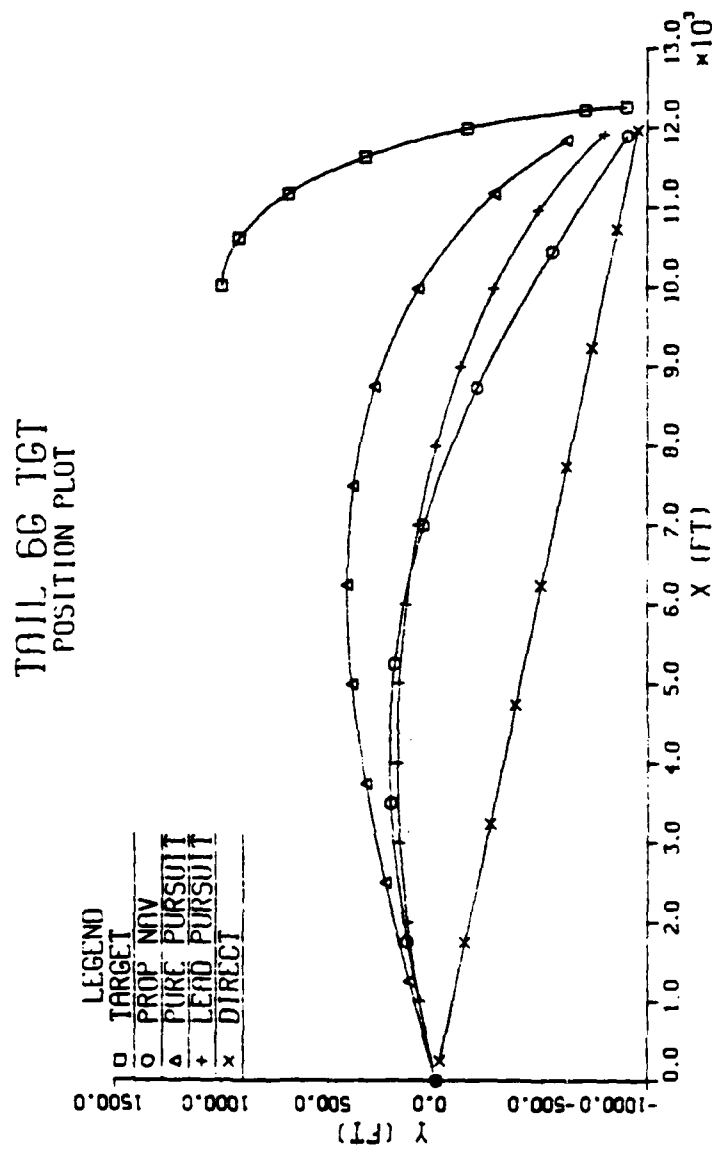


Figure II-22 Position Plot Tail  
Aspect Constant 6G Target Turn

# TAIL 6G TGT MISSILE HEADINGS

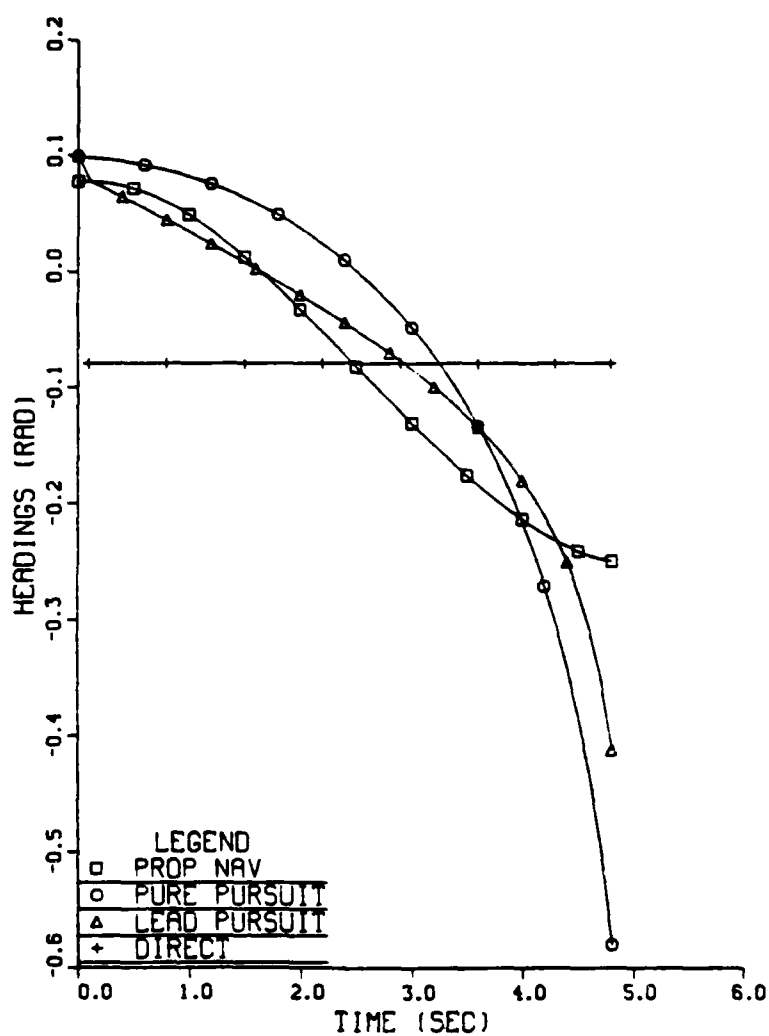


Figure II-23 Missile Heading Plot Tail  
Aspect Constant 6G Target Turn

# TAIL 6G TGT LINE OF SIGHT

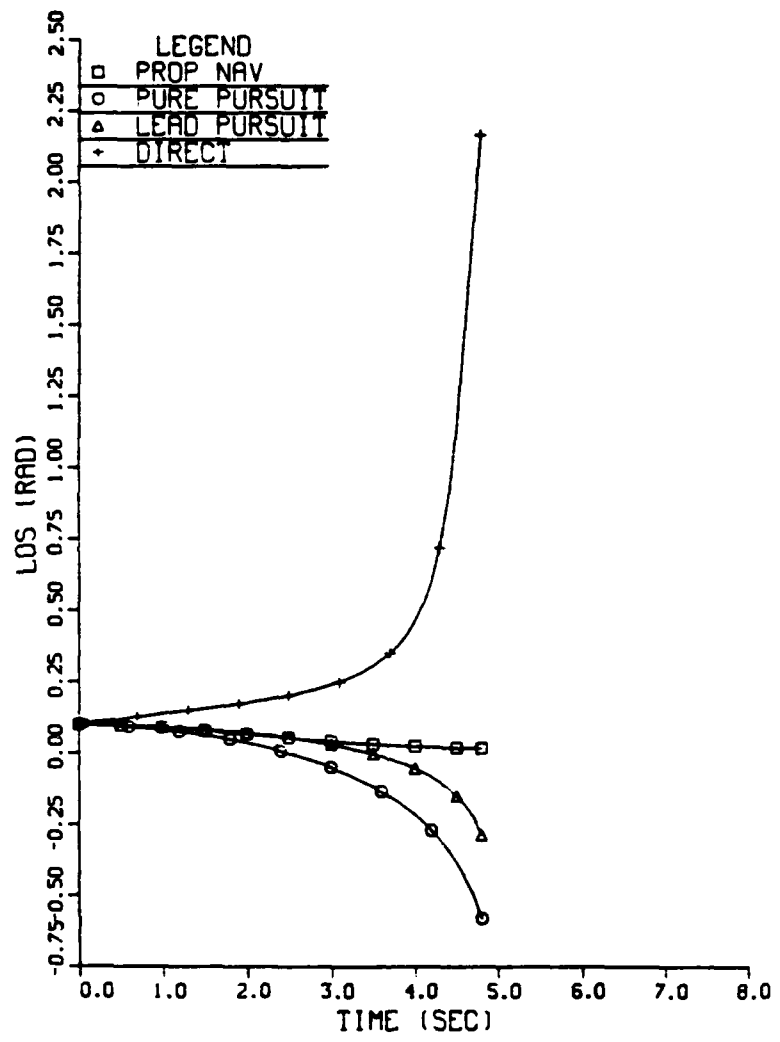


Figure II-24 Line of Sight Angle Plot Tail Aspect Constant 6G Target Turn

REPRODUCED AT GOVERNMENT EXPENSE

TAIL 6G TGT  
LOS RATE

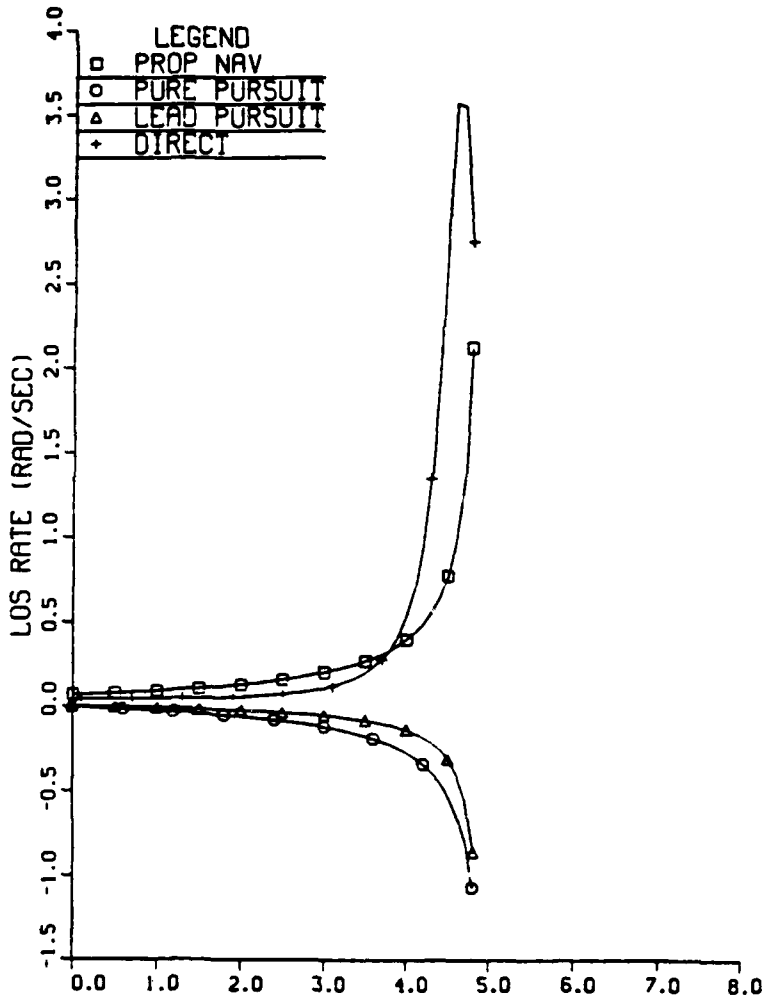


Figure II-25 Line of Sight Rate Plot Tail  
Aspect Constant 6G Target Turn

Figure II-25 Line of Sight Rate Plot Tail  
Aspect Constant 6G Target Turn

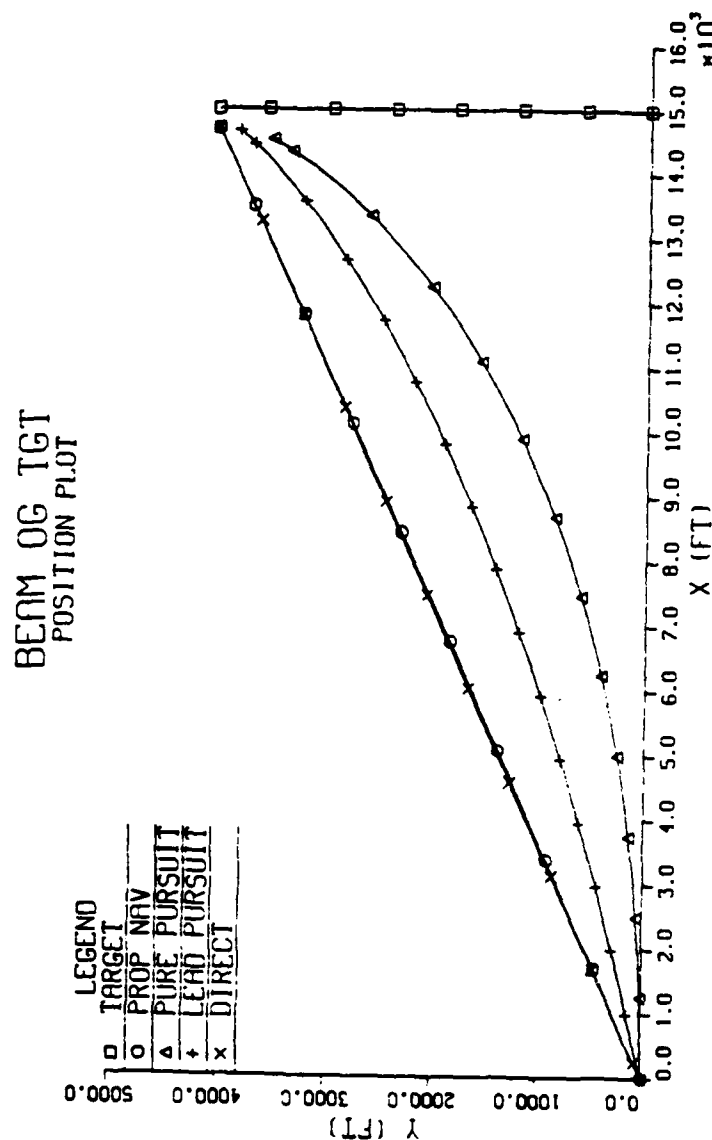


Figure II-26 Position Plot Beam  
Aspect Constant No Target Turn

Figure II-26 Position Plot Beam  
Aspect Constant No Target Turn



# BEAM OG TGT MISSILE HEADINGS

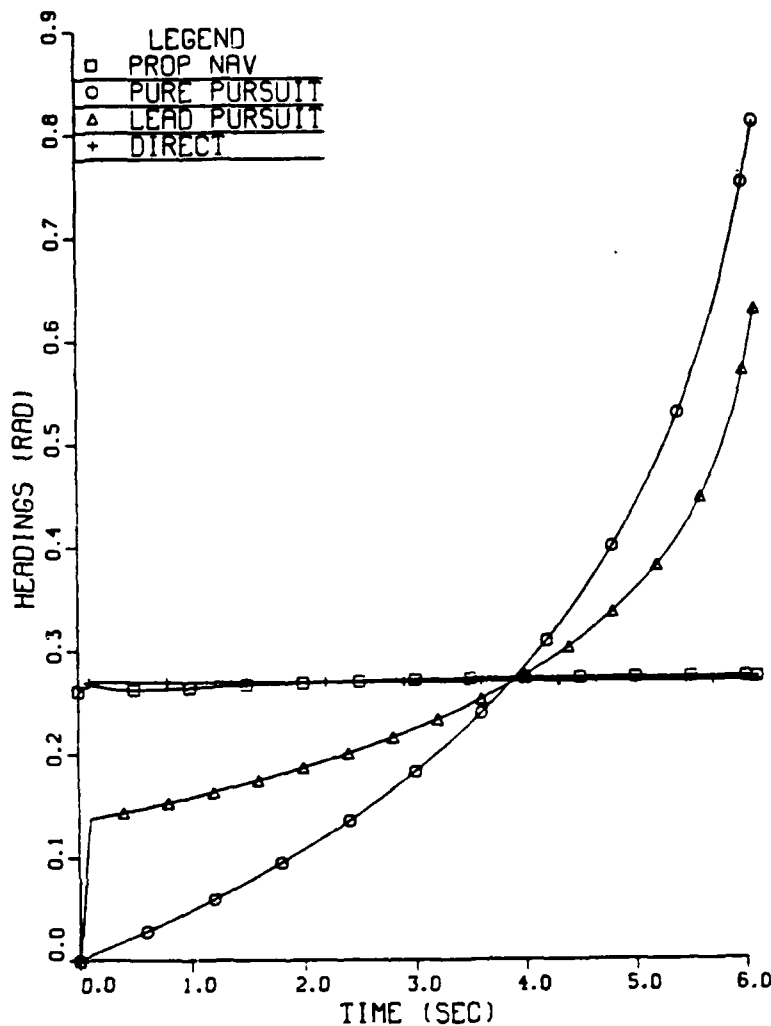
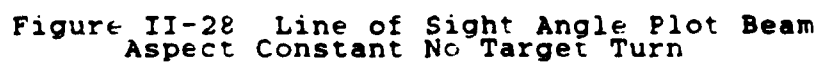


Figure II-27 Missile Heading Plot Beam  
Aspect Constant No Target Turn

Figure II-27 Missile Heading Plot Beam  
Aspect Constant No Target Turn



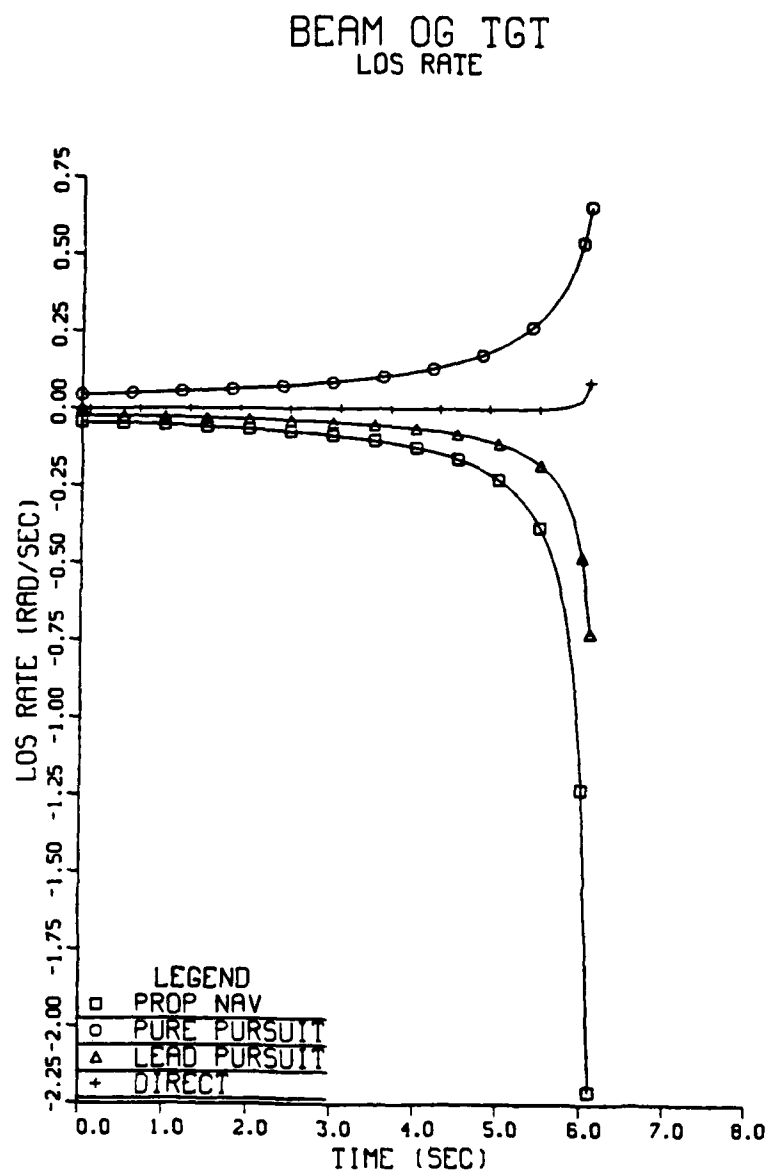


Figure II-29 Line of Sight Rate Plot Beam Aspect Constant No Target Turn

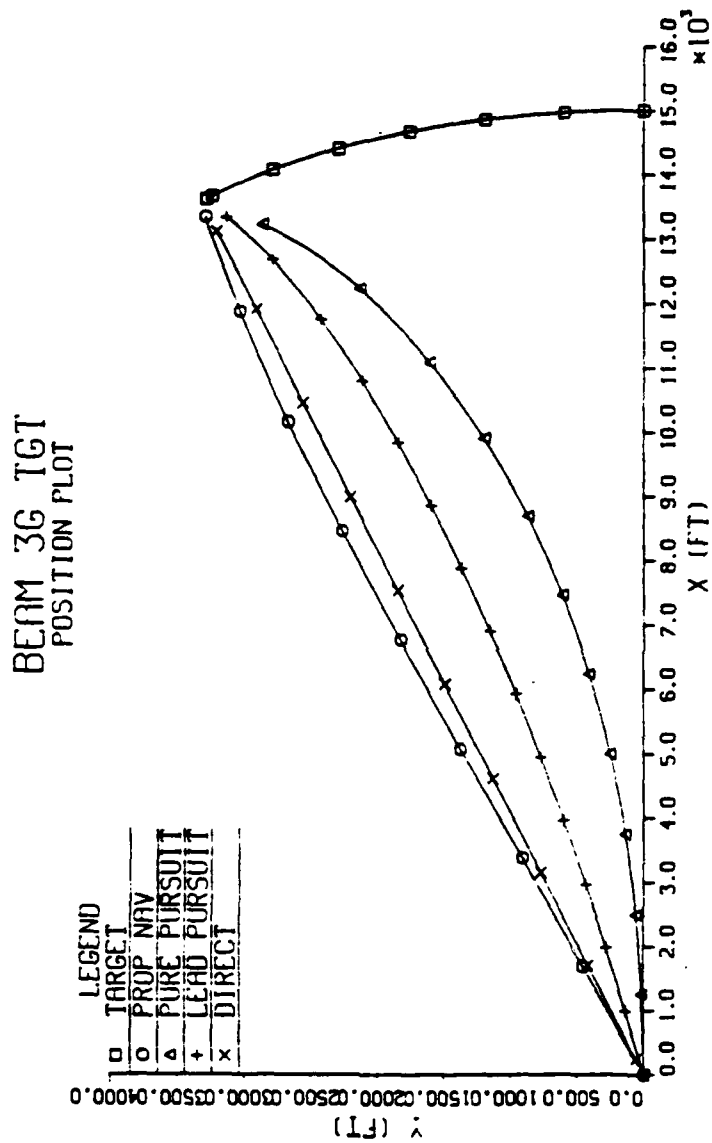


Figure II-30 Position Plot Beam  
Aspect Constant 3G Target Turn

# BEAM 3G TGT MISSILE HEADINGS

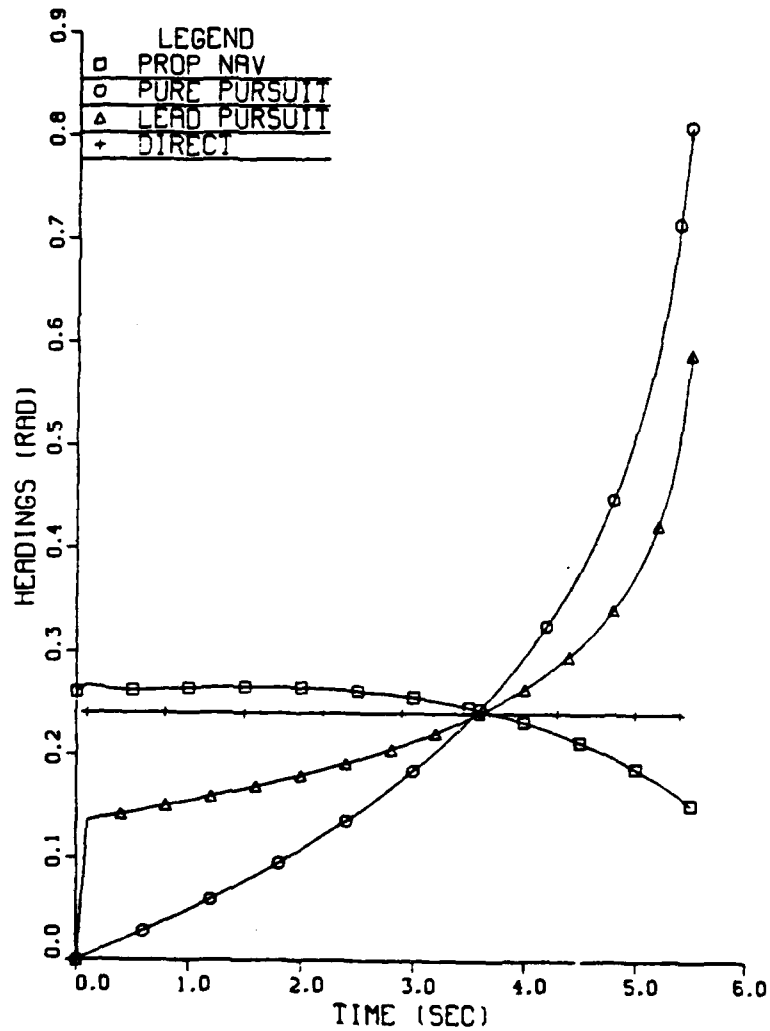


Figure II-31 Missile Heading Plot Beam  
Aspect Constant 3G Target Turn

REPRODUCED AT GOVERNMENT EXPENSE

# BEAM 3G TGT LINE OF SIGHT

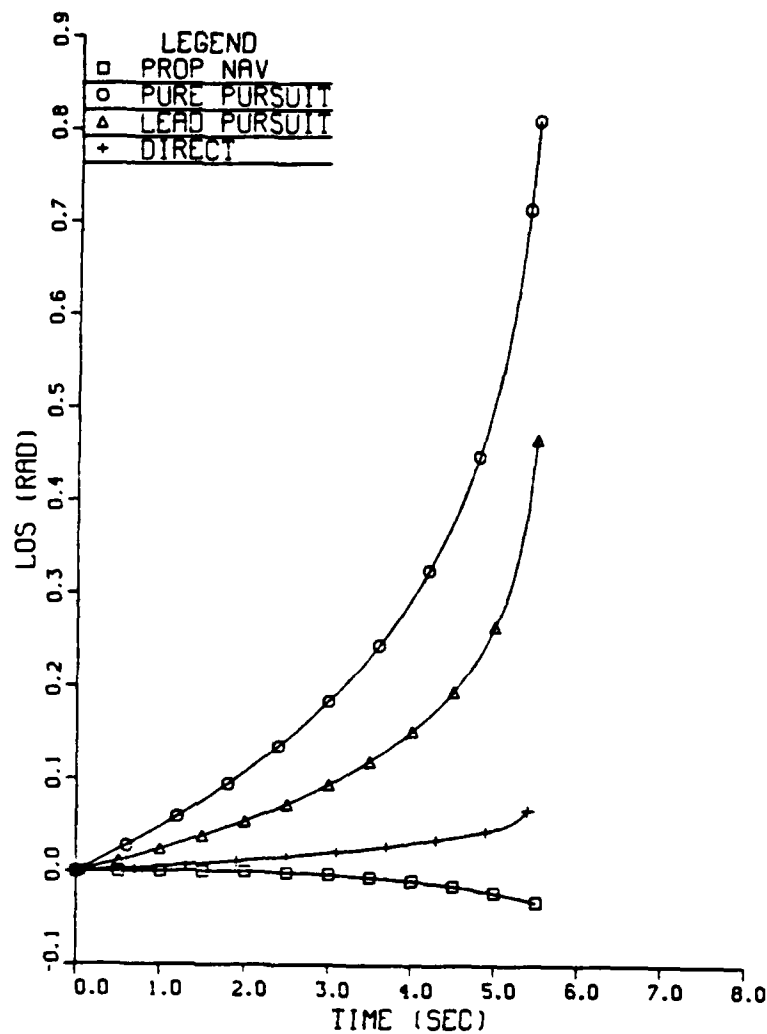


Figure II-32 Line of Sight Angle Plot Beam  
Aspect Constant 3G Target Turn

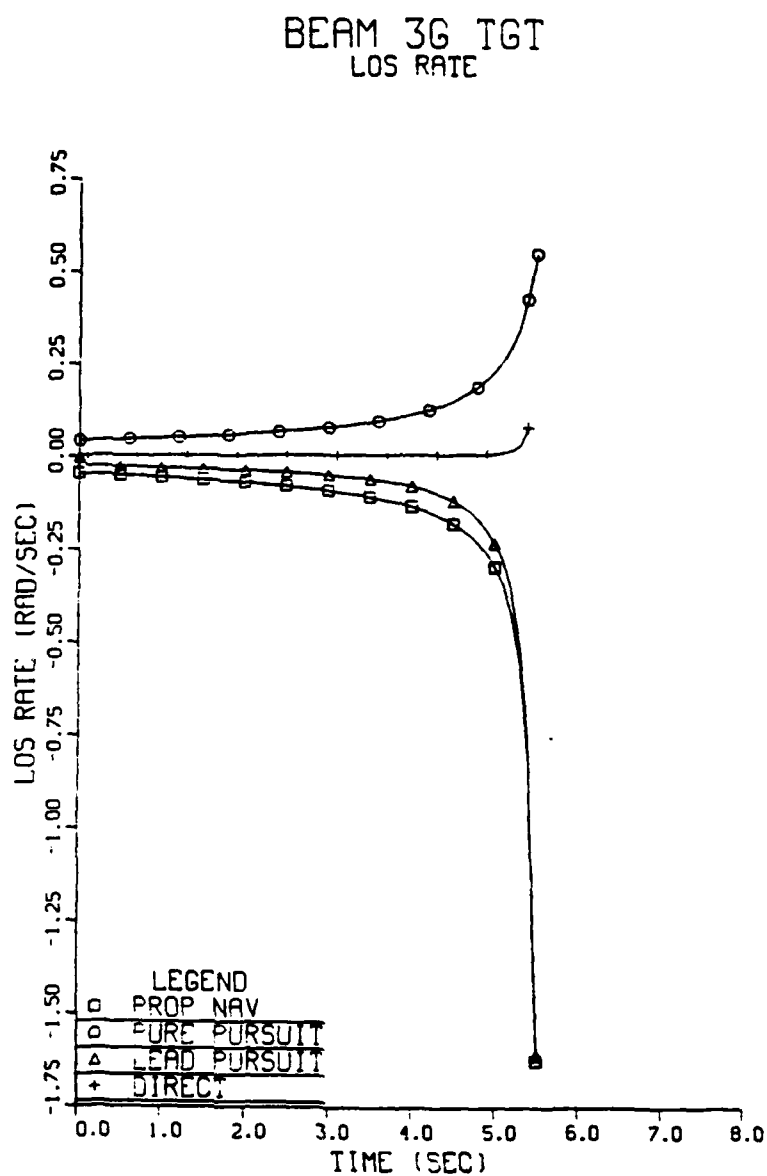


Figure II-33 Line of Sight Rate Plot Beam  
Aspect Constant 3G Target Turn

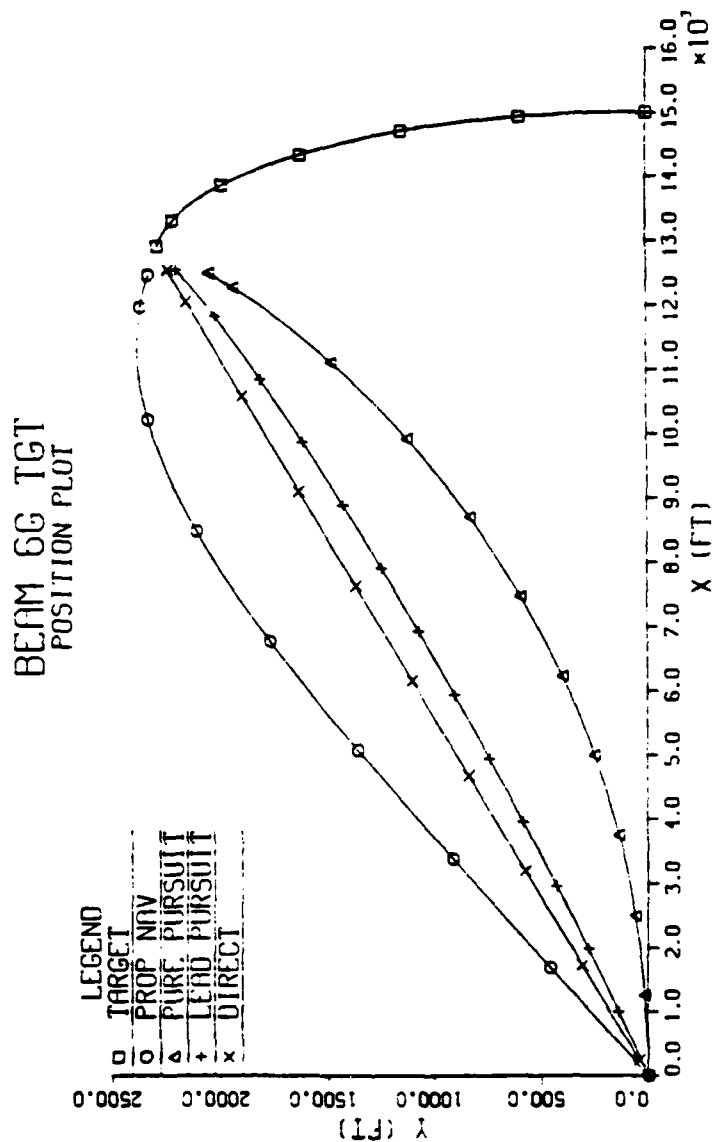


Figure II-34 Position Plot Beam  
Aspect Constant 6G Target Turn



# BEAM 6G TGT MISSILE HEADINGS

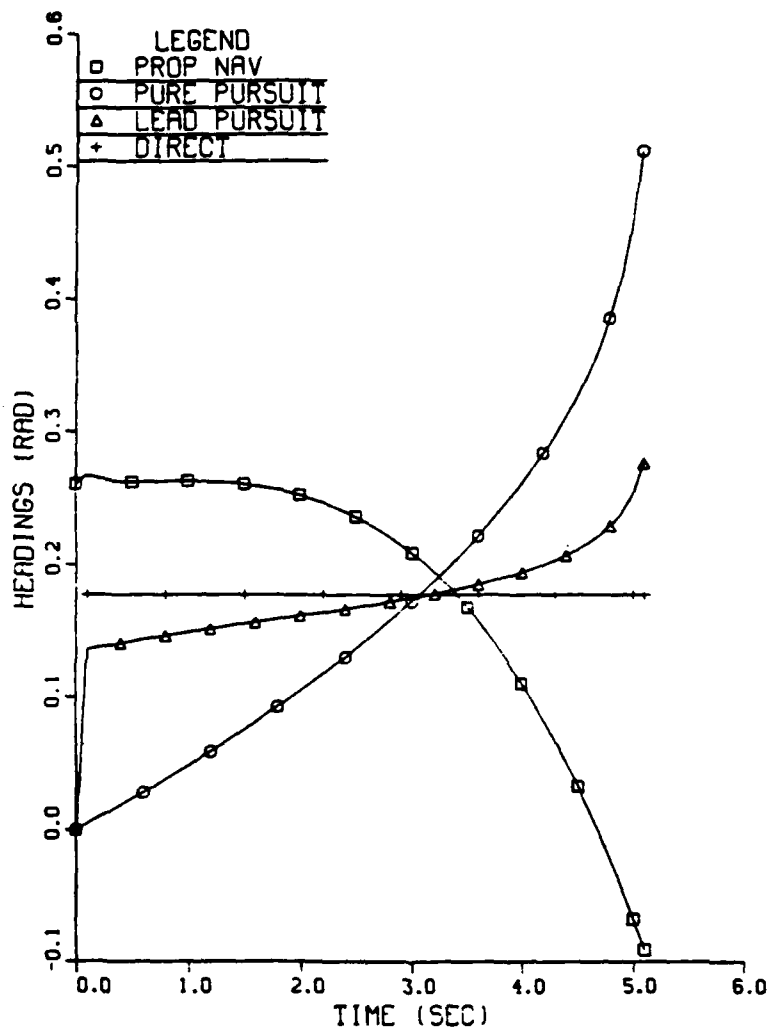


Figure II-35 Missile Heading Plot Beam  
Aspect Constant 6G Target Turn

# BEAM 6G TGT LINE OF SIGHT

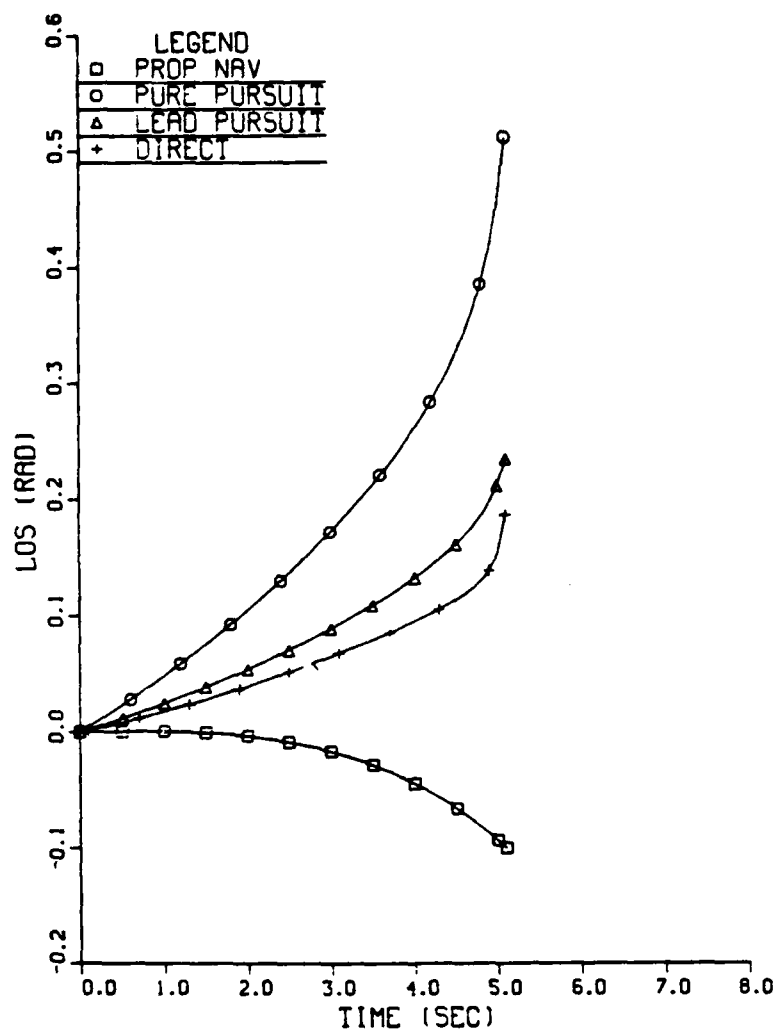


Figure II-36 Line of Sight Angle Plot Beam  
Aspect Constant 6G Target Turn

# BEAM 6G TGT LOS RATE

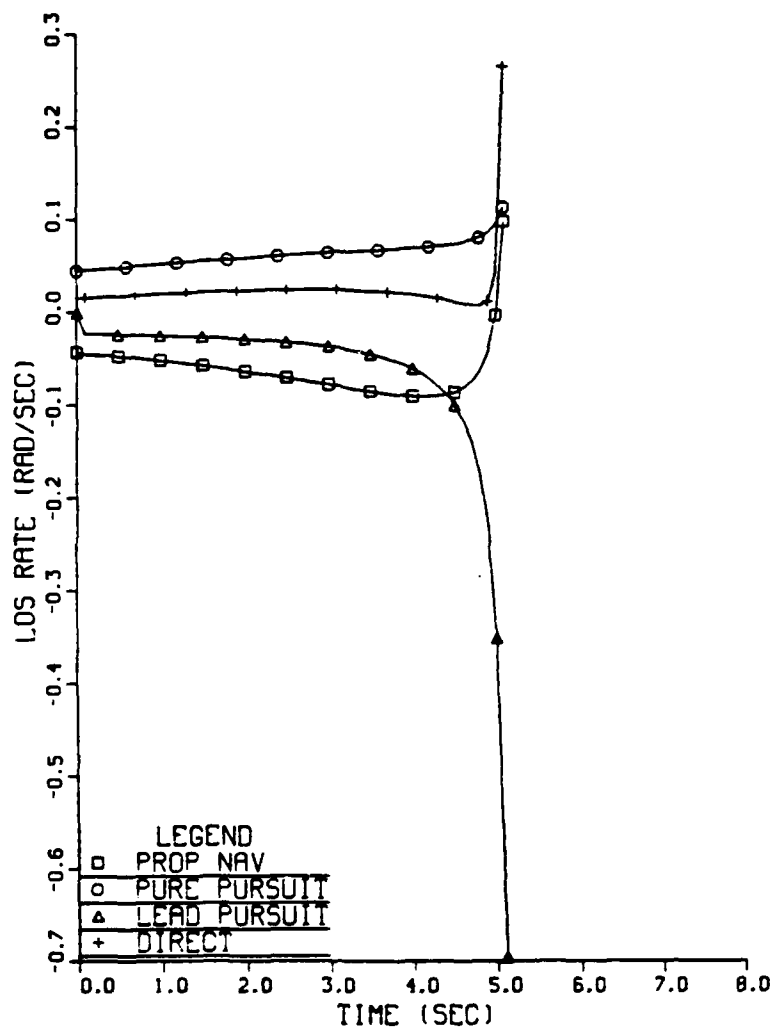


Figure II-37 Line of Sight Rate Plot Beam  
Aspect Constant 6G Target Turn

By applying the acceleration away from the missile the pilot will lose sight of the missile. This is undesirable, but a turn into the missile will help the missile, in the early stages, more than a turn away. With a turn into the missile, the pilot will also lose sight of the missile, during a constant acceleration turn.

#### 1. OG Target Acceleration

From the position plot, Figure II-2, it is seen that proportional navigation guidance is essentially the same as the direct path guidance. Any errors are due to initialization of the heading for the proportional navigation guidance. The pure pursuit guidance missile and the lead pursuit guidance missile fly curvilinear paths to target intercept. The curve for the lead pursuit guidance missile is less than the pure pursuit missile due to target lead.

The missile headings graph, Figure II-3, shows the relative heading changes involved for each missile guidance. After the initialization errors have been corrected, the proportional navigation guidance missile parallels the direct path missile. The heading changes for the lead pursuit are less than for the pure pursuit guidance method. Large increases in missile headings at the end of the intercept implies large lateral accelerations are required for the missile to complete the intercept.

The line of sight graph, Figure II-4, shows what would be expected for this case. The proportional navigation guidance and direct path missile maintain constant line of sight, approximately, while the line of sight increases for lead pursuit and pure pursuit guidance methods. The large change in line of sight at the end of the intercept also correlates to a high lateral acceleration required by the missile.

The line of sight rate graph, Figure II-5, gives some insight to the control inputs to the missile guidance

subsystem. The values from, Figure II-5, are the slew rates for the sensor subsystem. A positive slew rate is seen for the prop nav guidance only at the final stages of the intercept. Lead pursuit and pure pursuit guidance methods have accelerating positive slew rates throughout the intercept. The direct path missile has a negative slew rate, caused by the missile speed advantage (2500 : 667 ft/sec).

## 2. 3G Target Acceleration

The position graph, Figure II-6, shows a curvilinear path for all three guidance methods. The curvature of the target flight path is misleading, because of the axis scaling. The target is maintaining a constant acceleration. All three guidance methods appear to end up in a tail chase. The scaling is misleading again. Target heading change is approximately 50 degrees. The proportional navigation missile impacts in the beam while lead pursuit will be rear quarter and pure pursuit will be a tail chase.

The missile headings graph, Figure II-7, shows the proportional navigation guidance has the lowest heading slope and is approximately linear at the end of the intercept. Pure pursuit and lead pursuit guidance methods have accelerating missile heading slopes requiring higher missile acceleration.

The line of sight graph, Figure II-8, is similar to the Figure II-4, proportional navigation guidance method, which has low line of sight angles, slightly increasing due to target acceleration. Lead pursuit and pure pursuit guidance methods have line of sight angles which increase at an accelerated rate throughout the intercept. The direct missile has decreasing line of sight. The large negative LOS for the direct missile at the end of the intercepts is caused by the miss distance and heading initialization.

Line of sight rates, Figure II-9, correlate with the line of sight plot, Figure II-8. Line of sight rates are

small but show an acceleration at the end of the intercept, due to decreasing range. Proportional navigation guidance methods are reducing the line of sight angle while lead pursuit and pure pursuit increase the line of sight angle.

### 3. 6G Target Acceleration

Comparing the position plot, Figure II-10, with that of the 3G case, Figure II-6, similar statements can be made about all of the missile paths. Scaling is slightly deceiving; the target has made approximately 100° heading change. All flight paths are curvilinear with the proportional navigation guidance method being the shorter of the three methods.

Figure II-11, shows the heading changes for the missiles and the smaller missile maneuvering required for the proportional navigation missile. Figure II-12 and Figure II-13 show larger magnitudes for line of sight angle and line of sight rate than the 3G case, but follow the same trends. The direct path missile shows a reversal in line of sight rate as the target heading change is greater than 90°.

## B. TAIL ASPECT

Figure II-14 through Figure II-25 are the results of missile guidance comparisons for tail aspect initial condition with 0G, 3G and 6G constant target acceleration. The missile begins at the origin of the graph. The target initial position is X=10000 ft. and Y=1000 ft., with an initial heading of 090, parallel to the X axis. Applied target acceleration is directed into the missile, perpendicular to the target heading.

### 1. 0G Target Acceleration

The position plot, Figure II-14, shows the proportional navigation guidance missile flies a similar path as the direct path missile. The difference in the flight paths is due to errors in initialization. The

missile heading plot, Figure II-15, shows that the heading for proportional navigation guidance and direct path missiles are parallel after the initialization errors are corrected. Pure pursuit and lead pursuit guidance methods have continually changing headings with accelerating slopes at the final stage of the intercept.

Line of sight angles for the proportional navigation guidance and direct path are approximately constant and equal to the initial line of sight angle, giving a constant bearing decreasing range trajectory as seen by the target. The line of sight angle for pure pursuit and lead pursuit guidance decrease, but non linearly, as seen in Figure II-16 and Figure II-17.

### 2. 3G Target Acceleration

With target acceleration, all three missiles fly a curvilinear path. The proportional navigation guidance method has the shortest flight path, as seen in Figure II-19. Proportional navigation guidance gives a linear heading change, as seen in Figure II-19. Pure pursuit and lead pursuit guidance methods give higher heading slopes when the target applies lateral acceleration as compared to the OG heading plot, Figure II-15.

Line of sight angle changes are small for proportional navigation guidance, as shown in Figure II-20. Pure pursuit and lead pursuit guidance have decreasing line of sight angles, with corresponding decreasing line of sight rates, as seen in Figure II-20 and Figure II-21. Line of sight rates increase for proportional navigation guidance, as would be expected from the path the missile flies. The direct path gives both a nonlinear line of sight angle and line of sight rate throughout the intercept.

### 3. 6G Target Acceleration

When the target acceleration is increased, flight paths have a larger curvature, as seen in Figure II-22. The scaling gives some distortion, the target has gone through

approximately  $100^\circ$  of heading change. The missile heading changes, as per Figure II-23, are similar to those observed for the 6G head-on aspect, Figure II-11.

The line of sight angle and line of sight rate are larger for an increase in lateral target acceleration, as seen by comparing Figure II-24 and Figure II-25 with the 3G case, Figure II-20 and Figure II-21. The line of sight and line of sight rate for the direct path have a very large slope at the final intercept due to effects of decreased range. The reversal of line of sight rate for the direct path in Figure II-25 is where the target heading change is  $90^\circ$ .

### C. BEAM ASPECT

Figures II-26 through II-37 are the result of missile guidance comparisons for beam aspect initial conditions with 0G, 3G and 6G constant target accelerations. The missile begins at the origin of the graph. The target initial position is  $X=15000$ ,  $Y=0$ . Applied acceleration is directed into the missile.

#### 1. 0G Target Acceleration

As in the two previous cases, with no lateral target acceleration, proportional navigation guidance and direct path missiles have similar flight paths. Pure pursuit and lead pursuit guidance have curvilinear flight paths, as seen in Figure II-26. Heading changes are small for proportional navigation guidance and direct flight path missiles but not zero as what might be inferred from Figure II-27, because of scaling. The heading change for pure pursuit and lead pursuit guidance is accelerating throughout the flight time with the intercept ending in a tail chase.

Line of sight and line of sight rate, Figure II-28 and Figure II-29, are similar to the two previous cases, for no target acceleration and the analysis is the same.



## 2. 3G Target Acceleration

For the beam aspect initial condition, when lateral acceleration is applied, the difference between flight paths for proportional navigation guidance and direct path is opposite from the two previous cases for lateral acceleration. The proportional navigation guidance missile flight path is on the opposite side of the direct path from pure pursuit and lead pursuit guidance flight paths, Figure II-30, with the opposite curvature. Headings for proportional navigation guidance continually decrease while pure pursuit and lead pursuit guidance increase.

Differences between the methods are enhanced by the line of sight angle and line of sight rate plots in Figure II-32 and Figure II-33. Proportional navigation guidance decreases line of sight while the others have an increasing line of sight and appropriate line of sight rate.

## 3. 6G Target Acceleration

Increasing the target lateral acceleration magnifies the flight path differences between the guidance methods. As has been seen from the previous cases, the larger lateral acceleration increases the magnitudes of the values for Figure II-33 through Figure II-37, compared with similar graphs from the other cases, but the trends remain the same. Proportional navigation guidance parameters have smaller changes than pure pursuit and lead pursuit guidance, with parameters generally decreasing instead of increasing for pure pursuit and lead pursuit guidance.

## D. CONCLUSIONS

For scenarios with no applied target lateral acceleration the proportional navigation missile is the same as the direct missile. The pure pursuit and lead pursuit missiles finish in a 'tail chase' where a missile speed advantage is required to complete the intercept. The line

of sight remains constant for the proportional navigation missile but increases with the pursuit missiles. The line of sight rate increases with decreased range for the pursuit missiles but is zero for the proportional navigation and direct missiles.

When target lateral acceleration is applied, there is a deviation between the direct and the proportional navigation missiles. Since the target is turning into the missile, the line of sight angle decreases at an accelerated rate as range decreases. The proportional navigation missile accounts for the change of line of sight by turning into the target. The pursuit missiles fly a tail chase profile with higher line of sight accelerations due to the target turn.

For the direct missile, when target acceleration is applied, the line of sight is not constant and the rate of change depends on the applied acceleration. Implementation of a direct missile is impossible because the parameters used to guide the missile are dependent on the target flight path.

If an optimum missile is to be designed, proportional navigation guidance is the closest to an "ideal" missile. The better the proportional navigation missile can compensate for the effects of the target acceleration, the closer to "ideal" the missile will become.

### III. TARGET MODEL

A complete target model for use in computer simulation is very involved, time consuming and computer intensive. To simplify target simulation the target flight profile is based on the fact that the missile sees only the effects of the target command inputs and resultant flight path. The target model was simplified to include only the flight profile desired and not be concerned with the full target modeling. A constant speed, constant acceleration target is assumed for the simulation. A variable speed, variable acceleration target can be added at a later time. The missile simulation estimates and predicts target parameters of range, range rate, range acceleration, bearing, bearing rate, and bearing acceleration. Therefore, for proper evaluation of the missile guidance and missile flight profiles the target parameters in missile coordinates for all these parameters must be computed.

Complete analysis of target motion is obtained from a three dimensional derivation, but insight can be gained from two dimensional modeling. Three dimensional flight profiles are easily implemented on the computer but graphic display of the results are difficult. Two dimensional displays are easier to implement and comprehend. A two dimensional target model is assumed.

A target can accelerate at values ranging from negative maximum instantaneous acceleration to positive maximum instantaneous acceleration,  $A(\text{max inst})$ .  $A(\text{max inst})$  is defined as the aerodynamic acceleration given by the maximum deflection of control surfaces.  $A(\text{max inst})$  is dependent on airspeed and air density. High speeds and low altitudes produce the highest instantaneous accelerations. Maximum sustained acceleration,  $A(\text{max sust})$ , is defined as the aerodynamic acceleration to maintain constant airspeed and

constant altitude, at full thrust.  $A(\text{max sust})$  can be exceeded but must be compensated for by a reduction in airspeed or altitude.

In three dimensional maneuvering cross coupling exists between horizontal and vertical angle and angle rate components of target velocity and target acceleration. Applied accelerations and velocity changes in one direction will affect the parameters, seen by a missile, in the two other directions.

Thrust capabilities have a direct correlation to  $A(\text{max sust})$  and the airspeed of an aircraft. An aircraft with higher thrust can maintain a higher speed and compensate for drag induced by the applied acceleration. A modern aircraft with a relatively high thrust to weight ratio will have a very high  $A(\text{max sust})$  which is close to  $A(\text{max inst})$ .

Airspeed is a key element for maneuverability and survivability. Tactics incorporate optimum techniques for maintaining airspeed or recovering lost airspeed. Pilots learn to compensate for limitations of  $A(\text{max sust})$  by intentionally decreasing altitude and use the effects of gravity to maintain airspeed when lateral acceleration is applied. Another technique is to apply the lateral acceleration required to perform a maneuver then to reduce the acceleration, allowing excess thrust to restore the airspeed and altitude lost during the maneuver. There is a recovery time for the thrust to restore the lost energy, so to aid in restoring airspeed, a pilot will normally go to zero acceleration, reducing any induced drag, effectively increasing the aircraft thrust. This maneuver causes a loss in altitude due to gravity but improves airspeed restoration.

The probability of aircraft acceleration is used to determine parameters for the target model used in missile designs and simulations. Figure III-1 shows a typical acceleration probability graph used in missile design. The

figure does not account for pilot tendencies nor the difference between  $A(\text{max sust})$  and  $A(\text{max inst})$ . The graph assumes that a pilot will maneuver primarily at zero acceleration, straight and level, or maximum acceleration, for a turn, with some probability for any other possible acceleration. The design engineer assigns probabilities for the impulse functions at zero acceleration and at maximum acceleration depending on the type of target aircraft. A large bomber may have an  $A(\text{max sust})$  half that of a fighter aircraft, with less probability of turning than flying straight and level.

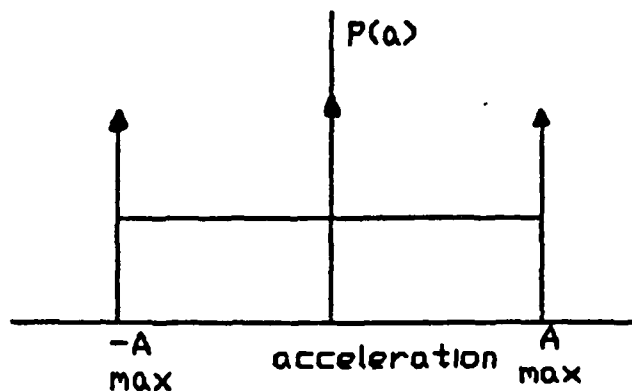


Figure III-1 Probability of Aircraft Acceleration [Ref. 2,3]

A proper target maneuver model should include some pilot tendencies and known tactics. A pilot is not always able to move the control surface to a precise location to cause a precise acceleration at an optimal time. A pilot will move the control surface, judge the acceleration induced then move the control surface to achieve a desired acceleration. The feel a pilot receives from the 'stick' is a prime feedback source to allow the pilot to set the desired acceleration. The more force the pilot applies, the more the control surface moves, and the higher is the acceleration. Modern aircraft may use computers to achieve the commanded acceleration, reducing any pilot induced errors on input.

## A. TACTICS FOR MISSILE DEFENSE

When a missile is fired at the target the battlefield scenario changes to an immediate survival situation. If the missile is undetected, the acceleration probabilities of Figure III-1 may be an adequate target model. If a pilot sees the missile, pilot reactions will change the probabilities. How the probabilities change may be of consequence to the missile guidance. An optimum missile design may be able to use pilot tendencies to increase missile performance. The overall acceleration probability from Figure III-1 is a zero mean function with a variance,  $\sigma^2$ , dependent on the probabilities assigned. Reference 2 discusses obtaining the parameters for the target acceleration probability model of Figure III-1.

When the pilot imposes a missile defense, the overall acceleration may not be zero mean, nor maintain the same variance. To account for the changes in acceleration probability a function similar to Figure III-2 might be used. This model accounts for some variance to the acceleration which the pilot is trying to achieve centered around  $A(\text{max sust})$ . If the pilot is trying to achieve  $A(\text{max inst})$ , it is assumed he will be decreasing airspeed and reducing actual acceleration until the applied acceleration is decreased to  $A(\text{max sust})$  or below. A smart pilot will either fly at a maximum acceleration or at zero acceleration, increasing the aircraft maneuverability.

Last ditch maneuvers are performed at  $A(\text{max inst})$  to avoid the missile, neglecting any adverse effects of applying acceleration, in order to increase survivability. If the last ditch maneuver is performed too soon, acceleration is decreased, due to loss of airspeed, negating the effectiveness of the maneuver. Further studies can be made correlating the use of  $A(\text{max inst})$  versus  $A(\text{max sust})$  for missile defense tactics.

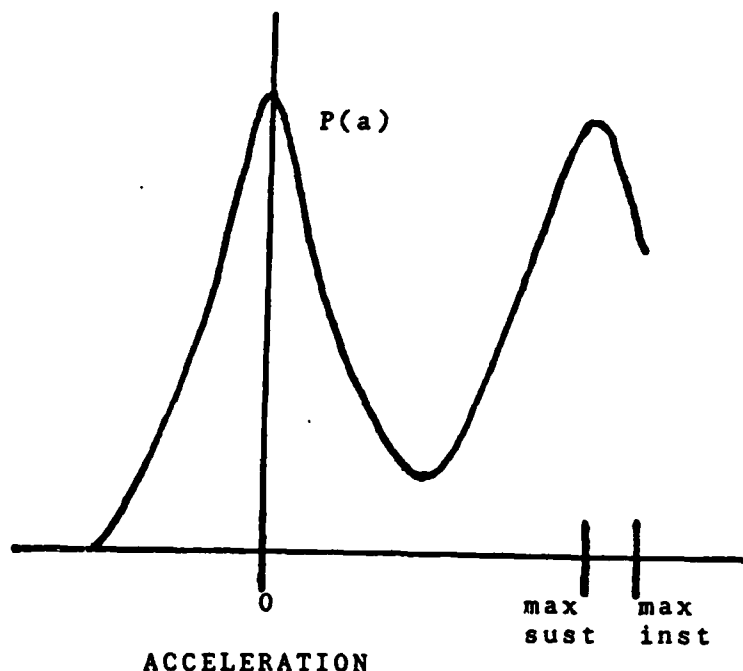


Figure III-2 Probability of Acceleration

If pilot reaction is taken as Gaussian when trying to achieve a desired acceleration, the overall acceleration probability will be Gaussian with a non-zero mean and a variance dependent on the combination of the two Gaussian terms. The probability assigned to each term determines the mean and variance.

Missile defense includes placing the missile on the beam, to utilize the largest acceleration vector, with maneuvers made out of phase, out of plane with the missile. The largest acceleration component comes from the elevator, perpendicular to the wings. By placing the wings parallel with the plane of the missile, the largest acceleration component is used to create the largest missile corrections, perpendicular to the plane of the missile. The plane of the missile is defined by three points: target position, missile position and the projected impact point.

A graph of a target acceleration, while performing missile evasion, might look like Figure III-3. The pilot commands  $A(\text{max sust})$  or  $A(\text{max inst})$  for a short time, then

reduces the acceleration to zero to regain lost energy, before applying the acceleration again. This process may be repeated 2,3 or more times during the missile flight time. The graph attempts to incorporate transient response induced by system time delays, transient responses of the control surfaces and pilot tendencies for maneuvering and control of the target.

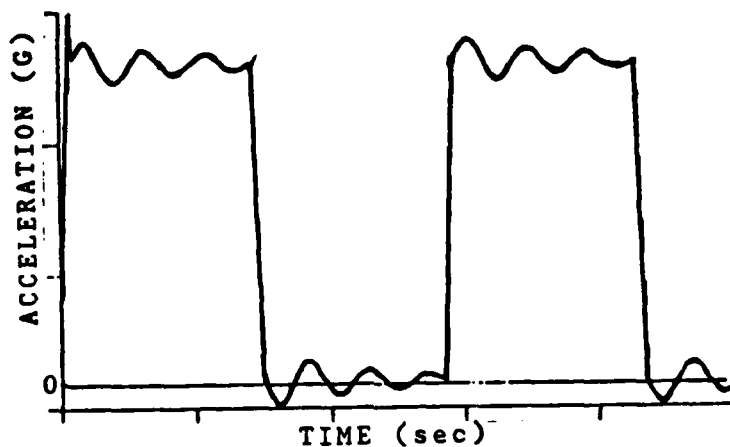


Figure III-3 Target Acceleration

The resultant average acceleration is non-zero, with a non-zero variance. The mean and variance of Figure III-3 can be estimated by the parameters assumed in Figure III-2.

Figure III-1 and Figure III-2 show total aircraft acceleration. The parameters as seen by the missile, in antenna coordinates, will vary depending on the three dimensional maneuver employed. The missile tracking subsystem must be designed to handle the maximum acceleration possible for each of the orthogonal components of the reference frame.

Proportional navigation missiles compensate for the applied target acceleration by decreasing the line of sight rate induced by the change of target velocities. With a good target model and detection of maneuvering effects, the missile guidance can predict target motion and position.



#### IV. SYSTEM MODEL

From the section on the ideal missile, it was ascertained that target parameters are not constant if lateral acceleration is applied. This thesis will attempt to incorporate as much sensor information as is available in defining the system models for an optimum missile. Current radars allow the measurement of range, range rate and off boresight bearing error. Measurements taken by the radar are referenced to a radar axis system. In order for the missile to use the information supplied by the radar, a common reference frame must be established.

##### A. COORDINATE SYSTEM

Each entity in the missile-target intercept problem has its own coordinate system. The overall geometry as seen from an "eye in the sky" would view it in space coordinates. An observer on the ground would view it in earth coordinates. The launching aircraft, missile and target aircraft will view it in an individual coordinate system, referenced to that specific platform. Trying to equate each coordinate system is not an easy task but one which is done.

By use of Euler angles any reference coordinate system can be related with Earth coordinates. By use of a directional cosine matrix transformation any reference coordinate system can be transformed to another reference coordinate system [Ref. 3].

The missile is concerned with flying to a point in space that will hopefully be occupied by the target at the completion of the intercept. The object is to guide the missile to the proper point where the target will be. The missile is concerned with its coordinate system and not that of the target. But on the missile itself there are

various coordinate system reference points. Each sensor has its own location on the missile and where it is mounted is its reference point. Any moving sensor, like the antenna, will have its special reference coordinate system. Missile parameters are normally referenced to the missile body frame of reference while target parameters are referenced to the antenna frame of reference. While very complicated, the frames of references can be transformed and equated. [Ref. 3]

To simplify simulation and evaluation of desired parameters, an inertial frame of reference will be used which is centered at the radar antenna location. This simplification will aid in better evaluation of the effects of the target parameters and the missile guidance without encumbrance of transformation errors. Although the simplification assumes ideal missile parameters, time delays can be incorporated later to account for first order modeling of the missile.

## B. EQUATIONS OF MOTION

In cartesian coordinates missile and target motion is described by the standard motion equation:

$$X(T) = X_0 + \int_0^T \dot{X}(t) dt + \iint_0^T \ddot{X}(t) dt dt \quad (7)$$

The equation is based on a fixed reference point. The orthogonal directions (Y and Z) will have the same equation.

The antenna frame of reference uses polar coordinates which have the equations:

$$r(t) = r_0 + \int_0^T \dot{r}(t) dt + \iint_0^T \ddot{r}(t) dt dt \quad (8)$$

$$\theta(t) = \theta_0 + \int_0^T \dot{\theta}(t) dt + \iint_0^T \ddot{\theta}(t) dt dt \quad (9)$$

$$\phi(t) = \phi_0 + \int_0^T \dot{\phi}(t) dt + \iint_0^T \ddot{\phi}(t) dt dt \quad (10)$$

where  $r(t)$  = the radial component of motion  
 $\theta(t)$  = horizontal component of motion  
 $\phi(t)$  = vertical component of motion

When the reference point is not fixed, extra terms and cross coupling are introduced into equation dynamics. The coriolis equation accounts for the moving reference point. Depicted in Figure IV-1 a change in the vector  $R$  is accounted for by both changes in the magnitude and the rotation effects by the moving reference point. Using the terms as defined in Figure IV-1 we can obtain the necessary equations to find  $r(t)$ ,  $\theta(t)$  and  $\phi(t)$ . For simplicity, only the derivation for  $r$  and  $\theta$  are shown with  $r$  and  $\phi$  relationships being a duality of derivation of  $r$  and  $\theta$ . The simulation of Section VI will be two dimensional.

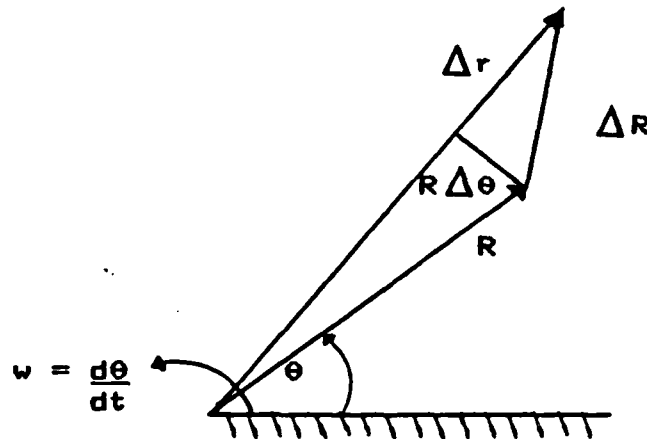


Figure IV-1 Rotating Vector Diagram

The coriolis equation to relate the time rate of change of the  $R$  vector to the rate of change in the  $r$  direction and the angular rate of motion is:

$$\dot{R} = \dot{r} + w \times R \quad (11)$$

where  $R$  = the directional vector  
 $r$  = the magnitude of the directional vector  
 $w$  = the angular rate of motion

The total change of the vector R is the sum of the change in the magnitude of R due to changes along the original vector R given by  $\dot{r}$  and the angular rotation due to the moving coordinate frame, given by  $\dot{w} \times R$ .

Utilizing the general rule for differentiating a vector<sup>1</sup> an expression is obtained for the acceleration of the R vector.

$$\dot{R} = \dot{r} + \dot{w} \times r + w \times \dot{r} + w \times R \quad (12)$$

$$\ddot{R} = \ddot{r} + \ddot{w} \times r + \dot{w} \times \dot{r} + w \times \ddot{r} + w \times \dot{w} \times r \quad (13)$$

$$\ddot{R} = \ddot{r} + \ddot{w} \times r + 2(w \times \dot{r}) + w \times w \times r \quad (14)$$

where  $R$  = directional vector  
 $r$  = the acceleration of the magnitude of  $R$   
 $w \times r$  and  $w \times r$  are perpendicular to the  $R$  vector  
 $w \times w \times r$  is centrifugal acceleration

This equation gives the cross correlation of range and angle to implement in a second order model. Applying the rule of differentiating a vector again will yield the equations for a third order model.

$$\frac{d(\ddot{R})}{dt} = \ddot{r} + \ddot{w} \times r + \dot{w} \times \dot{r} + 2(\dot{w} \times \dot{r}) + 2(w \times \ddot{r}) + \dot{w} \times w \times r + w \times \ddot{w} \times r + w \times w \times \dot{r} + w \times \ddot{R} \quad (15)$$

$$\frac{d(\ddot{R})}{dt} = \ddot{r} + \ddot{w} \times r + \dot{w} \times \dot{r} + 2(\dot{w} \times \dot{r}) + 2(w \times \ddot{r}) + \dot{w} \times w \times r + w \times \ddot{w} \times r + w \times w \times \dot{r} + w \times \ddot{R} + w \times 2(w \times \dot{r}) + w \times w \times w \times r \quad (16)$$

$$\ddot{R} = \ddot{r} + 3(\dot{w} \times \dot{r}) + 3(w \times \ddot{r}) + \ddot{w} \times r + \dot{w} \times w \times r + 2(w \times \ddot{w} \times r) + 3(w \times w \times \dot{r}) + w \times w \times w \times r \quad (17)$$

where  $\ddot{R}$  is the acceleration jerk of vector  $R$

---

<sup>1</sup> rule for differentiating a vector

$$\frac{dA}{dt} = \frac{\partial A}{\partial t} + w \times A$$

the total derivative is the sum of the time rate of change of the vector and the rotation of the vector.

$r$  is the magnitude of  $R$   
 $w_x r$  is perpendicular to  $R$   
 $w_x w_x r$  is in the negative direction of  $R$   
 $w_x w_x w_x r$  is perpendicular to  $R$

### C. SECOND ORDER MODEL

Beginning with equations 8-10, a second order state space system can be set up which would have the form:

$$r = r_0 + \int_0^T \dot{r} dt + \iint_0^T \ddot{r} dt \quad (18)$$

$$\theta = \theta_0 + \int_0^T \dot{\theta} dt + \iint_0^T \ddot{\theta} dt \quad (19)$$

$$\begin{bmatrix} \dot{r} \\ \ddot{r} \\ \dot{\theta} \\ \ddot{\theta} \end{bmatrix} = \begin{bmatrix} 0 & 1 & 0 & 0 \\ 0 & 0 & 0 & 0 \\ 0 & 0 & 0 & 1 \\ 0 & 0 & 0 & 0 \end{bmatrix} \begin{bmatrix} r \\ \dot{r} \\ \theta \\ \dot{\theta} \end{bmatrix} \quad (20)$$

The range portion of the second order system may be accomplished totally by the radar, since no other subsystems require the information. The radar receiver is designed to track the target in the radial direction without the need for an additional filter.

The more difficult state equations to implement in the missile are the angular directions. The second order, time invariant, constant velocity, zero acceleration, state feedback model makes the tracking much easier. The continuous system model can be given in a time derivative form as:

$$\dot{X} + k_1 \cdot \dot{X} + k_2 \cdot X = 0 \quad (21)$$

If the term given in the equation as  $X$  is actually the error of the angular position then

$$X = (\text{line of sight angle} - \text{antenna position angle})$$

where  $X$  can be directly measured by the antenna. The values of the  $k$ 's in the time derivative equation depend on the designer and the response desired. For the simulations of the proportional navigation missiles of Section II and Section VI,  $k_1 = 20$  and  $k_2 = 100$  were used. These constants give a response time constant of 0.1 sec.

The use of the coriolis equation to derive the second order model gives a time varying solution. Implementing time varying equations are difficult and often avoided by using a time invariant system and state feedback to cancel errors. The time variant space state model derived from equation 14 is shown below:

$$\ddot{R} = \ddot{r} + \dot{w}r + 2(w\dot{r}) + w\dot{w}r \quad (22)$$

Separating into orthogonal components of radial and transverse with scalar multiplication:

$$a_R = \ddot{r} + w\dot{r} \quad (23)$$

$$a_T = \dot{w}r + 2(w\dot{r}) \quad (24)$$

Rearranging into equations to implement into a system:

$$\ddot{r} = -\dot{\theta}^2 r + a_R \quad (25)$$

$$\dot{\theta} = -\frac{2\dot{\theta}\dot{r}}{r} + \frac{a_T}{r} \quad (26)$$

The state space model is difficult to represent unless divided into two channels with cross coupling given in the  $A$  matrix.

$$\begin{bmatrix} r \\ \dot{r} \end{bmatrix} = \begin{bmatrix} 0 & 1 \\ -\dot{\theta}^2 & 0 \end{bmatrix} \begin{bmatrix} r \\ \dot{r} \end{bmatrix} + \begin{bmatrix} 0 \\ 1 \end{bmatrix} a_R \quad (27)$$

$$\begin{bmatrix} \theta \\ \dot{\theta} \end{bmatrix} = \begin{bmatrix} 0 & 1 \\ 0 & -\frac{2\dot{r}}{r} \end{bmatrix} \begin{bmatrix} \theta \\ \dot{\theta} \end{bmatrix} + \begin{bmatrix} 0 \\ 1 \end{bmatrix} a_T \quad (28)$$

#### D. THIRD ORDER MODEL

The time invariant model, derived from equations similar to those deriving the time invariant second order model (equations 18 and 19), in state space form is given by:

$$\begin{bmatrix} \dot{r} \\ \ddot{r} \\ \ddot{r} \\ \dot{\theta} \\ \ddot{\theta} \\ \ddot{\theta} \end{bmatrix} = \begin{bmatrix} 0 & 1 & 0 & 0 & 0 & 0 \\ 0 & 0 & 1 & 0 & 0 & 0 \\ 0 & 0 & 0 & 0 & 0 & 0 \\ 0 & 0 & 0 & 0 & 1 & 0 \\ 0 & 0 & 0 & 0 & 0 & 1 \\ 0 & 0 & 0 & 0 & 0 & 0 \end{bmatrix} \begin{bmatrix} r \\ \dot{r} \\ \ddot{r} \\ \theta \\ \dot{\theta} \\ \ddot{\theta} \end{bmatrix} \quad (29)$$

Ranging may be accomplished by the radar receiver, as in the second order model, for similar reasons. Tracking angular positioning requires knowledge of the target angular acceleration as well as angular velocity. A filter is normally used to maintain a track of the target angular parameters. Common filters are  $\alpha$ - $\beta$ , Weiner, and Kalman. As compared in Reference 4, the Kalman is the best filter suited for air to air missiles, but also the most costly to implement. For the time invariant third order model a simple constant gain Kalman Filter can be used. The Kalman Filter will be discussed in the next section.

The time variant third order model is obtained from the second derivative of the coriolis equation derived in the previous section.

$$\begin{aligned} \ddot{\mathbf{R}} = \ddot{\mathbf{r}} + 3(\dot{\mathbf{w}}\mathbf{r}) + 3(\mathbf{w}\dot{\mathbf{r}}) + \dot{\mathbf{w}}\mathbf{x}\mathbf{r} + \mathbf{w}\mathbf{x}\mathbf{w}\mathbf{x}\mathbf{r} \\ + 2(\mathbf{w}\mathbf{x}\dot{\mathbf{w}}\mathbf{x}\mathbf{r}) + 3(\mathbf{w}\mathbf{x}\mathbf{w}\mathbf{x}\mathbf{r}) + \mathbf{w}\mathbf{x}\mathbf{w}\mathbf{x}\mathbf{w}\mathbf{x}\mathbf{r} \end{aligned} \quad (30)$$

The  $\ddot{\mathbf{R}}$  term is the change in the acceleration of the vector or a "jerk" term, a simple comprehension is the rate at which the pilot applies the commanded acceleration. Separating the equation into radial and tangential terms, the two orthogonal scalar equations are:

$$\ddot{a}_R = \ddot{r} - 3w^2r - 3w\dot{r} \quad (31)$$

$$\dot{a}_r = 3\dot{w}\dot{r} + 3w\dot{r} + \dot{w}r + w^3r \quad (32)$$

Converting the equation into primary coordinate axis, the equations obtained are:

$$\ddot{r} = \dot{a}_r + 3\dot{\theta}^2 r + 3\dot{\theta}(\dot{\theta})r \quad (33)$$

$$\ddot{\theta} = \dot{a}_r - \frac{3(\dot{\theta})\dot{r}}{r} - \frac{3\dot{\theta}(\dot{r})}{r} - \dot{\theta}^3 \quad (34)$$

The disassociated space state model looks like:

$$\begin{bmatrix} \dot{r} \\ \dot{r} \\ \ddot{r} \end{bmatrix} = \begin{bmatrix} 0 & 1 & 0 \\ 0 & 0 & 1 \\ 3\dot{\theta}(\dot{\theta}) & 3\dot{\theta}^2 & 0 \end{bmatrix} \begin{bmatrix} r \\ \dot{r} \\ \ddot{r} \end{bmatrix} + \begin{bmatrix} 0 \\ 0 \\ 1 \end{bmatrix} \dot{a}_r \quad (35)$$

$$\begin{bmatrix} \dot{\theta} \\ \dot{\theta} \\ \ddot{\theta} \end{bmatrix} = \begin{bmatrix} 0 & 1 & 0 \\ 0 & 0 & 1 \\ 0 & -\frac{3\dot{r}}{r} & -\frac{3\dot{r}}{r} \end{bmatrix} \begin{bmatrix} \theta \\ \dot{\theta} \\ \ddot{\theta} \end{bmatrix} + \begin{bmatrix} 0 \\ 0 \\ 1 \end{bmatrix} \dot{a}_r \quad (36)$$

It is readily observed that a very high cross coupling of the radial and transverse components exists. The range, range rate and range acceleration are required to adequately compute the angular acceleration. The angular velocity and acceleration is required in computing the range acceleration. All of these quantities are time varying requiring a time varying filter to implement this model.

The cubic term of angle rate in the angle channel is insignificant compared to the other terms and is neglected. The second order model uses the simplifying assumption of constant velocity and constant acceleration. For the full third order model, no simplifying assumptions will be made. This third order model should account for all of the cross coupling between the bearing and angle channels.

A Kalman Filter can be employed to track the target in both range and bearing to implement the time variant third order model. The Kalman Filter will be discussed in the next section.



## V. KALMAN FILTER

Given a system model, where the plant can be modeled by a set of first order differential equations and the output can be measured, a set of state equations can be defined similar to:

$$\dot{X} = A X + B U + W \quad (37)$$

$$Y = C X + V \quad (38)$$

where  $X$  is the state vector

$Y$  is the system output vector

$A, B, C$  and  $D$  are matrices

$U$  is the system input

$W$  is plant disturbances

$V$  is measurement noise

The system can be modeled in discrete time as:

$$X(k+1) = \Phi X(k) + \Gamma U(k) + W(k) \quad (39)$$

$$Y(k) = H X(k) + V(k) \quad (40)$$

A Kalman Filter is the best filter to track the output of a discrete system [Ref. 3]. The Kalman Filter equations are given as:

$$\hat{X}(k|k) = \hat{X}(k|k-1) + G(k) \cdot [Y(k) - \hat{Y}(k|k-1)] \quad (41)$$

$$\hat{X}(k+1|k) = \Phi \cdot \hat{X}(k|k) + \Gamma \cdot U(k) \quad (42)$$

$$\hat{Y}(k+1|k) = H \cdot \hat{X}(k+1|k) \quad (43)$$

where  $\hat{X}(k|k)$  = the state estimate at time  $k$  given information through time  $k$ .

$\hat{X}(k+1|k)$  = the state estimate at time  $k+1$  given information through time  $k$ .

$\hat{Y}(k+1|k)$  = the output estimate at time  $k+1$  given information through time  $k$ .

$G(k)$  = the filter gain at time  $k$ .

For linear, time invariant systems, the  $\Phi$  and  $\Gamma$  matrices are easy to calculate and follow directly from the state space model, where  $\Phi = e^{At}$  and  $\Gamma = \int e^{At} dt$ . For non linear systems, an extended Kalman filter can be used. For the extended Kalman filter, the  $\Phi$  and  $\Gamma$  matrices are linearized about the projected operating point. One method of estimating the linearization is to take the partial derivatives of the non linear state space matrices:

$$\Phi = \left. \frac{A}{X} \right| \begin{matrix} X = X_0 \\ U = U_0 \\ W = 0 \end{matrix} \quad (44)$$

$$\Gamma = \left. \frac{B}{U} \right| \begin{matrix} X = X_0 \\ U = U_0 \\ W = 0 \end{matrix} \quad (45)$$

The gain matrix  $G(k)$  will vary with the parameters of the filter.  $G(k)$  is the weighting factor for the system error. The solution to the filter gain  $G(k)$  requires the solution of Riccati equations:

$$G(k) = P(k|k-1) H^T [H P(k|k-1) H^T + R(k)]^{-1} \quad (46)$$

$$P(k|k-1) = \Phi P(k|k-1) \Phi^T + \delta Q \delta^T \quad (47)$$

$$P(k|k) = P(k|k-1) - G(k) H P(k|k-1) \quad (48)$$

where  $G(k)$  = Kalman Filter gain at time  $k$   
 $P(k|k-1)$  = Covariance of predicted estimate  
 $R(k)$  = measurement covariance matrix,  $E\{VV^T\}$   
 $Q(k)$  = maneuver covariance matrix,  $E\{UU^T\}$   
 $P(k|k)$  = Covariance of filtered estimate  
 $\delta$  = maneuvering weighting matrix

A constant gain matrix can also be used in the Kalman filter. Instead solving the full Riccati equations for each

change of variables, a constant value is used throughout the problem. A constant gain matrix will simplify implementation of the Kalman filter.

One implementation of the third order model, as discussed in the previous section, is to model the system as linear, time invariant, given by the space state model:

$$\begin{bmatrix} \dot{r} \\ \ddot{r} \\ \dddot{r} \\ \dot{\theta} \\ \ddot{\theta} \\ \dddot{\theta} \end{bmatrix} = \begin{bmatrix} 0 & 1 & 0 & 0 & 0 & 0 \\ 0 & 0 & 1 & 0 & 0 & 0 \\ 0 & 0 & 0 & 0 & 0 & 0 \\ 0 & 0 & 0 & 0 & 1 & 0 \\ 0 & 0 & 0 & 0 & 0 & 1 \\ 0 & 0 & 0 & 0 & 0 & 0 \end{bmatrix} \begin{bmatrix} r \\ \dot{r} \\ \ddot{r} \\ \theta \\ \dot{\theta} \\ \ddot{\theta} \end{bmatrix} \quad (49)$$

The Kalman Filter equations for this third order model are:

$$\hat{X}(k|k) = \hat{X}(k|k-1) + G(k) \cdot [Y(k) - \hat{Y}(k|k-1)] \quad (50)$$

$$\hat{X}(k+1|k) = \Phi \cdot \hat{X}(k|k) \quad (51)$$

$$\hat{Y}(k+1|k) = H \cdot \hat{X}(k+1|k) \quad (52)$$

where  $X = \begin{bmatrix} r \\ \dot{r} \\ \ddot{r} \\ \theta \\ \dot{\theta} \\ \ddot{\theta} \end{bmatrix}$  and  $H = \begin{bmatrix} 1 & 0 & 0 & 0 & 0 & 0 \\ 0 & 1 & 0 & 0 & 0 & 0 \\ 0 & 0 & 1 & 0 & 0 & 0 \\ 0 & 0 & 0 & 1 & 0 & 0 \\ 0 & 0 & 0 & 0 & 1 & 0 \\ 0 & 0 & 0 & 0 & 0 & 1 \end{bmatrix}$

Using a Kalman Filter on this third order model is very simple and requires few on line calculations. The gain matrix can be considered either constant or time varying. If time varying gains are used, they can be computed off-line and stored in memory. The Filter then utilizes the precomputed gain schedule and can select a gain depending on

the accuracy of the filter at that time. If a maneuver causes the filter to loose accuracy then a higher gain term can be utilized. If constant gains are used then they must be high enough to compensate for any maneuver the target might make. A high gain matrix will make the missile more responsive to any unwanted noise terms in the system since the missile cannot distinguish a noise input from a target maneuver.

As discussed previously, a Kalman Filter is not required for the range channel. The radar can measure range and range rate directly. Since the actual values of the range channel are not used by any other elements of the guidance subsystem, the radar is able to maintain its own tracking of the target in the center of the range gate, which has no consequences on the rest of the missile guidance. Some noise information can be gained when estimating the range channel with a Kalman Filter. A Kalman Filter is used for the range channel in the simulation of Section VI for completeness of simulation and practical experience.

A second implementation of the third order model is by using the equations obtained through the coriolis equations. The disassociated state space model is given as:

$$\begin{bmatrix} \dot{r} \\ \ddot{r} \\ \ddot{r} \end{bmatrix} = \begin{bmatrix} 0 & 1 & 0 \\ 0 & 0 & 1 \\ 3\dot{\theta}(\dot{\theta}) & 3\dot{\theta}^2 & 0 \end{bmatrix} \begin{bmatrix} r \\ \dot{r} \\ \ddot{r} \end{bmatrix} + \begin{bmatrix} 0 \\ 0 \\ 1 \end{bmatrix} \ddot{a}_r \quad (53)$$

$$\begin{bmatrix} \dot{\theta} \\ \ddot{\theta} \\ \ddot{\theta} \end{bmatrix} = \begin{bmatrix} 0 & 1 & 0 \\ 0 & 0 & 1 \\ 0 & -\frac{3\dot{r}}{r} & -\frac{3\ddot{r}}{r} \end{bmatrix} \begin{bmatrix} \theta \\ \dot{\theta} \\ \ddot{\theta} \end{bmatrix} + \begin{bmatrix} 0 \\ 0 \\ 1 \end{bmatrix} \ddot{a}_r \quad (54)$$

Two possible ways to implement the Kalman filter are to create an extended Kalman filter by linearizing the  $\Phi$  matrix, reducing the time dependence and cross coupling of the range and bearing channel, or keep the cross coupling

components and have the Kalman Filter maintain the values of the time varying  $\Phi$ . If  $\Phi$  is linearized, some of the cross coupling and time dependence lost by linearization can be compensated for by the maneuver covariance matrix  $Q$ . Given the target acceleration probability model, Figure III-1, the  $Q$  matrix can be calculated, as derived in Reference 3, as time varying and relates the cross coupling of the bearing and range channel as:

$$QR = \begin{bmatrix} 0 & 0 & 0 \\ 0 & 0 & 0 \\ 0 & 0 & \sigma^2_a \end{bmatrix} \quad \text{and} \quad QS = \begin{bmatrix} 0 & 0 & 0 \\ 0 & 0 & 0 \\ 0 & 0 & \frac{\sigma^2_a}{R} \end{bmatrix} \quad (55)$$

where  $\sigma^2_a$  = acceleration variance

As discussed in the reference the  $Q(3,3)$  element can be increased to make the missile gain matrix put more weight on any target acceleration elements.

If the  $\Phi$  matrix is maintained as time varying and nonlinear then the  $Q$  matrix can be constant. The constant  $Q$  matrix can be calculated as:

$$Q = K I \quad (56)$$

where  $K$  = matrix gain

$I$  = identity matrix

Since the reference deals extensively with the time invariant  $\Phi$  and the time varying  $Q$  matrix, this thesis will deal with the time varying  $\Phi$  and constant  $Q$ .

If Figure III-4 is used to define the maneuver probability then a non-zero mean is established. The  $Q$  matrix maintains the same properties just discussed with a different calculation for  $\sigma^2_a$ . The non-zero mean can be implemented by increasing  $Q(3,3)$ , increasing the weighting matrix  $\delta$ , or by not assuming the  $U(k)$  term is zero.

Kalman filter equations for this third order model are:

$$\hat{X}(k|k) = \hat{X}(k|k-1) + G(k) \cdot [Y(k) - \hat{Y}(k|k-1)] \quad (57)$$

$$\hat{X}(k+1|k) = \Phi \cdot \hat{X}(k|k) + \Gamma \cdot \hat{U}(k) \quad (58)$$

$$\hat{Y}(k+1|k) = H \cdot \hat{X}(k+1|k) \quad (59)$$

$$P(k|k-1) = \Phi \cdot P(k|k-1) \cdot \Phi^T + \delta \cdot Q \cdot \delta^T \quad (60)$$

$$G(k) = P(k|k-1) \cdot H^T \cdot [H \cdot P(k|k-1) \cdot H^T + R(k)]^{-1} \quad (61)$$

$$P(k|k) = P(k|k-1) - G(k) \cdot H \cdot P(k|k-1) \quad (62)$$

## VI. SIMULATION

To aid in the efforts of simulation, the Dynamic Simulation Language (DSL) was used to integrate the equations of motion for the target and missiles, as well as the antenna angle channel. Two programs were written and are listed in Appendix B. The first program is the time varying third order model. The second program is the time invariant third order model and the second order model.

The output of the simulation is a set of graphs to compare the three missile models and their effectiveness in tracking the target.

The Kalman Filter is implemented in a Fortran subroutine at the end of the DSL main program. The basic filter equations used were described in the previous section.

### A. ASSUMPTIONS

The following assumptions are made to simplify the implementation of the Kalman Filter and determine the effects of the time varying third order model.

- "Ideal" missile autopilot.
- Inertial cartesian reference frame for angle measurements.
- Final portion of intercept only.
- Cross coupled effects of missile motion on antenna stabilization system disregarded.
- Missile initialized to collision course.
- Missile constant speed of 1500 kts (Mach 1.5) or 2500 ft/sec.
- Target constant speed of 400 kts (Mach .75) or 667 ft/sec.
- Target lateral acceleration applied perpendicular to target velocity vector.
- Angle of Attack not accounted for in velocity vector calculations.
- Missile located at the center of the cartesian reference frame.

- Target located to the right of the origin of the reference frame.
- No noise.

#### B. INITIALIZATION

The user is asked at the beginning of the program to establish the geometry by giving the target initial position, heading, speed and acceleration. The target heading is oriented relative to a vertical line, parallel to the Y axis, defining the North or 000 heading. The initial missile headings are calculated for constant velocity, zero acceleration collision course with a time to go estimate of range/misssile velocity. Antenna parameters are initialized to initial line of sight and zero angular rate.

#### C. SECOND ORDER MODEL

The second order model is implemented using a proportional navigation constant of four and two s-plane poles at  $s=-10$ . This gives the equation for angular acceleration as:

$$\dot{\beta} = -20 \dot{\beta} + 100 (\text{LOS} - \beta) \quad (63)$$

where  $\dot{\beta}$  = the antenna angular acceleration  
 $\dot{\beta}$  = the antenna angle rate  
 $\beta$  = the antenna angle position  
 LOS = the actual angle to the target

#### D. THIRD ORDER MODEL

The Kalman filter is used to implement the third order model. The DSL main program calls the Kalman Filter subroutine at a sampling time of  $h=0.01$  seconds. The Kalman Filter is executed, then control is passed back to the DSL program. A proportional navigation constant of four is used as discussed in Section II.



### 1. Time Invariant, Constant Phi Model

The discrete time invariant third order model divided into two Kalman filters for range and bearing is:

$$\text{RNG}(k+1 | k) = \text{RPHI} \cdot \text{RNG}(k | k) \quad (64)$$

$$\text{RNG}(k | k) = \text{RNG}(k | k-1) + \text{GR}(k) \cdot \begin{bmatrix} \text{DELR} \end{bmatrix} \quad (65)$$

$$\text{S}(k+1 | k) = \text{SPHI} \cdot \text{S}(k | k) \quad (66)$$

$$\text{S}(k | k) = \text{S}(k | k-1) + \text{GS}(k) \cdot \begin{bmatrix} \text{SDEL} \end{bmatrix} \quad (67)$$

where

$$\text{RPHI} = \text{SPHI} = \begin{bmatrix} 1 & .01 & .0005 \\ 0 & 1 & .01 \\ 0 & 0 & 1 \end{bmatrix}$$

$$\text{DELR} = \begin{bmatrix} \text{RM} - \text{RKP1} \\ \text{RDM} - \text{RDKP1} \end{bmatrix}$$

$$\text{SDEL} = \begin{bmatrix} \text{LOS} - \text{SKP1} \\ \text{LOSD} - \text{SDKP1} \end{bmatrix}$$

Using Matlab functions of Aker and Place, with eigenvalues of 0.5, 0.5 and 0.5 constant gain matrices were obtained for range and bearing, given by GR and GS, respectively.

$$\text{GR} = \begin{bmatrix} 0.5 & 0.0125 \\ 0.0025 & 1.0 \\ 0.125 & 24.9 \end{bmatrix}$$

$$\text{GS} = \begin{bmatrix} 1.5 \\ 12.5 \\ 1250.0 \end{bmatrix}$$

### 2. Time Variant, Variable Phi Model

The discrete, time variant third order model divided into two Kalman filters for range and bearing is:

$$\text{RNG}(k | k) = \text{RNG}(k | k-1) + \text{GR}(k) \cdot \begin{bmatrix} \text{DELR} \end{bmatrix} \quad (68)$$

$$\text{RNG}(k+1 | k) = \text{RPHI} \cdot \text{RNG}(k | k) \quad (69)$$

$$PR(k|k-1) = RPHI \cdot PR(k|k-1) \cdot RPHI^T + QR \quad (70)$$

$$GR(k) = PR(k|k-1) \cdot HR^T \left[ HR \cdot PR(k|k-1) \cdot HR^T + RMCOV(k) \right]^{-1} \quad (71)$$

$$PR(k|k) = PR(k|k-1) - GR(k) \cdot HR \cdot PR(k|k-1) \quad (72)$$

$$S(k|k) = S(k|k-1) + GS(k) \cdot [SDEL] \quad (73)$$

$$S(k+1|k) = SPHI \cdot S(k|k) \quad (74)$$

$$PS(k|k-1) = SPHI \cdot PS(k|k-1) \cdot SPHI^T + QS \quad (75)$$

$$GS(k) = PS(k|k-1) \cdot HS^T \cdot [HS \cdot PS(k|k-1) \cdot HS^T + RSCOV(k)]^{-1} \quad (76)$$

$$PS(k|k) = PS(k|k-1) - GS(k) \cdot HS \cdot PS(k|k-1) \quad (77)$$

The time variant model uses two different  $\Phi$  matrices, one for range and the other for bearing. Two other matrices must be specified for each filter, the initial error covariance matrix and the target maneuvering covariance matrix. The two  $\Phi$  matrices are:

$$RPHI = \begin{bmatrix} 1 & .01 & .00005 \\ .00005 \cdot A & 1 + .00005 \cdot B & .01 \\ .01 \cdot A & .01 \cdot B & 1 + .00005 \cdot B \end{bmatrix} \quad (78)$$

$$SPHI = \begin{bmatrix} 1 & .01 & .00005 \\ 0 & 1 + .00005 \cdot C & .01 + .00005 \cdot D \\ 0 & .01 \cdot C + .00005 \cdot D & 1 + .01 \cdot D + .00005 \cdot (C+D) \end{bmatrix} \quad (79)$$

where  $A = -3\dot{\theta} \ (\dot{\theta}')$

$$B = -3\dot{\theta}^2$$

$$C = -3\dot{r}/r$$

$$D = -3\ddot{r}/r$$

The initial error covariance matrices are given as:

$$PR(0|0) = \begin{bmatrix} 500 & 0 & 0 \\ 0 & 500 & 0 \\ 0 & 0 & 500 \end{bmatrix}$$

$$PS(^0 | _0) = \begin{bmatrix} 1e4 & 0 & 0 \\ 0 & 1e4 & 0 \\ 0 & 0 & 1e4 \end{bmatrix}$$

The maneuvering covariance matrix can either be time varying or constant as discussed previously. The maneuvering covariance matrix accounts for the capabilities of the target as discussed in Section IV. Reference 3 gives the derivation for the time varying matrix for a constant  $\Phi$  matrix. The  $\Phi$  matrix also accounts for any time variance of the target model so the maneuvering covariance matrix can be constant. A constant matrix is assumed since  $\Phi$  is time varying. The maneuvering covariance matrix (QR AND QS) are given as:

$$QR = \begin{bmatrix} 500 & 0 & 0 \\ 0 & 500 & 0 \\ 0 & 0 & 500 \end{bmatrix}$$

$$QS = \begin{bmatrix} .01 & 0 & 0 \\ 0 & .01 & 0 \\ 0 & 0 & .01 \end{bmatrix}$$

The simulation calculates the range model then the bearing model. The results of each filter are used in the other filter to calculate the  $\Phi$  values.

## E. RESULTS

Similar simulations of the ideal missile cases, Section II, were used to evaluate the missiles. The simulation consists of head-on, tail and beam aspects with 0G, 3G and 6G target acceleration. The results of the computer simulation is shown in graph form in Figure VI-1 through VI-31. The computer program listings are contained in Appendix B.

### 1. Gains

Gain comparison plots are given in Figure VI-1 through Figure VI-4. The resultant gains from the time variant, varying Phi third order missile are the same for each scenario.

In predicting  $R(k+1|k)$ , the varying Phi model weights the range error by .5 and the range rate error by 0. The constant Phi model uses weights of .5 and .0125, approximately the same, Figure VI-1.

Gains for predicting  $RD(k+1|k)$ , for varying Phi, are .001 and .6 while those of the constant Phi are .0025 and 1.0, Figure VI-2. Little emphasis is placed on the range error, because the radar is measuring range rate, with a higher weighting factor.

In predicting  $RDD(k+1|k)$ , small gains are calculated by the varying Phi while the constant Phi model places a high emphasis on range rate error. The noise of the system will be noticed more in the prediction of  $RDD(k+1|k)$  than the other parameters, because of the higher weighting factor.

Bearing channel gains give unusual curves for the varying Phi model, Figure VI-4. There is little weight placed on non-observed parameters as in SG2 and SG3, during most of the intercept, except in the initial stage and final stage. The gains are highest during the critical stages of the intercept. SG1 is a constant 1.0 giving equal weighting to the current estimate and the error. The constant Phi model has higher gains giving more weight to any errors.

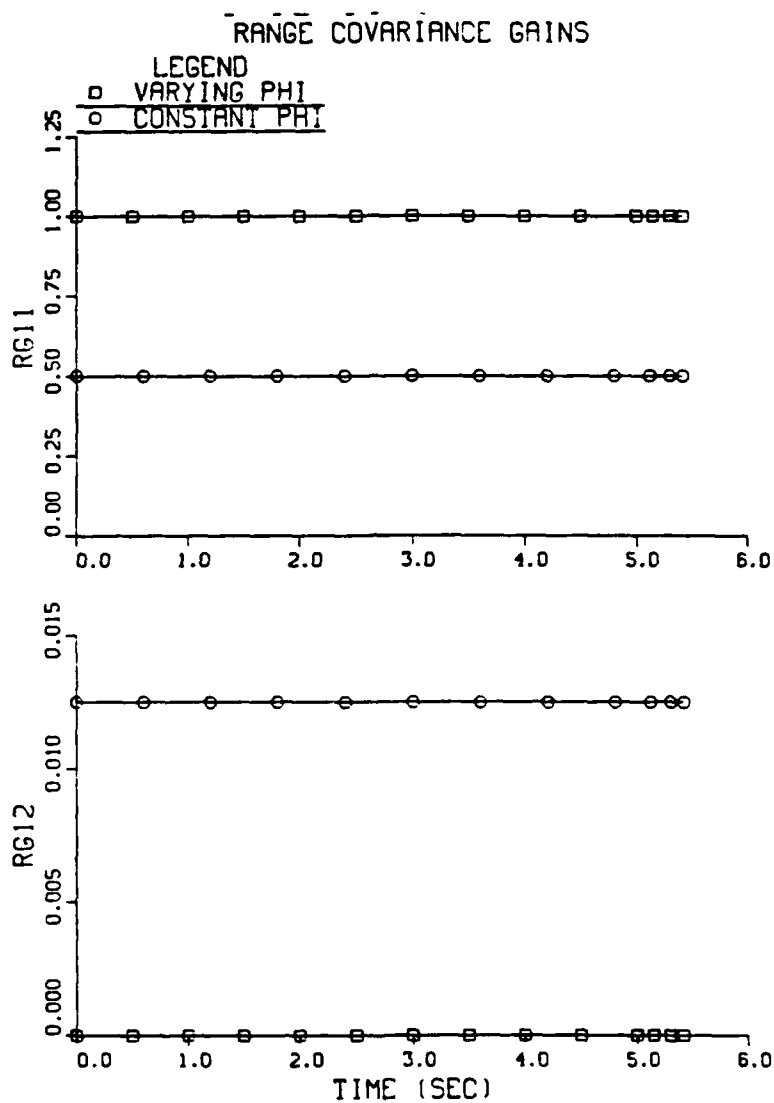


Figure VI-1 Range Covariance Gains RG11 and RG12

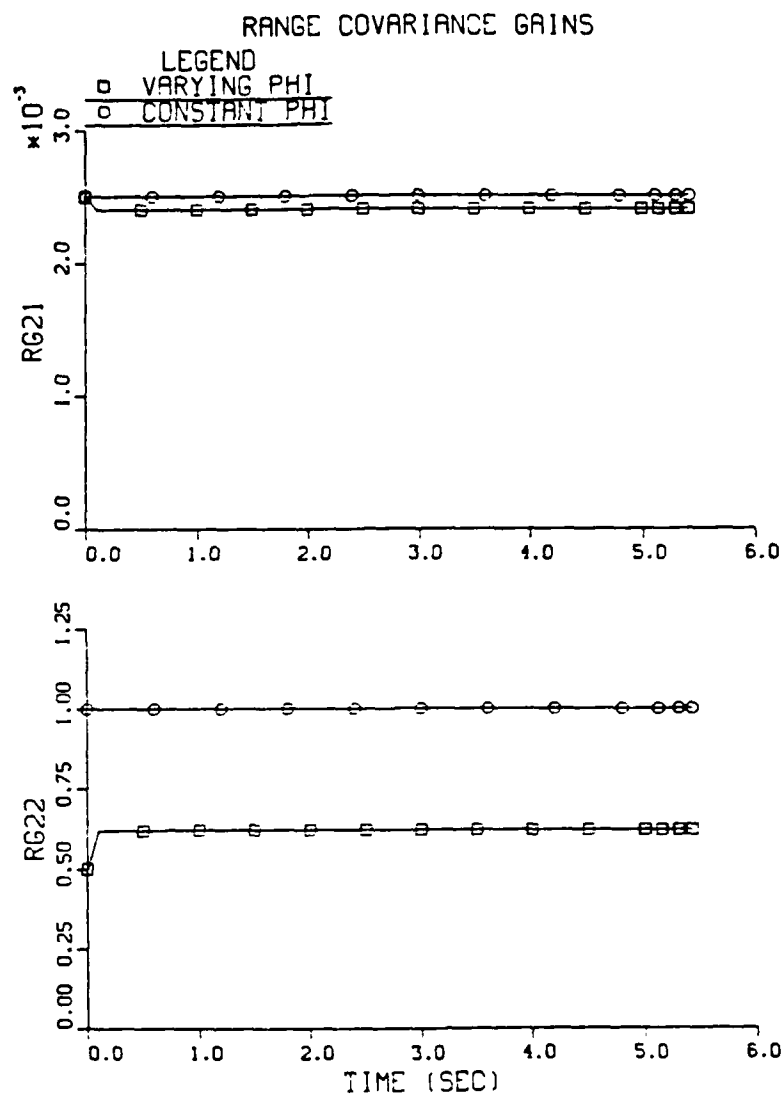


Figure VI-2 Range Covariance Gains RG21 and RG22

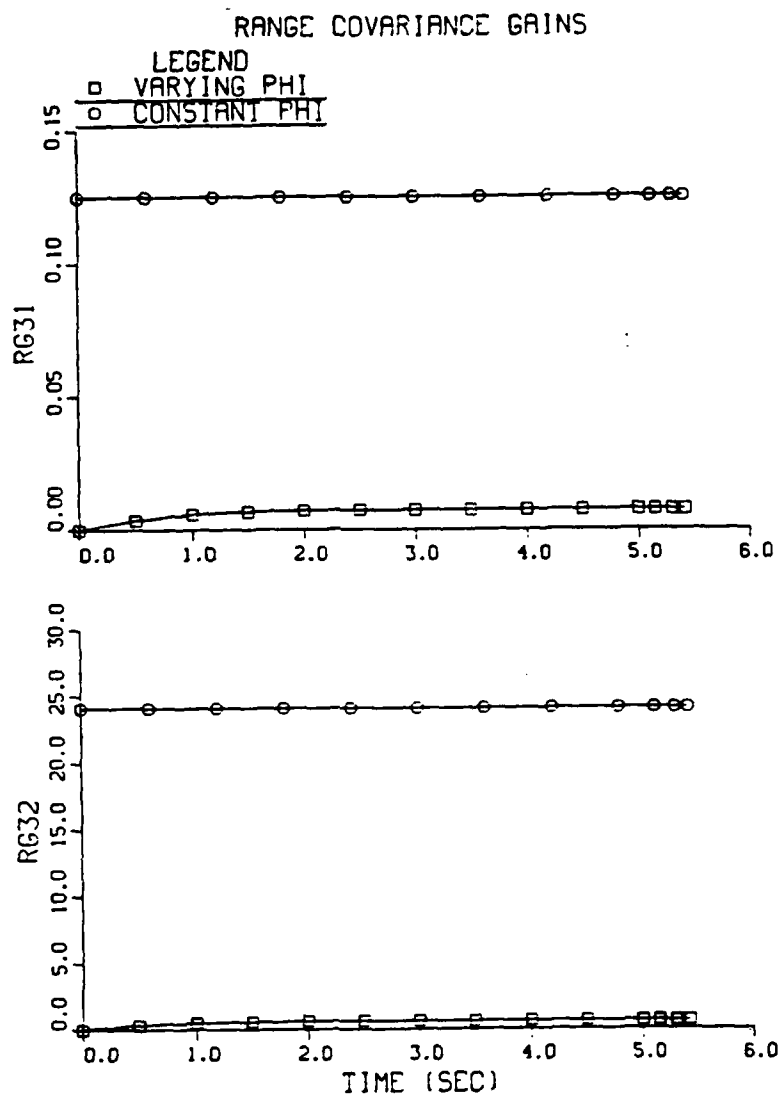


Figure VI-3 Range Covariance Gains RG31 and RG32

# BEAM OG TGT BEARING COVARIANCE GAINS

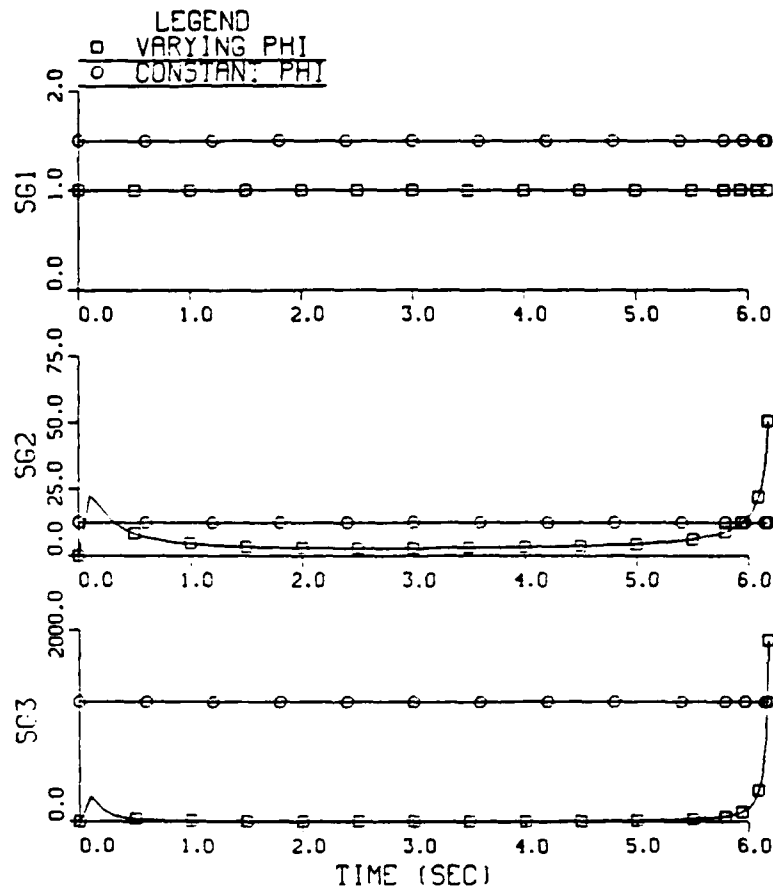


Figure VI-4 Bearing Covariance Gains SG1, SG2 and SG3



# HEAD-ON OG TGT POSITION PLOT

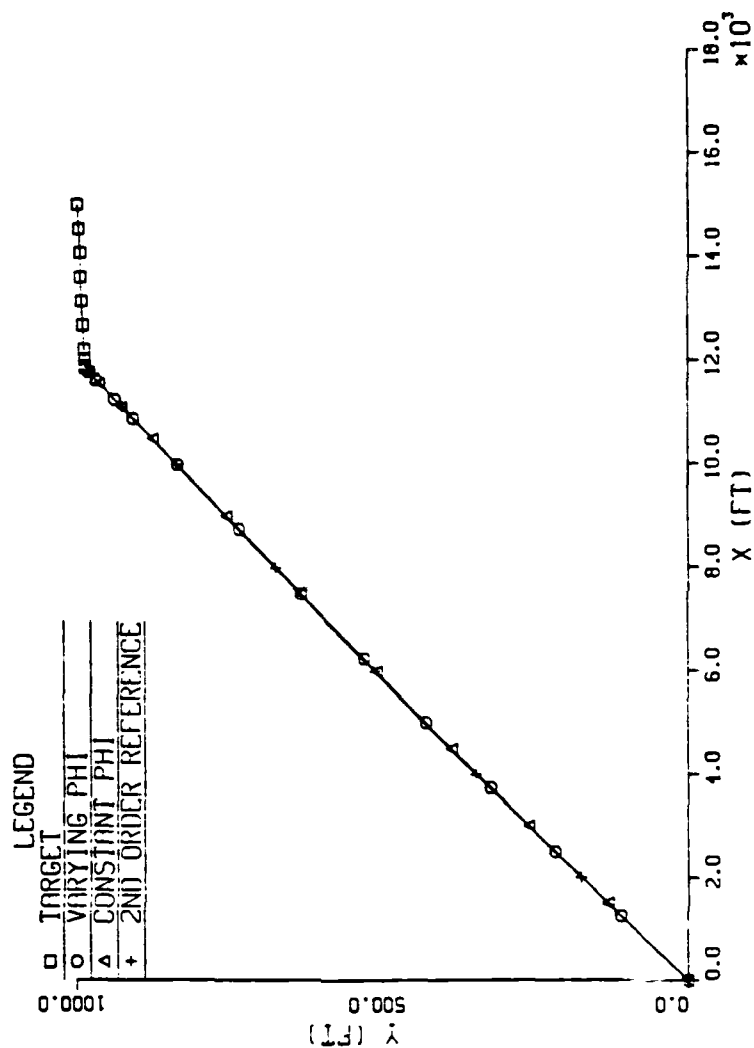


Figure VI-5 Position Plot for Head-on  
Aspect No Target Turn

# HEAD-ON OG TGT LINE OF SIGHT

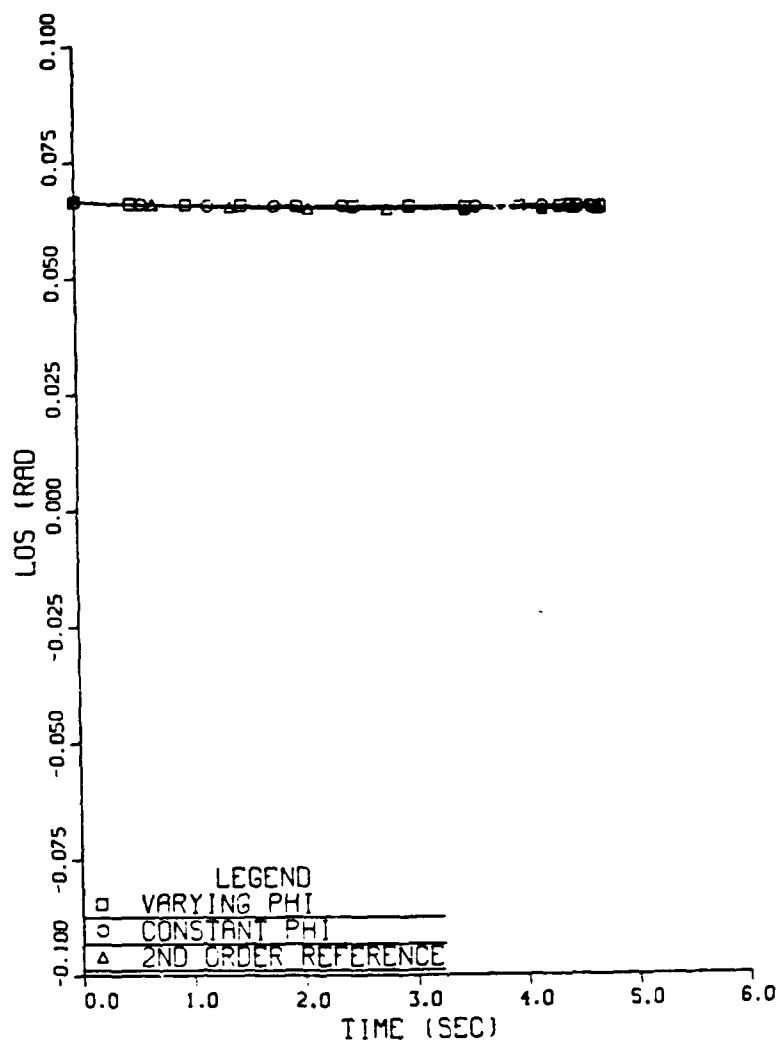


Figure VI-6 Line of Sight Angle Plot for Head-on  
Aspect No Target Turn

# HEAD-ON OG TGT MISSILE COMMANDED ACCELERATION

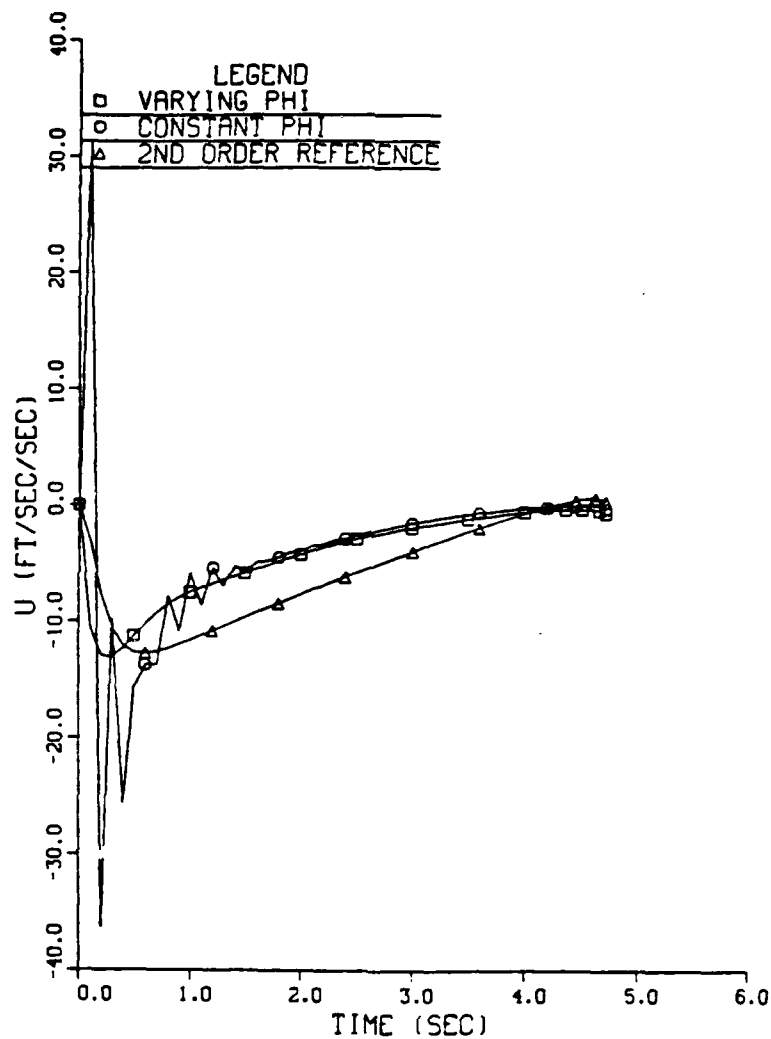


Figure VI-7 Missile Commanded Acceleration Plot for Head-on Aspect No Target Turn

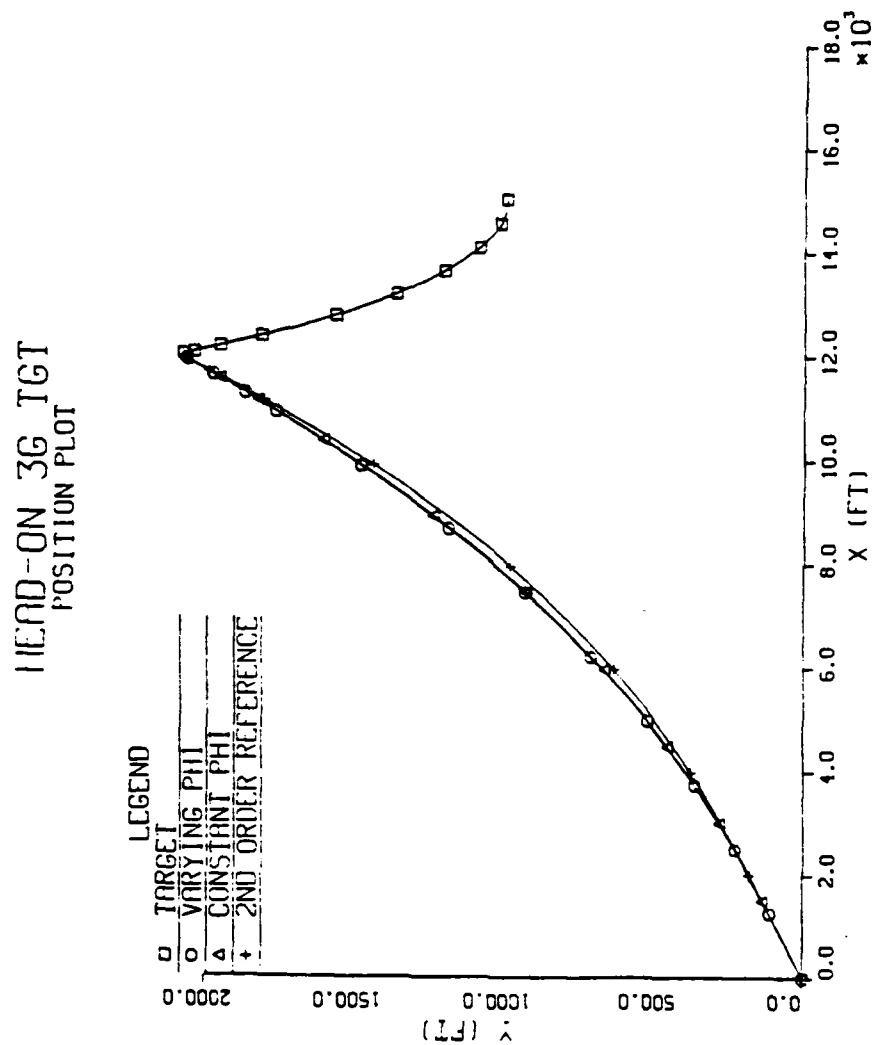


Figure VI-8 Position Plot for Head-on  
Aspect 3G Target Turn

# HEAD-ON 3G TGT LINE OF SIGHT

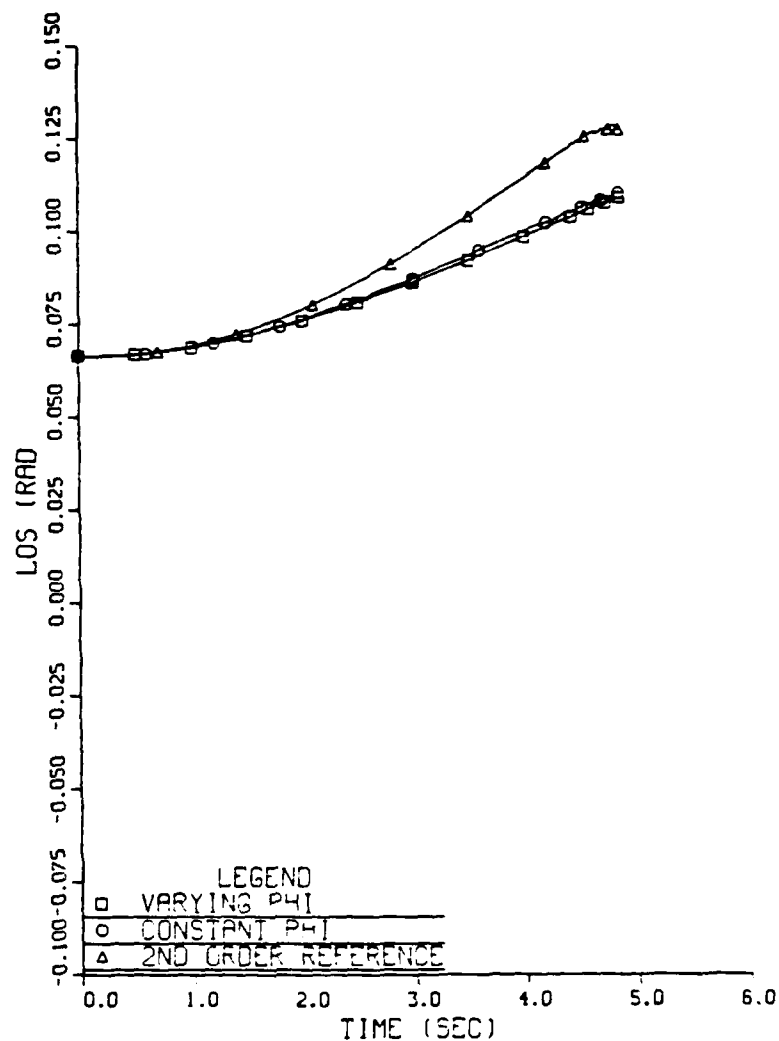


Figure VI-9 Line of Sight Angle Plot for Head-on Aspect 3G Target Turn

# HEAD-ON 3G TGT MISSILE COMMANDED ACCELERATION

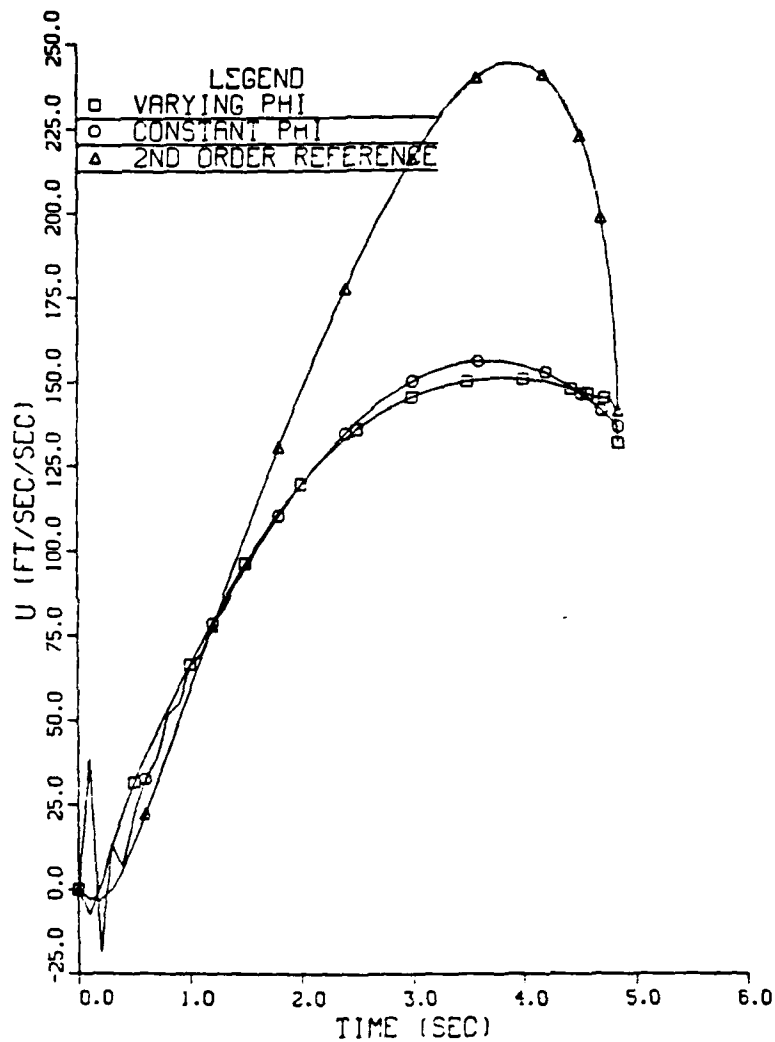


Figure VI-10 Missile Commanded Acceleration Plot for Head-on Aspect 3G Target Turn

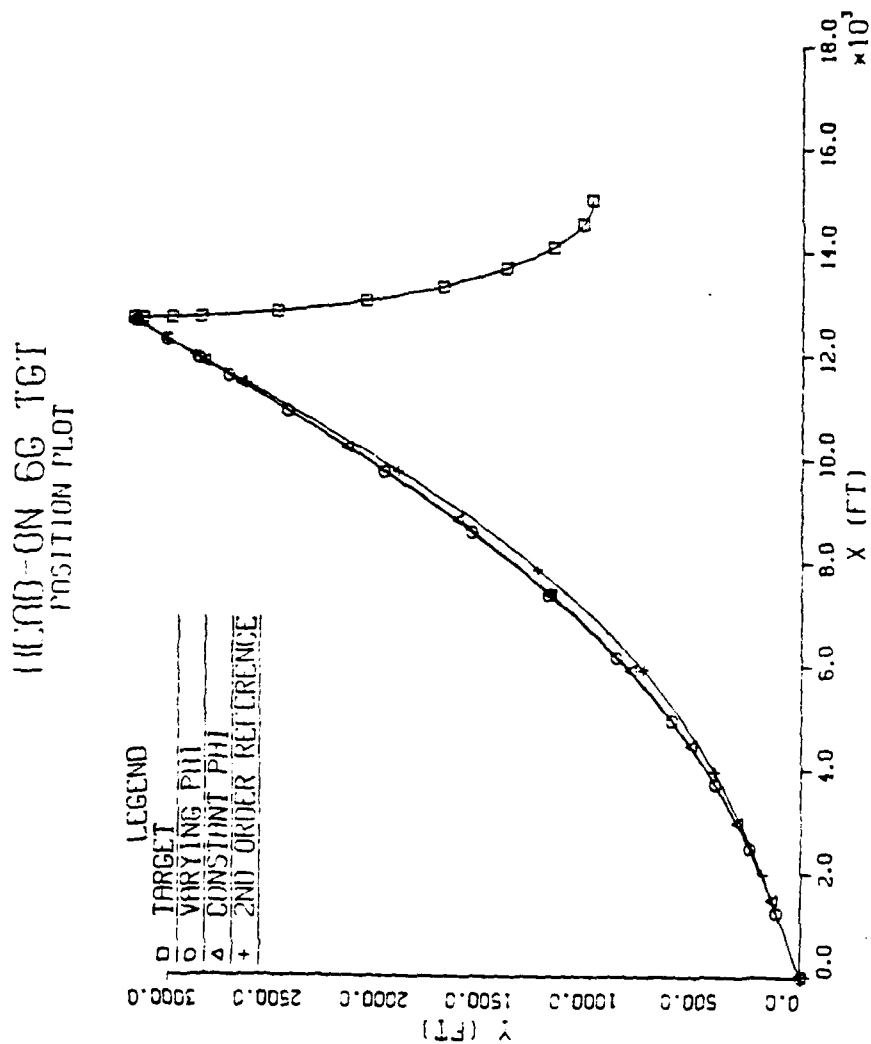


Figure VI-11 Position Plot for Head-on Aspect 6G Target Turn

# HEAD-ON 6G TGT LINE OF SIGHT

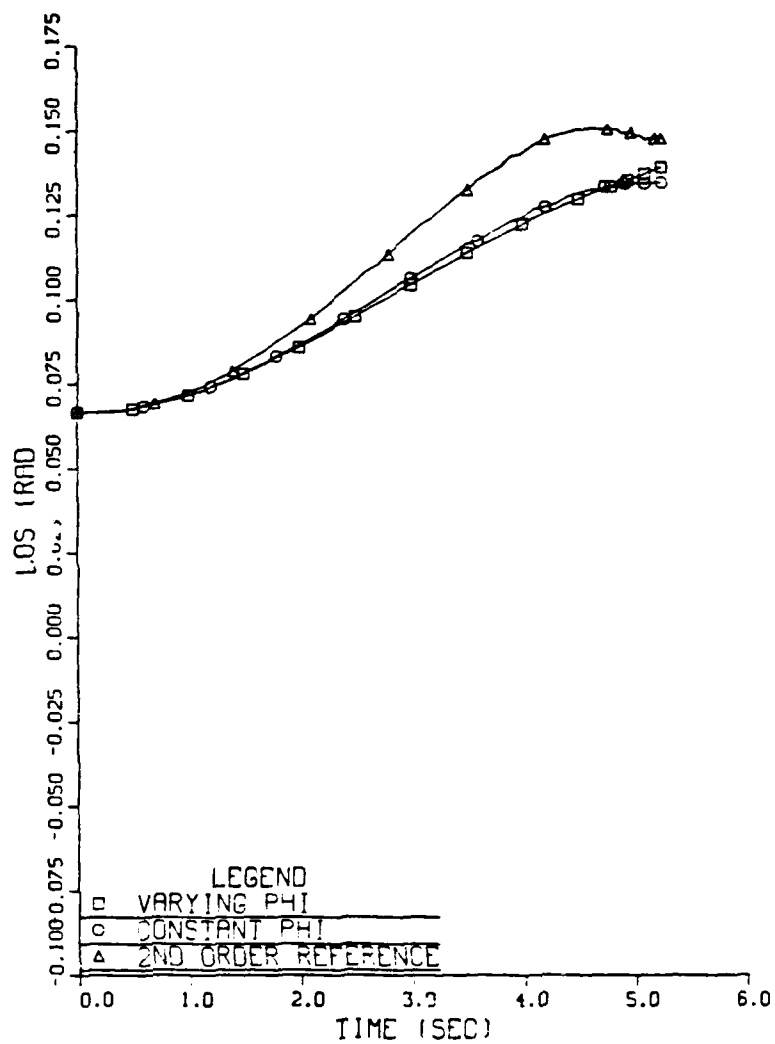


Figure VI-12 Line of Sight Plot for Head-on  
Aspect 6G Target Turn



# HEAD-ON 6G TGT MISSILE COMMANDED ACCELERATION

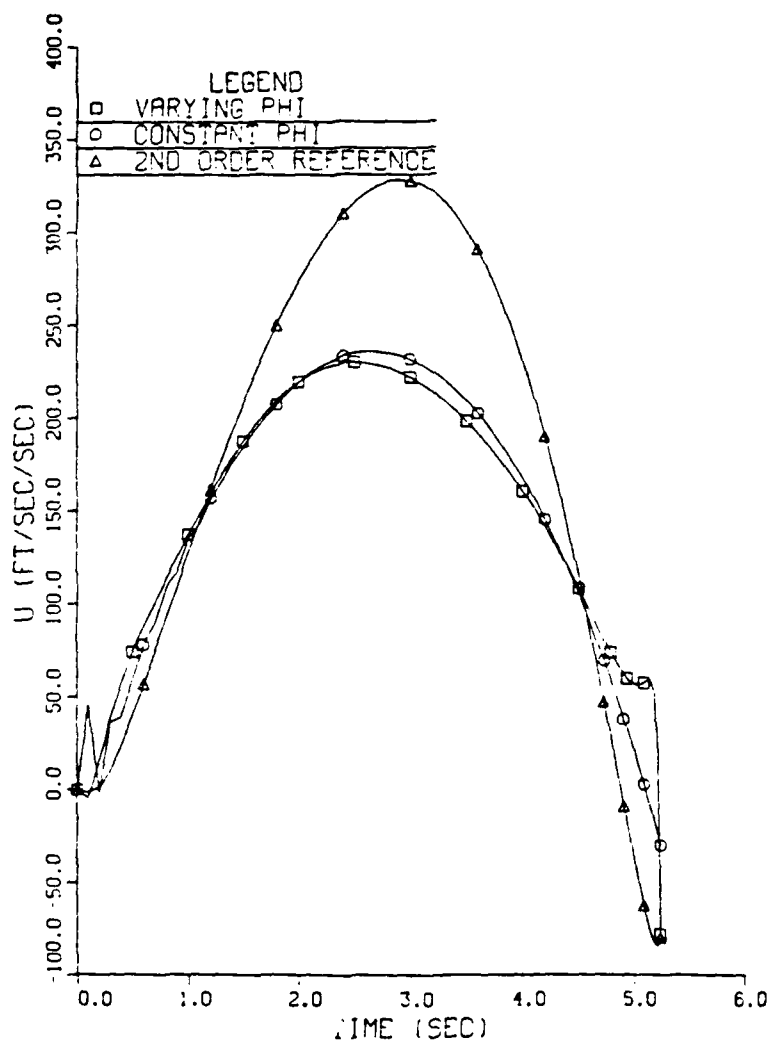
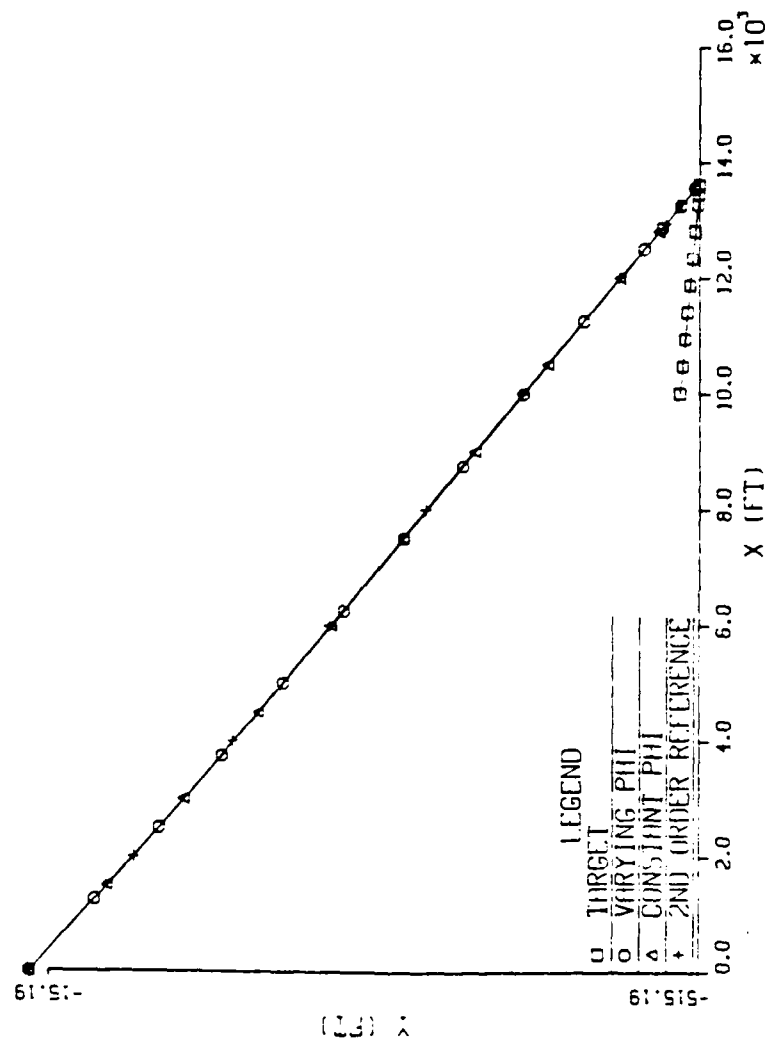


Figure VI-13 Missile Commanded Acceleration Plot for Head-on Aspect 3G Target Turn



85

# TAIL OG TGT LINE OF SIGHT

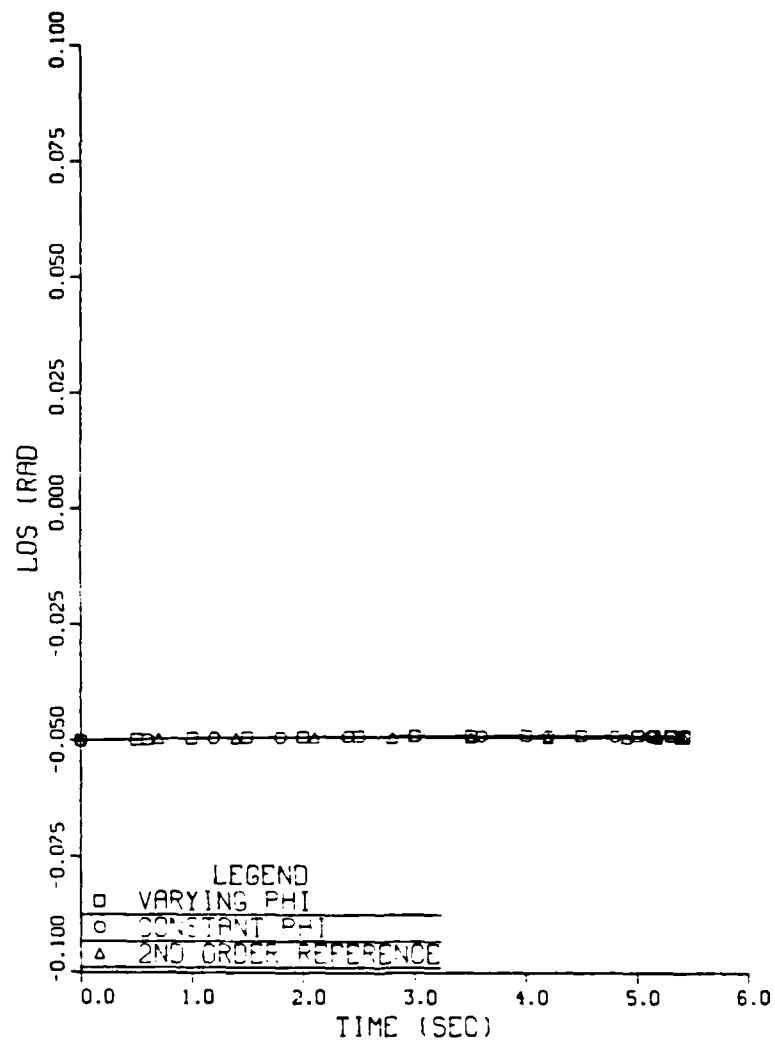


Figure VI-15 Line of Sight Angle Plot for Tail Aspect No Target Turn

# TAIL OG TGT MISSILE COMMANDED ACCELERATION

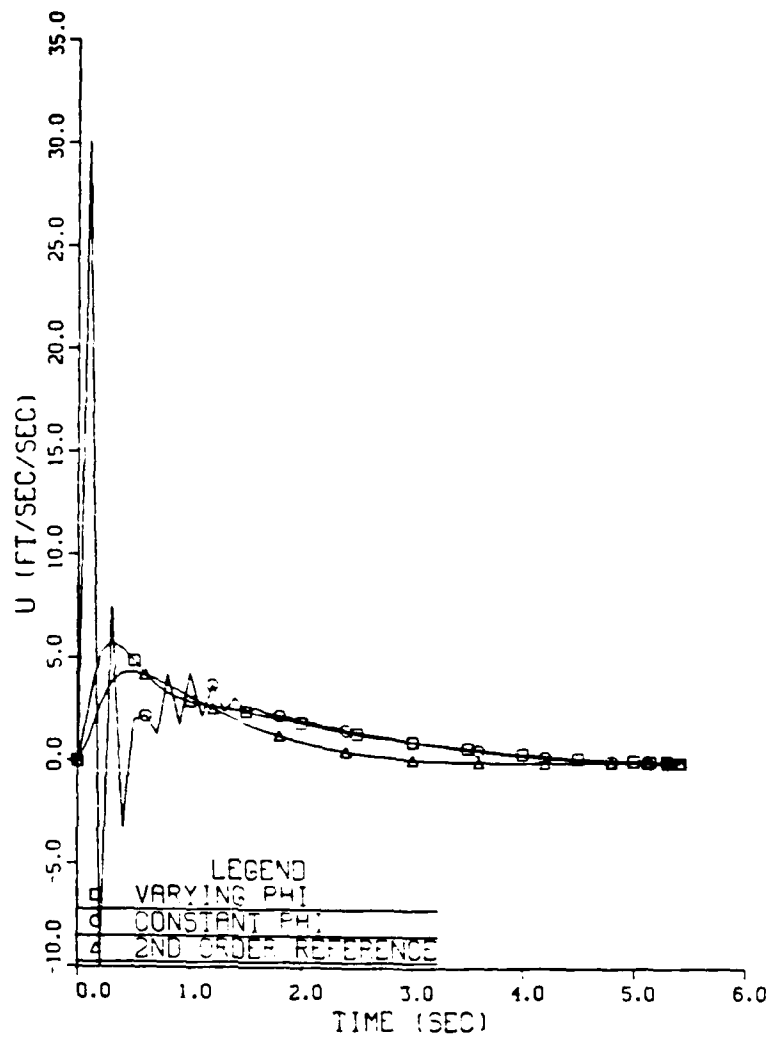


Figure VI-16 Missile Commanded Acceleration Plot for Tail Aspect No Target Turn

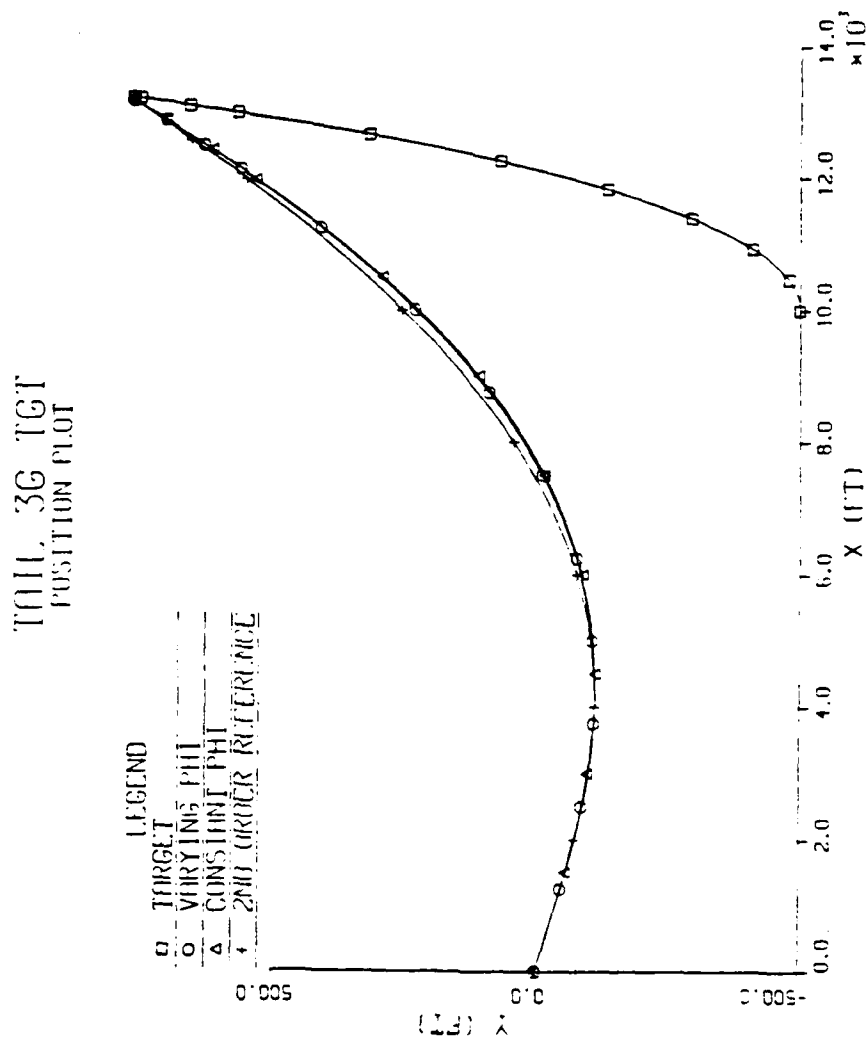


Figure VI-17 Position Plot for Tail Aspect 3G Target Turn

# TAIL 3G TGT LINE OF SIGHT

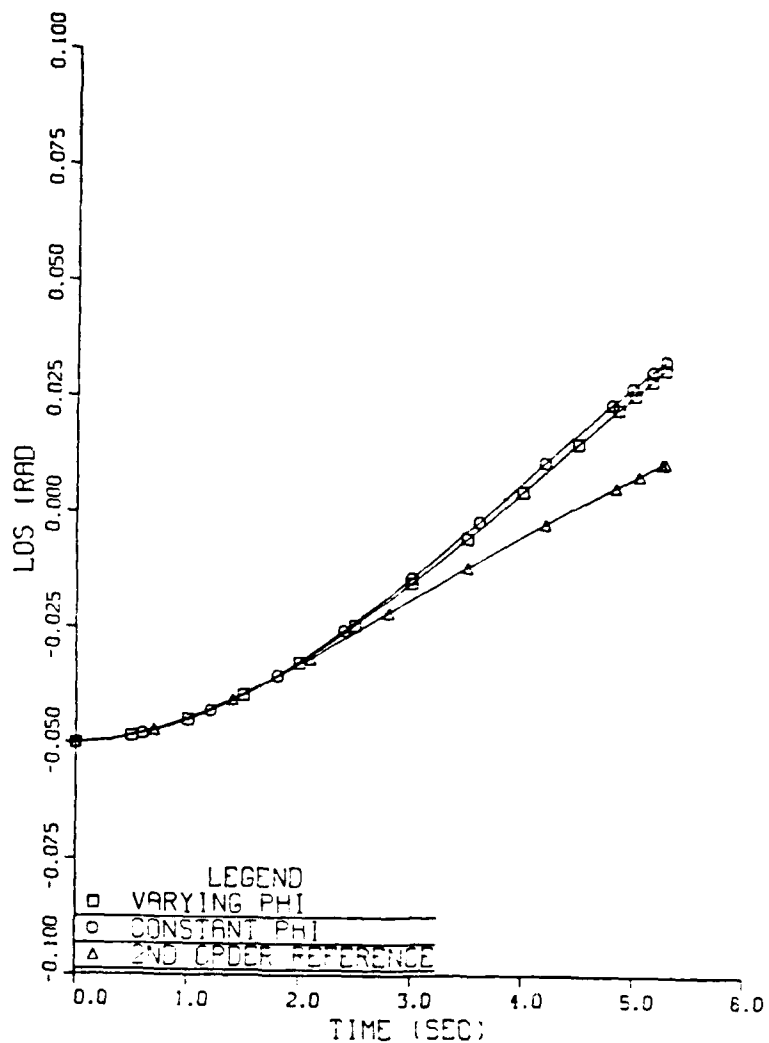


Figure VI-18 Line of Sight Angle Plot for Tail Aspect 3G Target Turn

# TAIL 3G TGT MISSILE COMMANDED ACCELERATION

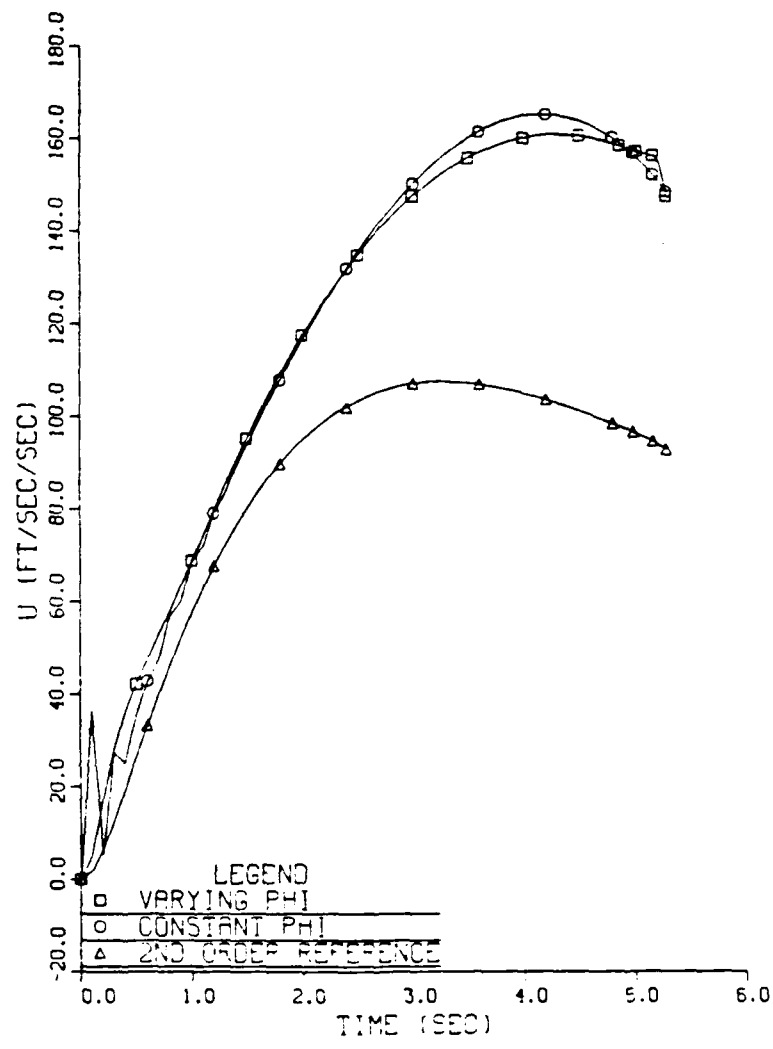


Figure VI-19 Missile Commanded Acceleration Plot for Tail Aspect 3G Target Turn

# TAIL 6G TGT POSITION PLOT

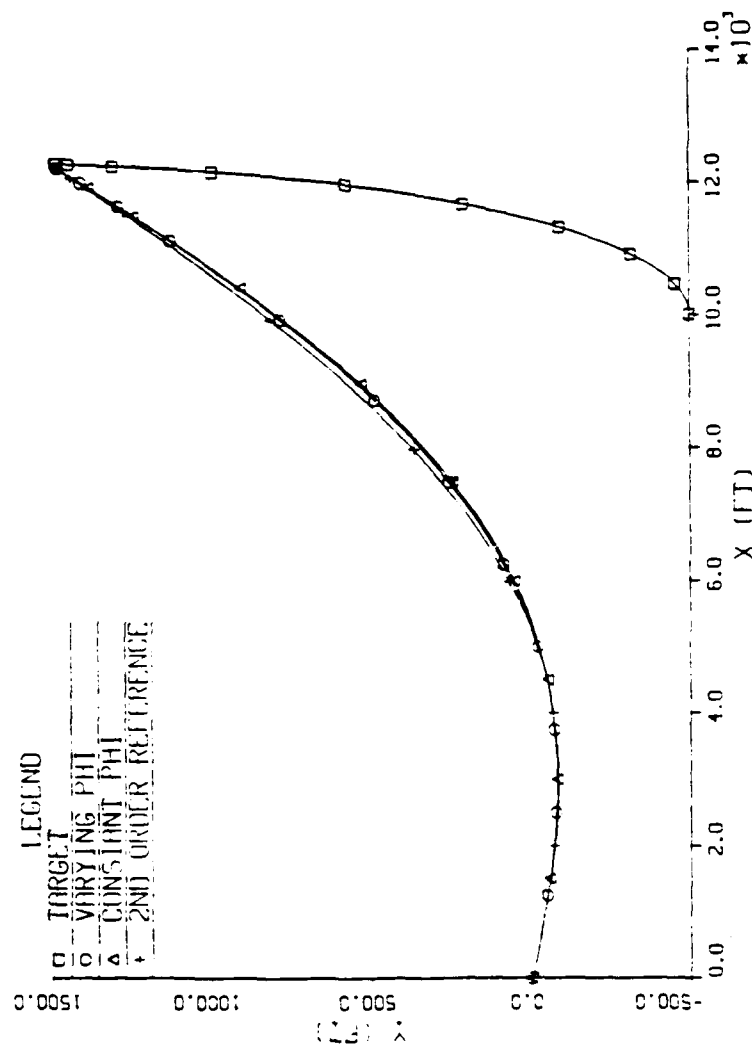


Figure VI-20 Position Plot for Tail Aspect 6G Target Turn



# TAIL 6G TGT LINE OF SIGHT

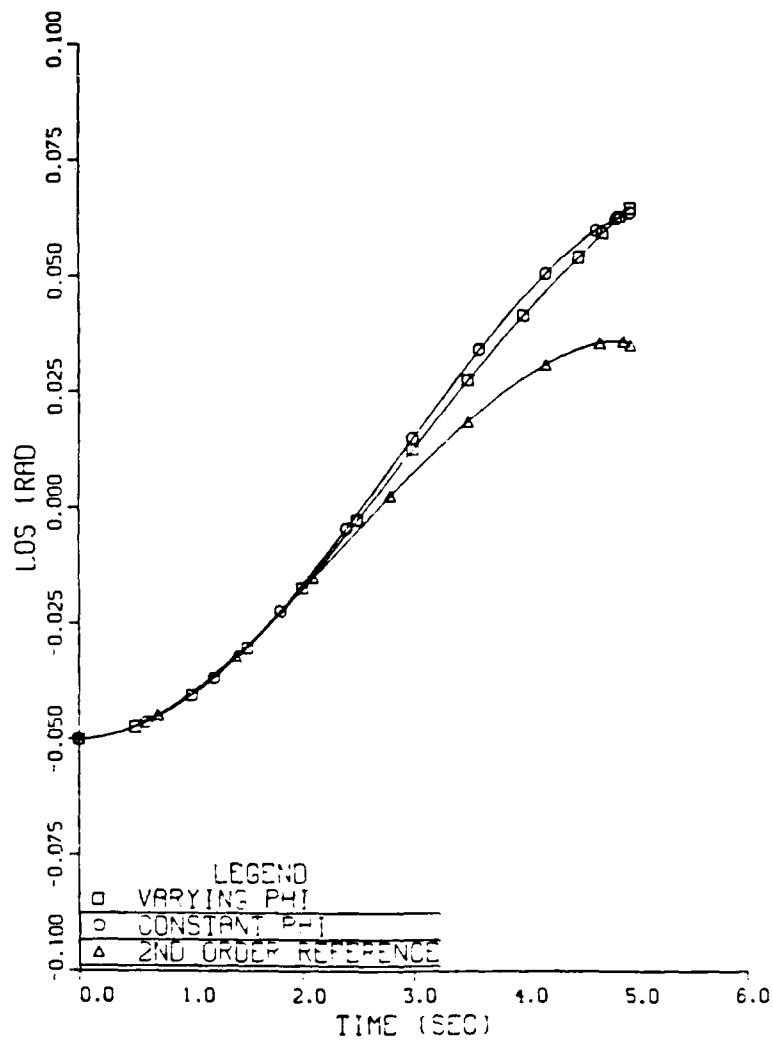


Figure VI-21 Line of Sight Angle Plot for Tail Aspect 6G Target Turn

# TAIL 6G TGT MISSILE COMMANDED ACCELERATION

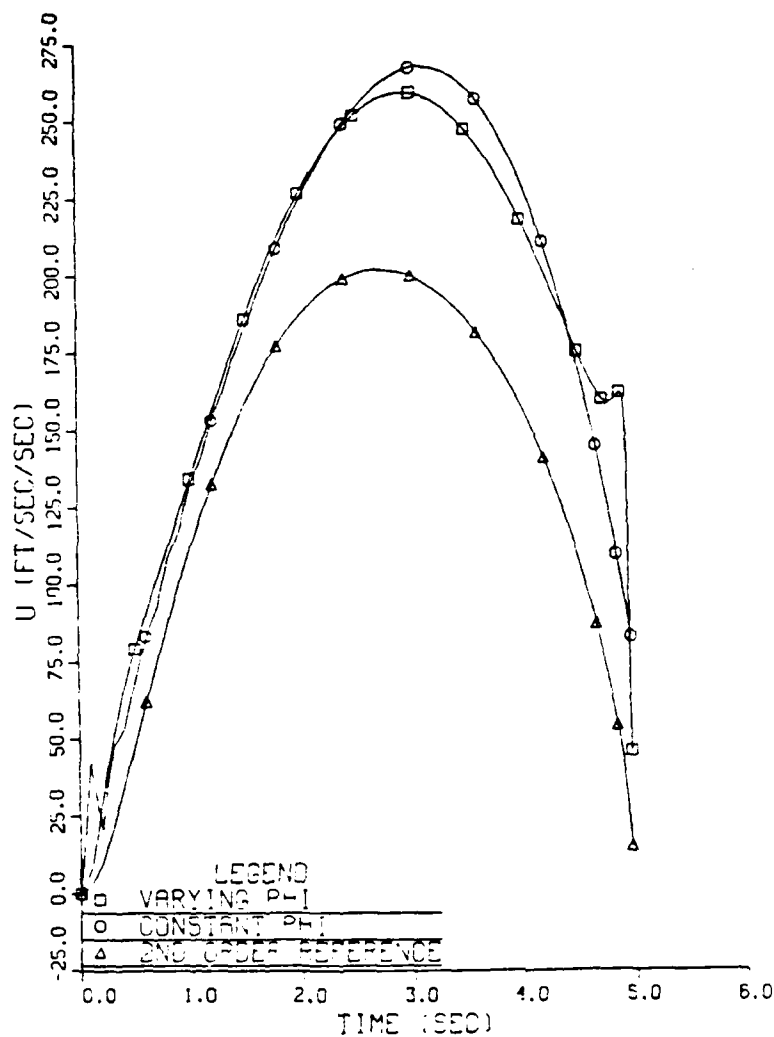


Figure VI-22 Missile Commanded Acceleration Plot for Tail Aspect 6G Target Turn

# BLOM OG TGT POSITION PLOT

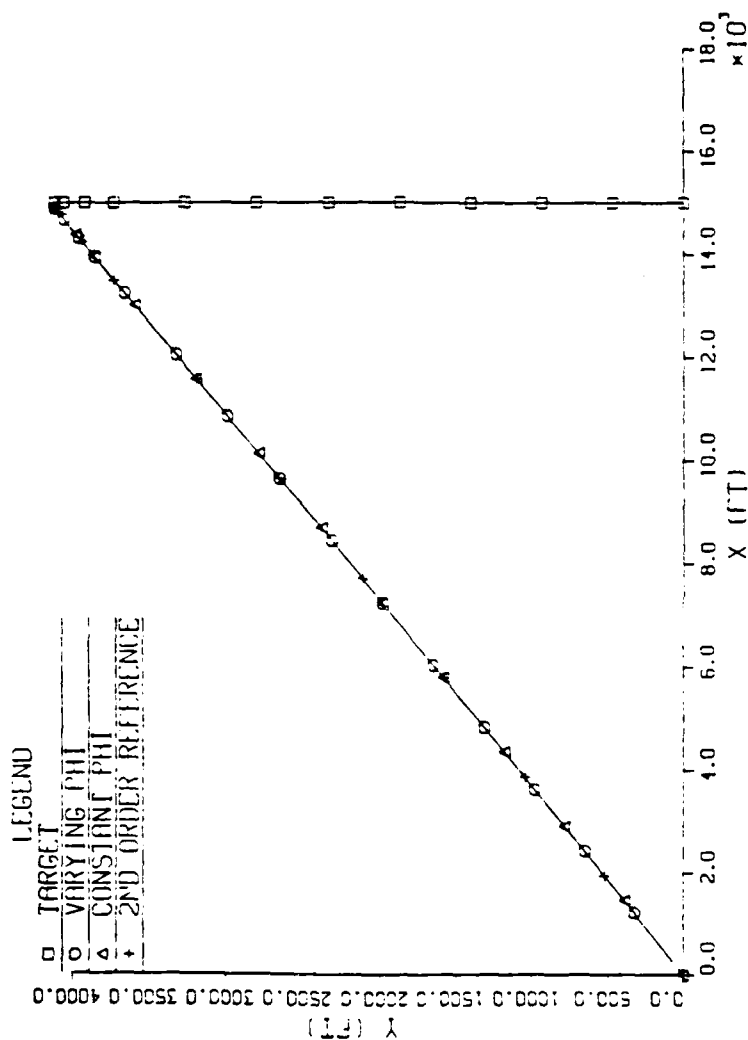


Figure VI-23 Position Plot for Beam  
Aspect No Target Turn

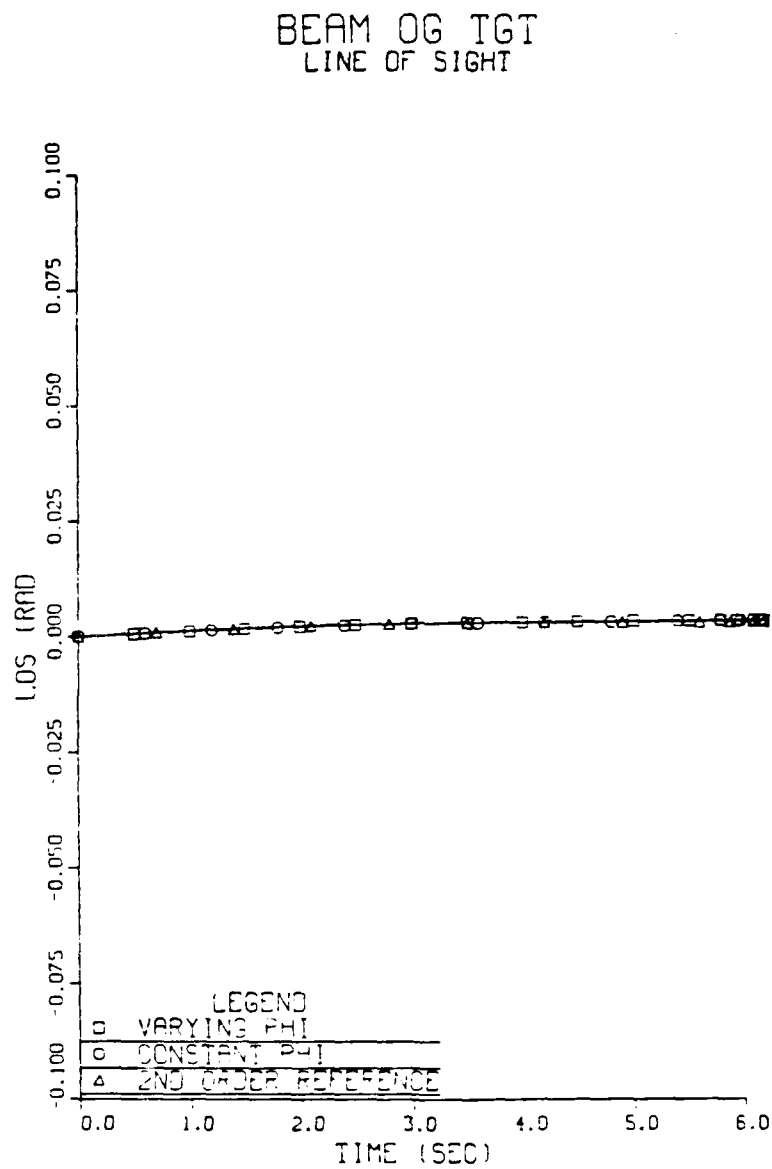


Figure VI-24 Line of Sight Angle Plot for Beam Aspect No Target Turn

# BEAM OG TGT MISSILE COMMANDED ACCELERATION

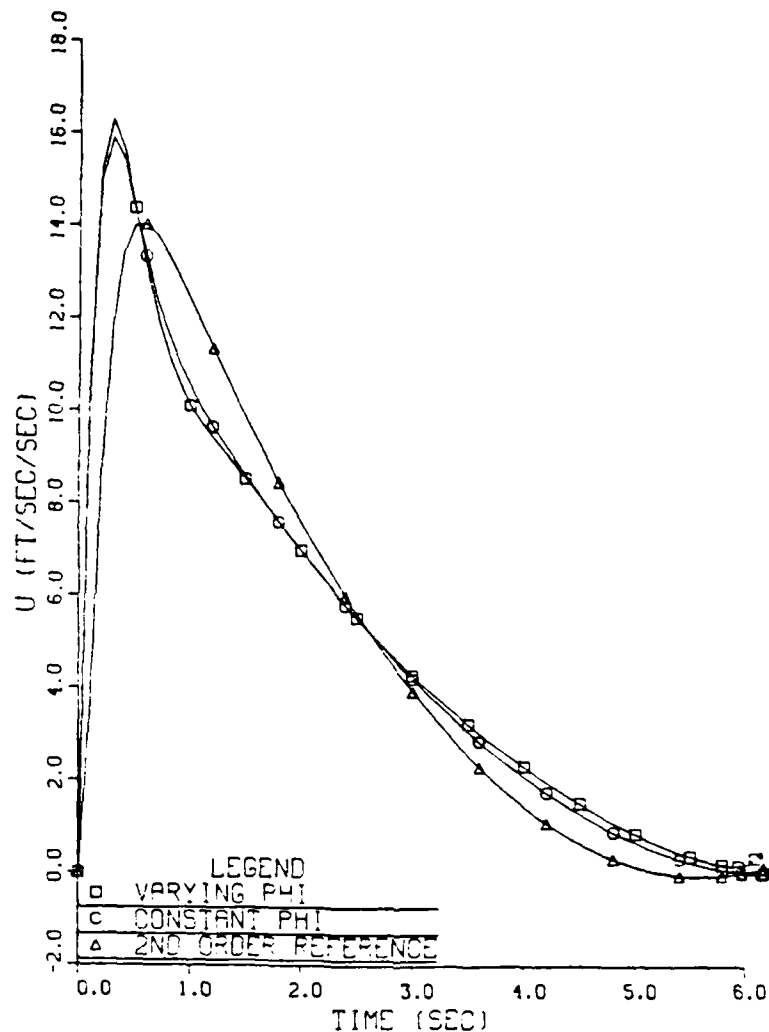


Figure VI-25 Missile Commanded Acceleration Plot for Beam Aspect No Target Turn

BEAM 3G TGT  
POSITION PLOT

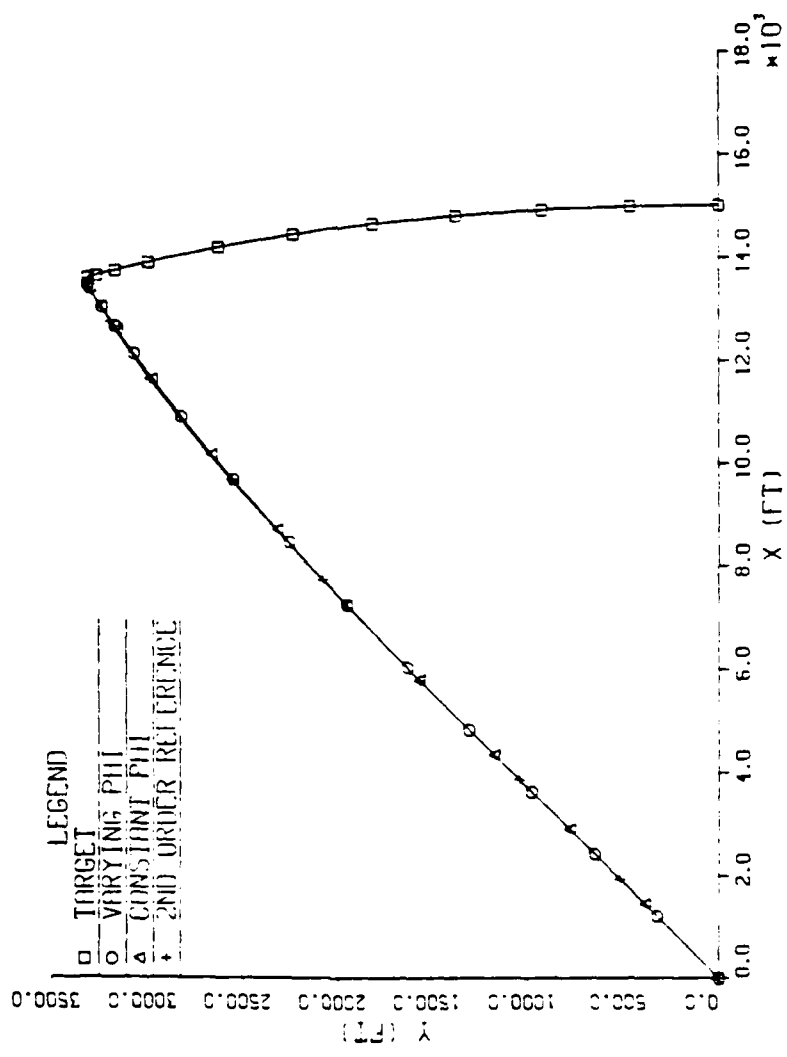


Figure VI-26 Position Plot for Beam  
Aspect 3G Target Turn

# BEAM 3G TGT LINE OF SIGHT

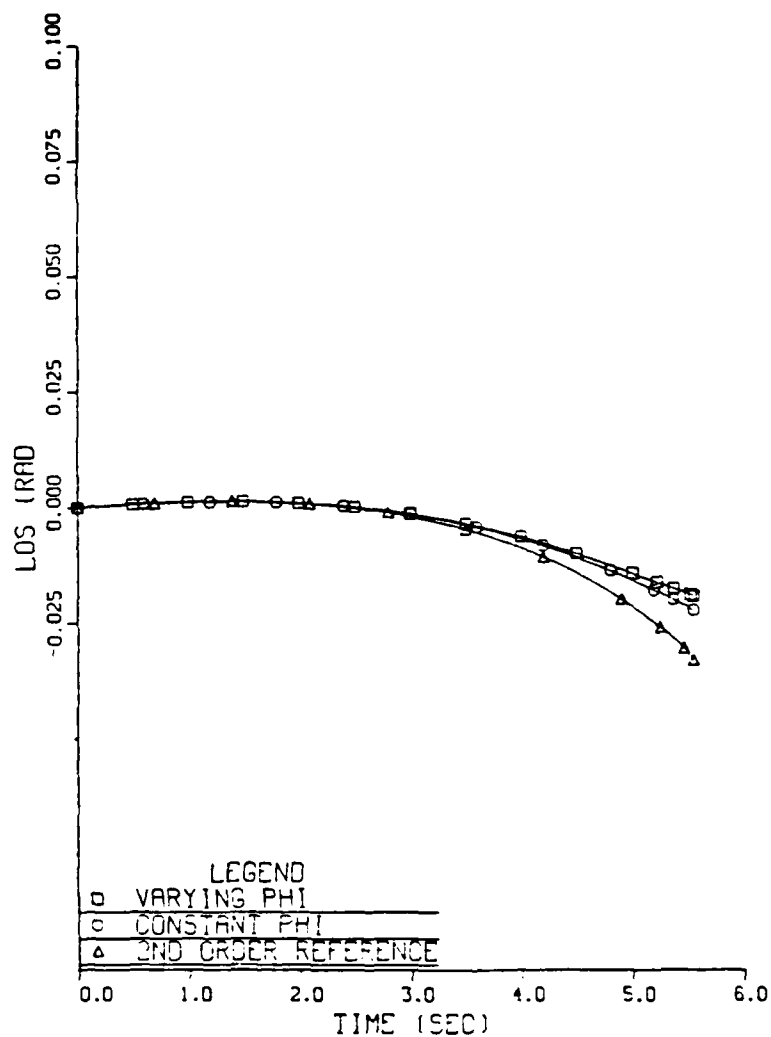


Figure VI-27 Line of Sight Angle Plot for Beam Aspect 3G Target Turn

# BEAM 3G TGT MISSILE COMMANDED ACCELERATION

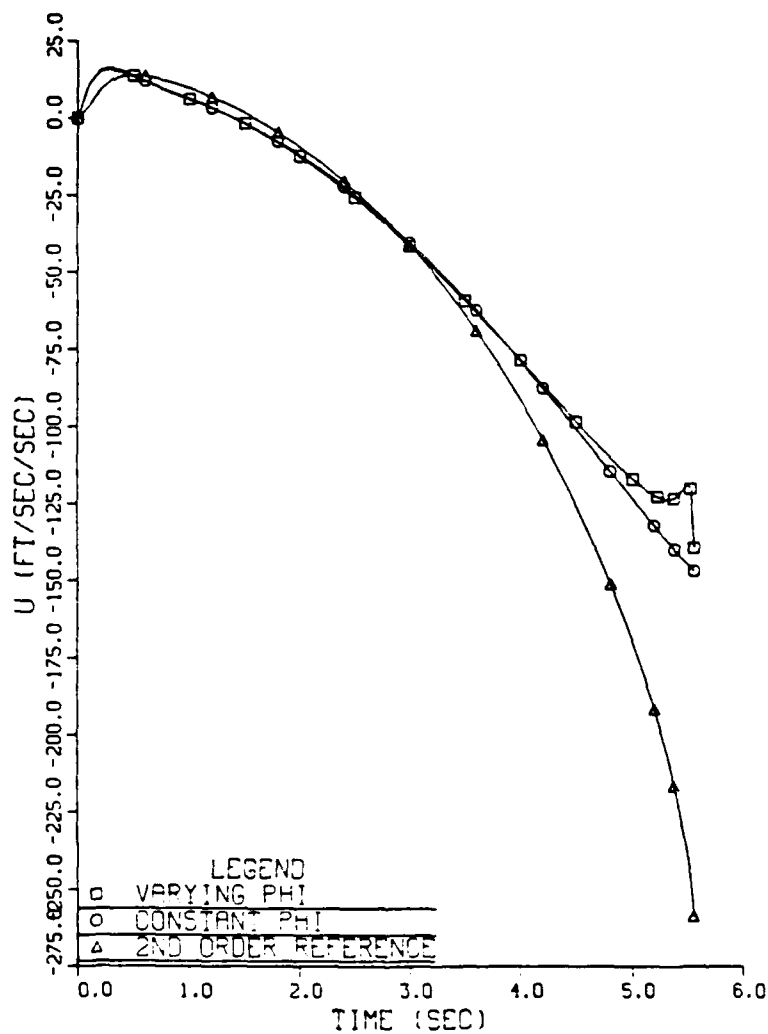


Figure VI-28 Missile Commanded Acceleration Plot for Beam Aspect 3G Target Turn



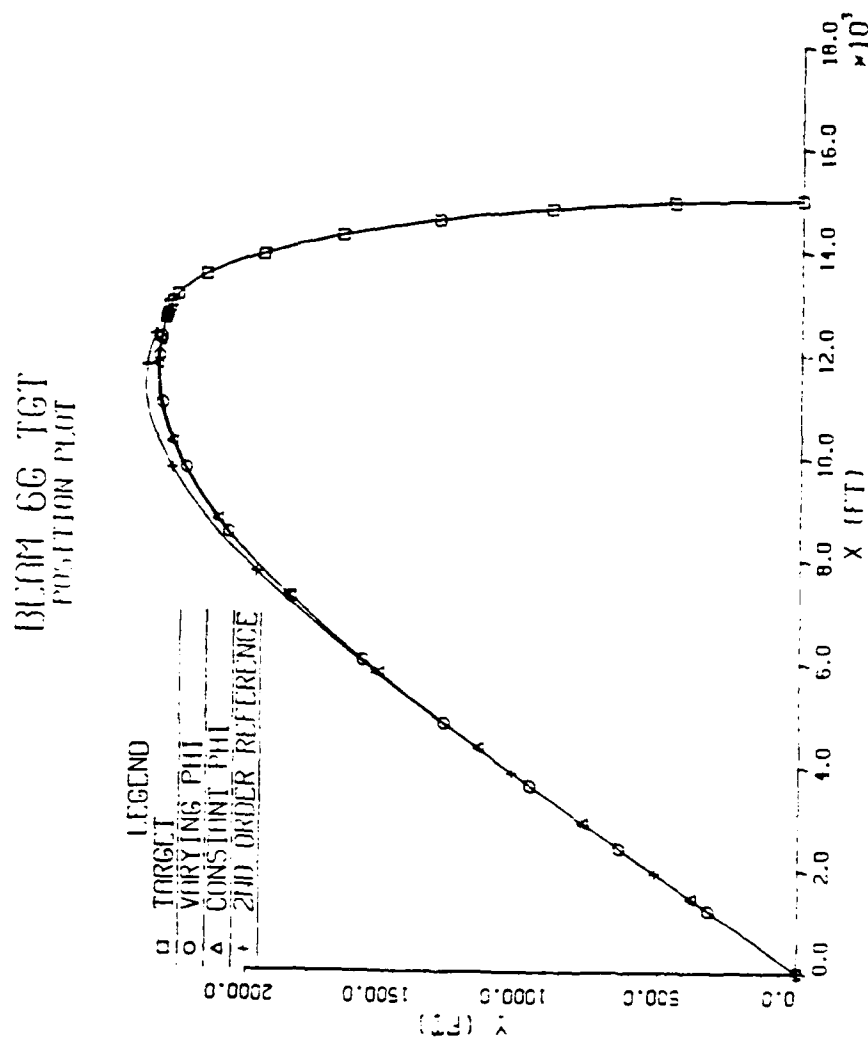


Figure VI-29 Position Plot for Beam  
Aspect 6G Target Turn

# BEAM 6G TGT LINE OF SIGHT

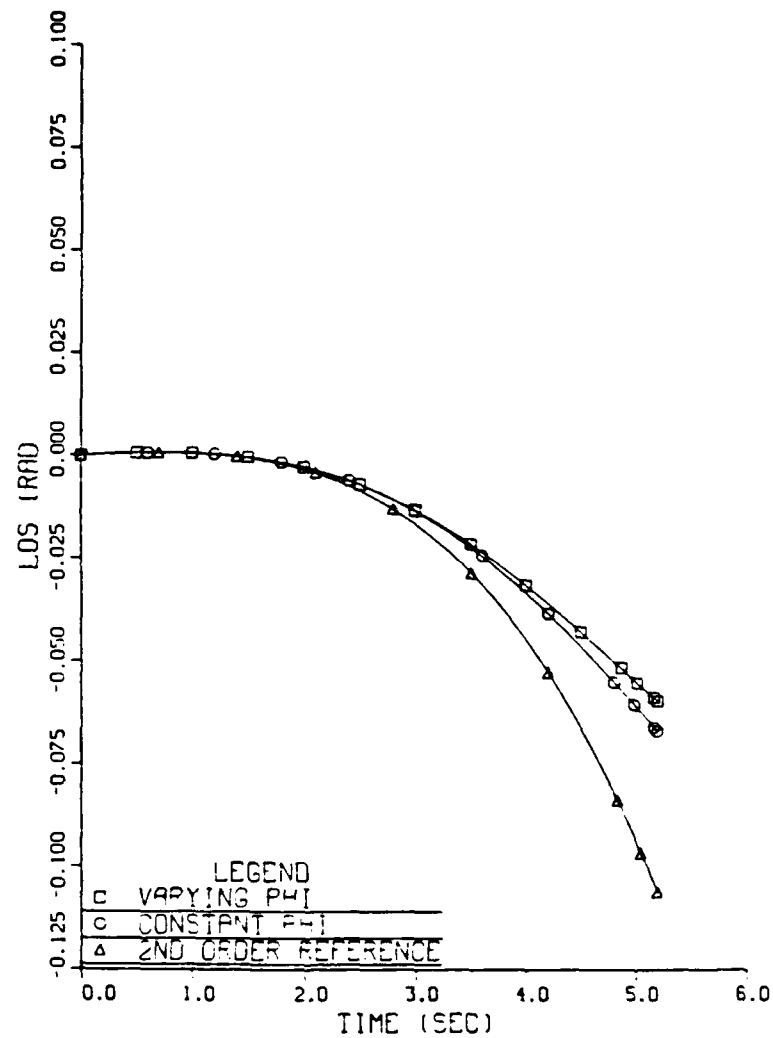


Figure VI-30 Line of Sight Angle Plot for Beam Aspect 6G Target Turn

# BEAM 6G TGT MISSILE COMMANDED ACCELERATION

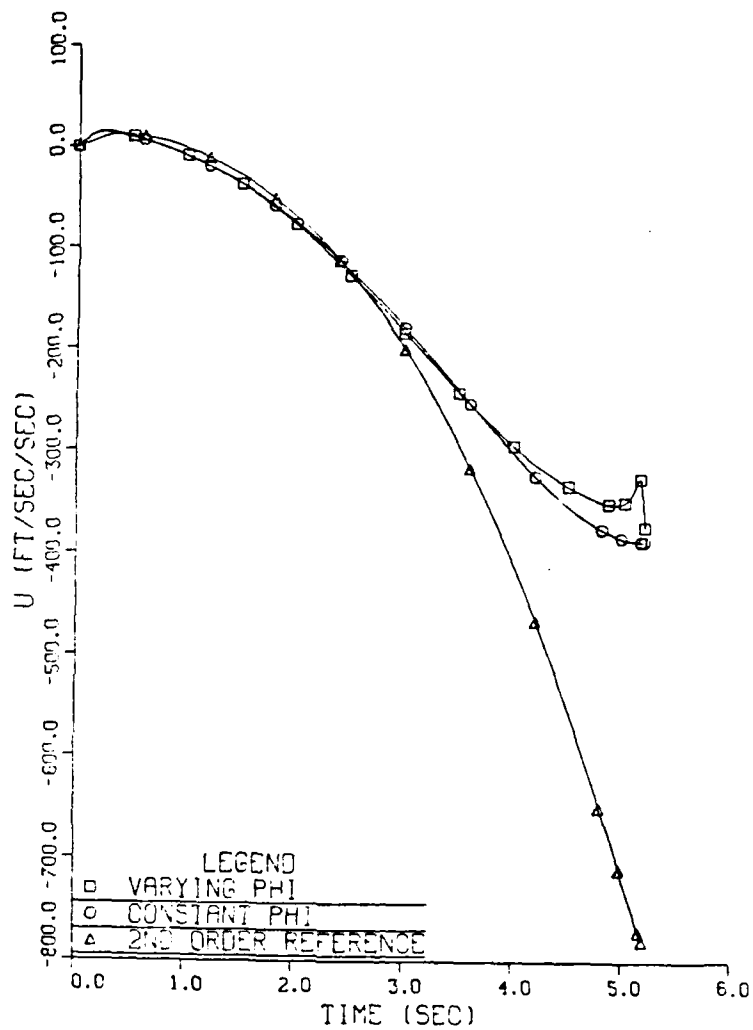


Figure VI-31 Missile Commanded Acceleration Plot for Beam Aspect 6G Target Turn

## 2. Head-on Aspect

Figures VI-5 through VI-16 are the results of missile guidance comparisons for head-on aspect initial condition with 0G, 3G and 6G constant target acceleration. The missile begins at the origin of the graph. The target initial position is at  $x = 10000$  ft,  $y = 1000$  ft. Applied lateral target acceleration is away from the missile.

### a. 0G Target Acceleration

Flight paths for the three models are shown in Figure VI-5. All three paths appear to be the same, within the accuracy of the plotter. The line of sight angle, Figure VI-6 remains relatively constant for all three models, at the initial value, giving a constant bearing decreasing range, no maneuver intercept.

Commanded Missile Acceleration, Figure VI-7, shows that the second order model pulls more lateral acceleration than third order models. Higher gain terms make the constant  $\Phi$  third order model erratic when compensating for initialization error.

### b. 3G Target Acceleration

In the position plot, Figure VI-8, the second order model begins to lag the third order model. The lagging means the missile is slower to compensate for line of sight rates. This is further illustrated by Figure VI-9, the line of sight angle plot. The change in line of sight is greater for the second order model.

Commanded acceleration, Figure VI-10 shows a larger increase for the second order model. The second order model requires approximately 7.5G to intercept a 3G target while the third order model require 4.66G.

c. 6G Target Acceleration

Increased target acceleration increases the lag of the second order model, Figure VI-11. Magnitude of line of sight is larger for the second order model, Figure VI-12, but the missile is compensating for the errors. The two third order models are fairly close. The difference is only fractions of radians.

The constant Phi third order model has less initial oscillations in commanded acceleration when the target acceleration increases. The second order model requires approximately 11G for a 6G target, 7.5G is required for the third order models.

3. Tail Aspect

Figures VI-13 through Figure VI-21 are the results of missile guidance comparisons for tail aspect initial condition with 0G, 3G and 6G constant target acceleration. The missile begins at the origin of the graph. The target initial position is at  $x = 15000$  ft,  $y = -500$  ft. Applied lateral target acceleration is into the missile.

a. 0G Target Acceleration

As shown in Figure VI-13, there is little difference in flight paths for the three missiles in the no target acceleration case. Line of sight angles remain constant, Figure VI-14, throughout the intercept.

There is some slight difference in commanded accelerations, Figure VI-15, with the second order model being the smaller of the three models.

b. 3G Target Acceleration

As the target applies acceleration, the lag of the second order missile gives a shorter flight path, than the third order missiles, Figure VI-16. Line of sight angles are smaller for the second order model, Figure VI-17.

Acceleration required for the second order model is 3.4G and 5.3G for the third order models, Figure VI-18. By lagging the other missiles, the second order model allows

the target to complete part of the intercept, which allows the missile to pull less acceleration.

c. 6G Target Acceleration

With higher target acceleration, the flight paths, Figure VI-19 have approximately the same differences as the 3G case. The second order model maintains a better flight path throughout the intercept. The slope of the line of sight curves, Figure VI-20, are higher with the second order model maintaining a smaller angle difference.

Commanded acceleration is much smaller for the second order model than the third order models, Figure VI-21. To intercept the 6G target, the second order model requires 6.2G and the third order models require 8.1G.

4. Beam Aspect

Figures VI-22 through VI-30 are the results of missile guidance comparisons for head-on aspect initial condition with 0G, 3G and 6G constant target acceleration. The missile begins at the origin of the graph. The target initial position is at  $x = 15000$  ft,  $y = 0$  ft. Applied lateral target acceleration is away from the missile.

a. 0G Target Acceleration

Figure VI-22 through VI-24, show the three missiles are practically the same for a no target acceleration, beam aspect intercept. All three missiles maintain a constant bearing decreasing range, small acceleration intercept.

b. 3G Target Acceleration

Only slight differences are noticed when target acceleration is applied. Flight paths, Figure VI-25, shows very little deviation. The line of sight angle difference of .01 rad between the models is approximately .575. Acceleration is higher for the second order missile to allow it to fly the same path as the third order models, Figure VI-27.

c. 6G Target Acceleration

Flight paths have a pronounced difference with a higher target acceleration, Figure VI-28. Line of sight angles, Figure VI-29, have larger magnitudes and higher slopes. Commanded acceleration increases dramatically, now 25G is required of the second order model and 9.3G for the third order models.

## VII. CONCLUSIONS

In analyzing second and third order missile tracking and guidance subsystems, the following conclusions are made:

- Proportional navigation guidance is the optimum method for missiles, given current design tradeoffs.
- Target modeling is very difficult and requires the analysis of many factors. Acceleration probabilities make modeling easier, but the proper acceleration model must be chosen.
- Cross coupling between coordinate reference axis components does exist and gives errors if not accounted for in the system model.
- Kalman filters are the best predictors for airborne missiles, if one is required.
- Complete time varying third order models give better results than approximated linear, time invariant third order models.
- Only small differences are noticed in parameter values between second and third order models. Higher accelerations are required for the second order model.
- Second order missiles are better than third order missiles in tail aspect, constant acceleration intercepts.
- Implementation of a Kalman filter requires considerable amounts of computer resources, with limited time to complete the calculations.
- Some parameter terms are of the approximate order as system noise or non significant calculations.

Some recommendations for future study and consideration are:

- A study of miss distance analysis for second and third order models.
- Analysis of the effects of the Q and P matrix initialization.
- Analyze the target acceleration probability model to find optimum values to assign to the probability model.
- Determine missile cross couple effect of heading changes and autopilot torques on the sensor subsystem.
- Add noise to the system to determine the effects of the high gain terms on a noisy system.



#### REFERENCES

1. Titus, Hal, "Missile Guidance Notes", Naval Postgraduate School, Monterey, California, 1987, unpublished.
2. Singer, Robert A., "Estimating Optimal Tracking Filter Performance for Manned Maneuvering Targets", IEEE Transactions on Aerospace and Electronic Systems, Vol. AES-6, No. 4, July 1970.
3. Fitts, John Murray, "Aided Tracking as Applied to High Accuracy Pointing Systems", IEEE Transactions on Aerospace and Electronic Systems, Vol. AES-9, No. 3, May 1973.
4. Singer, Robert A. and Behnke, Kenneth W., "Real-Time Tracking Filter Evaluation and Selection for Tactical Applications", IEEE Transactions on Aerospace and Electronic Systems, Vol. AES-7, No. 1, January 1971.

# APPENDIX A. IDEAL MISSILE PROGRAM LISTING

```

C      MISSILE PROGRAM FOR FLIGHT PATH COMPARISON IN THE
C      THESIS, THIS PROGRAM IS DESIGNED TO FOLLOW THREE IDEAL
C      MISSILES USING DIFFERENT GUIDANCE TECHNIQUES TO TARGET
C      INTERCEPT. THE GUIDANCE TECHNIQUES ARE: PROPORTIONAL
C      NAVIGATION, PURE PURSUIT AND LEAD PURSUIT. PARAMETERS
C      ARE ALSO OBTAINED FOR A FOURTH MISSILE USING A DIRECT
C      FLIGHT PATH.
INITIAL
CONST
G=32.2,D2R=.0175,K2F=1.66667,PITCH=2.7,PI=3.14159,RM1=20000
      K=0
      NN=0
      MISSX0=0.0
      MISSY0=0.0
      VM = 2500.0
      READ (2,5) VT,AT,THDG,TGTX0,TGTY0
5      FORMAT (F6.1,2X,F5.1,2X,F6.1,2(2X,F10.2))
      TGTV=VT*K2F
      TGTA=-AT*G
      THDG=THDG*D2R
      TGTVX0=TGTV*SIN(THDG)
      TGTVY0=TGTV*COS(THDG)
C
C      INITIALIZATION OF DIRECT INTERCEPT MISSILE
      DXT=MISSX0
      DYT=MISSY0
C
C      INITIALIZATION OF PROP NAV MISSILE CONSTANT VELOCITY,
ZERO ACCEL
      R0=((TGTX0 - MISSX0)**2 + (TGTY0 - MISSY0)**2)**.5
      TTGO= R0/VM
      LOS = ATAN2(TGTY0-MISSY0,TGTX0-MISSX0)
      PHDG=ATAN2(TGTY0+TGTVY0*TTGO-MISSY0,-
TGTX0+TGTVX0*TTGO-MISSX0)
      BDO = TGTV*COS(THDG)/(COS(LOS) * R0)
      BO = LOS
C
C      INITIALIZATION OF LEAD PURSUIT MISSILE
      GO = BO
      GDO = 0
      LPHDGO = LOS
C      * * * * *
METHOD RKSPX
DERIVATIVE
C
C      TARGET POSITION UPDATING
C      TGTHDG=INTGRL(THDG,(-1*AT)*PITCH*D2R)
      TGTAX=TGTA*COS(TGTHDG)
      TGTAY=-TGTA*SIN(TGTHDG)
      TVELX=INTGRL(TGTVX0,TGTAX)
      TVELY=INTGRL(TGTVY0,TGTAY)
      XT=INTGRL(TGTX0,TVELX)
      YT=INTGRL(TGTY0,TVELY)
      TGTHDG = ATAN2(TVELX,TVELY)
C
C      PROP NAV MISSILE POSITION UPDATING
      BDDOT = -20*BDO + 100*(PNLOS-B)
      BDCT = INTGRL(BDO,BDDOT)
      B = INTGRL(BO,BDO)
      PNHDG = INTGRL(PHDG,4*BDO)
      PKM=INTGRL(MISSX0,VM*COS(PNHDG))
      PYM=INTGRL(MISSY0,VM*SIN(PNHDG))
C
C      PURE PURSUIT MISSILE

```

```

PPHDG = ATAN2(YT-PPYM,XT-PPXM)
PPXM = INTGRL(MISSX0,VM*COS(PPHDG))
PPYM = INTGRL(MISSY0,VM*SIN(PPHDG))

C
C   LEAD PURSUIT MISSILE
C   LPHDG
C   ATAN2(YT+TVELX*0.5*TTG-LPYM,XT+TVELX*0.5*TTG-LPXM)
C   LPXM = INTGRL(MISSX0,VM*COS(LPHDG))
C   LPYM = INTGRL(MISSY0,VM*SIN(LPHDG))
C
C   * * * * *
C
C DYNAMIC
C
C   PROP NAV MISSILE GEOMETRY UPDATE
C   PNAM = 4*BDOT*PNRD
C   PNR=((XT-PXM)**2 + (YT-PYM)**2)**.5
C   PNLOS = ATAN2(YT-PYM,XT-PXM)
C   PNRD=TVELX*COS(PNLOS) +VM*COS(PNHDG-PNLOS)
C   PNLOSD = (-TVELX*SIN(PNLOS)-VM*SIN(PNHDG-PNLOS))/PNR

C
C   PURE PURSUIT GEOMETRY UPDATE
C   PPR = ((XT-PPXM)**2 + (YT-PPYM)**2)**.5
C   PPLOS = ATAN2(YT-PPYM,XT-PPXM)
C   PPRD = TVELX*COS(PPLOS) - VM*COS(PPHDG-PPLOS)
C   PPLOSD = -TVELX*SIN(PPLOS)/PPR

C
C   LEAD PURSUIT GEOMETRY UPDATE
C   LPR = ((XT-LPXM)**2 + (YT-LPYM)**2)**.5
C   LPLOS = ATAN2(YT-LPYM,XT-LPXM)
C   LPRD = TVELX*COS(LPLOS) - VM*COS(LPHDG-LPLOS)
C   LPLOSD = (-TVELX*SIN(LPLOS))/LPR
C   VM*SIN(LPHDG-LPLOS))/LPR
C   TTG = - LPR/LPRD

C
C   DIRECT INTERCEPT MISSILE GEOMETRY UPDATE
C   RD=((YT-MISSY0)**2 + (XT-MISSX0)**2)**.5
C   DXT,DYT,FON= CHECK(RD,TIME,VM,XT,YT)
C   IF (PXM.GT. XT) CALL ENDRUN

C
C   IF (K.LE. 0.0) THEN
C     NN=NN+1
C     WRITE (31,50) XT,YT,PXM,PYM
C     WRITE (32,50) PPXM,PPYM,LPXM,LPYM
C     WRITE (33,51) TIME,PNLOS,PPLOS,LPLCS
C     WRITE (34,52) TIME,PNLOSD,PPLOSD,LPLOSD
C     WRITE (36,54) TIME,PNHDG,PPHDG,LPHDG
C     FORMAT(4(F10.2,2X))
C     FORMAT(F5.2,3(2X,F10.5))
C     FORMAT(F5.2,3(2X,F10.5))
C     FORMAT(F5.3,2X,3(F10.6,2X))
C     K=10
C
C   IF (PNR.LT.0.1*R0) THEN
C     K=1
C   ENDIF
C   ENDIF
C   K=K-1

C
C   SAMPLE
C   SAVE (A) 0.1,XT,YT,PXM,PYM,PPXM,PPYM,LPXM,LPYM
C   PRINT 1.0,XT,YT,LPXM,LPYM,GDOT,LPLOS,LPHDG
C   CONTROL FINTIM= 8.0,DELT=.01
C   TERMINAL
C     DHDG = ATAN2(DYT-MISSY0,DXT-MISSX0)
C     GRAPH (A/A,DE=TEK618) XT
C     (SC=1600,LO=0.00),YT(SC=750,LO=0.0,PO=16000)
C     GRAPH (A/A,OV)
C     PXM(SC=1600,LO=0.0,AX=OMIT),PYM(SC=750,LO=0)

```

```

C                                     GRAPH (A/A,OV)
PPXM(SC=1600,LO=0.0,AX=OMIT),PPYM(SC=750,LO=0,AX=OMIT)
C                                     GRAPH (A/A,OV)
LPXM(SC=1600,LO=0.0,AX=OMIT),LPYM(SC=750,LO=0,AX=OMIT)
      WRITE (2,15) DHDG,FON
15      FORMAT (F10.7,2X,F5.2)
      WRITE (1,16) NN
16      FORMAT (F4.0)

END
STOP
FORTRAN
      SUBROUTINE CHECK (RD,TIME,VM,XT,YT,DXT,DYT,FON)
      REAL*8 RD,TIME,VM,XT,YT,DXT,DYT,FON,DMISS
      DMISS = VM*TIME
      IF (DMISS .LT. RD) THEN
          DXT = XT
          DYT = YT
          FON = TIME
      ENDIF
      RETURN
      END

```

```

C      THIS IS A DSL PROGRAM TO FIND THE LOS AND RANGE OF A
C      TARGET IN A CONSTANT G TURN FROM A MISSILE ON A
C      DIRECTPATH.
C
C      INITIAL
C      CONST
G=32.2,D2R=.0175,PITCH=2.7,K2F=1.66667,I=1.0,PI=3.14159,K=0
      READ (2,10) VT,AT,THDG,TGT X0,TGT Y0
      READ (2,11) MISHDG,DONE
10     FORMAT (F6.1,2X,F5.2,2X,F6.2,2(2X,F10.2))
11     FORMAT (F10.7,2X,F5.2)
C      MISSILE PARAMETERS
      MISSX0 = 0.0
      MISSY0 = 0.0
      VM = 2500.0
C      TARGET PARAMETERS
      TGTHDG=THDG*D2R
      TGT V=VT*K2F
      TGTG =-AT*G
      TGT TVELX0=TGT V*SIN(TGTHDG)
      TGT TVELY0=TGT V*COS(TGTHDG)
C      EQUATIONS OF MOTION
METHOD RKSF
DERIVATIVE
      TGTHDG=INTGRL(THDG,-AT*PITCH*D2R)
      TGT AX=TGTG*COS(TGTHDG)
      TGT AY=-TGTG*SIN(TGTHDG)
      TVELX=INTGRL(TGT TVELX0,TGT AX)
      TVELY=INTGRL(TGT TVELY0,TGT AY)
      XT=INTGRL(TGT X0,TVELX)
      YT=INTGRL(TGT Y0,TVELY)
C      MISSILE POSITION UPDATE
      XM = INTGRL(MISSX0,VM*COS(MISHDG))
      YM = INTGRL(MISSY0,VM*SIN(MISHDG))
DYNAMIC
      R=((XT-XM)**2 + (YT-YM)**2)**.5
      LOS = ATAN2(YT-YM,XT-XM)
      RD = TVELX*COS(LOS) - VM*COS(MISHDG-LOS)
      LOS = (TVELY*COS(LOS) - VM*SIN(MISHDG-LOS))/R
      IF (K.EQ.10) THEN
      MM = MM+1
      WRITE (37,15) XM,YM
      WRITE (38,16) TIME,LOS,LOSD,MISHDG
15     FORMAT (2(F9.2,3X))
16     FORMAT (F5.2,2X,2(F10.5,2X),F7.4)
      K=0
      ENDF
      K=K+1
      IF (TIME .GT. DONE) CALL ENDRUN
SAMPLE
CONTROL FINTIM=10.0,DELT=.01
C      PRINT 1.0,XT,YT,XM,YM,LOS,R
C      SAVE (D) 0.1,XT,YT,XM,YM,R,LOS
TERMINAL
      READ (1,26) NN
      WRITE (1,26) MM
26     FORMAT (F5.0)
C      GRAPH (A/D,DE=TEK618) XT(SC=1500,LO=0),YT(PO=15000)
C      GRAPH (A/D,DE=TEK618,OV) XM(SC=1500,LO=0,AX=OMIT),YM
C      GRAPH (A/D,DE=TEK618) TIME,LOS
C      GRAPH (A/D,DE=TEK618) TIME,R
END
STOP

```

# APPENDIX B. THIRD ORDER SIMULATION PROGRAM LISTING

```

C      PROP NAV MISSILE PROGRAM FOR THESIS
INITIAL
D      PS(3,3),PR(3,3),RMCOV(2,2),RNG(3),S(3),DELR(3),SG(3)
D      DIMENSION RG(3,3)
D      K=0
D      MM=0
D      HH=0

C      METHOD RKSF
CONST  G=32.2,D2R=.0175,K2F=1.66667
      TR = .01
      MISSX0=0.0
      MISSY0=0.0
      VM = 2500.0
      AMO = 0.0
10     READ (2,10) VT,AT,THDG,TGTGX0,TGTGY0
      FORMAT (F6.1,2X,F5.1,2X,F6.1,2X,F10.2,2X,F10.2)
      TGTV=VT*K2F
      TGTGTA=(-1*AT)*G
      THDG=THDG*D2R
      TGTVX0=TGTV*SIN(THDG)
      TGTVY0=TGTV*COS(THDG)

C      INITIAL PS(0/0) MATRIX
C      PS(1,1)=1.0E+4
C      PS(1,2)=0.0
C      PS(1,3)=0.0
C      PS(2,1)=PS(1,2)
C      PS(2,2)=1.0E+4
C      PS(2,3)=0.0
C      PS(3,1)=PS(1,3)
C      PS(3,2)=PS(2,3)
C      PS(3,3)=1.0E+4

C      INITIAL PR(0/0) MATRIX
C      PR(1,1) = 500
C      PR(1,2) = 0
C      PR(1,3) = 0
C      PR(2,1) = PR(1,2)
C      PR(2,2) = 500
C      PR(2,3) = 0.0
C      PR(3,1) = PR(1,3)
C      PR(3,2) = PR(2,3)
C      PR(3,3) = 500

C      INITILIZE THE RANGE MEASUREMENT COVARIANCE MATRIX
C      RMCOV(1,1) = 0.0
C      RMCOV(1,2) = 0.0
C      RMCOV(2,1) = RMCOV(1,2)
C      RMCOV(2,2) = 0.0

C      INITIALIZE THE BEARING MEASUREMENT NOISE COVARIANCE
C      MATRIX
C      SMCOV = 0.0

C      INITIALIZATION OF PROP NAV MISSILE CONSTANT VELOCITY,
C      ZERO ACCEL
      LOS = ATAN2(TGTGY0 - MISSY0, TGTGX0 - MISSX0)
      R=((TGTGX0 - MISSX0)**2 + (TGTGY0 - MISSY0)**2)**.5
      TTGO= R/VM
      PHDG=ATAN2(TGTGY0+TGTVY0*TTGO-MISSY0,TGTGX0+-
TGTVX0*TTGO-MISSX0)
      VMX0 = VM*COS(PHDG)

```

```

      VMYO = VM*SIN(PHDG)
      RKP1 = R
      RDKP1 = -VM*COS(PHDG-LOS) + TGTV*SIN(THDG)/COS(LOS)

      RDDKP1 = 0
      SKP1 = LOS
      SDKP1 = (TGTVYO/COS(LOS) - VM*SIN(PHDG-LOS))/R
      SDDKP1 = 0
      BO = LOS
      BDO = 0
C
      RNG(1) = RKP1
      RNG(2) = RDKP1
      RNG(3) = RDDKP1
      S(1) = SKP1
      S(2) = SDKP1
      S(3) = SDDKP1
C
DERIVATIVE
C
C      TARGET POSITION UPDATING
      TGTHDG = ATAN2(TVELX,TVELY)
      TGTAX = TGTA*COS(TGTHDG)
      TGTAY = (-1*TGTA)*SIN(TGTHDG)
      TVELX = INTGRL(TGT VX0,TGTAX)
      TVELY = INTGRL(TGT VY0,TGTAY)
      XT = INTGRL(TGT X0,TVELX)
      YT = INTGRL(TGT Y0,TVELY)
C
C
C      THIRD ORDER PROP NAV MISSILE POSITION UPDATING
      BDOT = INTGRL(BDO,BDDOT)
      B = INTGRL(BO,BDOT)
      AM = U
      MVELX = INTGRL(VMX0,-AM*SIN(PNHDG))
      MVELY = INTGRL(VMY0,AM*COS(PNHDG))
      PNHDG = ATAN2(MVELY,MVELX)
      PXM = INTGRL(MISSX0,MVELX)
      PYM = INTGRL(MISSY0,MVELY)
C
DYNAMIC
C
C      THIRD ORDER PROP NAV MISSILE GEOMETRY UPDATE
      RM = ((XT-PXM)**2 + (YT-PYM)**2)**.5
      LOS = ATAN2(YT-PYM,XT-PXM)
      RDOTM = TGTV*SIN(TGTHDG)/COS(LOS)
      VM*COS(PNHDG-LOS)
      RDDOTM = TGTA*COS(TGTHDG-LOS)
      LOSD = (TVELX*SIN(LOS) + VM*SIN(PNHDG-LOS))/RM
      LOSDD = TGTAY*COS(LOS)/RM
C
      COMPUTE THE ERROR TERMS
      DELR(1) = RM - RKP1
      DELR(2) = RDOTM - RDKP1
      SDEL = LOS - SKP1
C
C
      CALL
      KALMAN(RNG,RM,RDOTM,RDDOTM,RK,RDK,RDDK,RKP1,RDKP1,RDDKP1,...
      K,DEL R,PR,RMCOV,S,LOS,LOSD,LOSDD,SK,SDK,SDDK,TIME,SKP1,...
      SDKP1,SDDKP1,SDEL,SMCOV,PS,TK,RG,SG,HH)
      BDDOT = SDDKP1 + 10*(SDK-BDOT) + 33.33333*(LOS-B)
      U = -4*BDOT*RDOTM
C
      SAVE VALUES OF THE GAIN MATRICES
      GR11=RG(1,1)
      GR12=RG(1,2)
      GR21=RG(2,1)
      GR22=RG(2,2)

```

```

GR31=RG(3,1)
GR32=RG(3,2)
GS1=SG(1)
GS2=SG(2)
GS3=SG(3)
IF ( PXM .GT. XT ) THEN
  CALL ENDRUN
ENDIF
C
IF (K .LE. 0) THEN
  MM=MM+1
  WRITE (40,20) XT,YT,PXM,PYM
  WRITE (42,21) TIME,GR11,GR12,GR21,GR22,GR31,GR32
  WRITE (44,22) TIME,GS1,GS2,GS3
  WRITE (46,23) TIME,LOS,LOSD,LOSDD,U
  K=10
  IF (RM .LT. .1*R) THEN
    K=3
  ENDIF
ENDIF
K=K-1
20  FORMAT(4(2X,F10.2))
21  FORMAT (F5.2,6(1X,F10.4))
22  FORMAT (F5.2,3(2X,E12.5))
23  FORMAT (F5.2,3(2X,E11.4),2X,E14.6)
SAMPLE
C  STATEMENTS TO SAVE DATA FOR USE WITH GRAFAEL
C  SAVE (A) 0.1,XT,YT,PXM,PYM
C  SAVE (B) 0.1, LOS,B,SK
C  SAVE (C) 0.1,LOSD,BDOT,SDK
C  SAVE (D) 0.1,SDEL
C  SAVE (E) 0.1,RM,RK,RDDOTM,RDDK
C  SAVE (F) 0.1,U,BDDOT
C  SAVE (G) 0.1,GS1,GS2,GS3
C  SAVE (H) 0.1,GR11,GR12,GR21,GR22
C  PRINT 0.1,RM,RKP1,RK,RDOTM,RDKP1,RDK,RDDOTM,RDDKP1,RDDK
C  PRINT 0.1,PNHDG,LOS,B,SK,LOSD,BDOT,SDK,LOSDD,BDDOT,SDDK
CONTROL FINTIM=10.0,DELT=.01
TERMINAL
  WRITE (1,30) MM
30  FORMAT (F6.1)
C  STATEMENTS FOR PLOTTING WITH GRAFAEL
C  GRAPH (A/A,DE=TEK618) (A/A,DE=TEK618) XT
(SC=1600,LO=0.0),YT(SC=500,PO=16000)
C  GRAPH (A/A,OV) PXM (SC=1600,AX=OMIT),PYM(SC=500)
C  GRAPH (B/B,DE=TEK618) TIME,LOS(SC=.025,LO=-.1)
C  GRAPH (B/B,OV) TIME(AX=OMIT),B(PO=7.5,SC=.025,LO=-.1)
C  GRAPH (C/C,DE=TEK618) TIME,LOSD
C  GRAPH (C/C,OV) TIME(AX=OMIT),BDOT(PO=7.5)
C  GRAPH (C/C,OV) TIME(AX=OMIT),SDK(AX=OMIT)
C  GRAPH (D/D,DE=TEK618) TIME,SDEL
C  GRAPH (E/E,DE=TEK618) TIME,RM(SC=2000.0,LO=0.0)
C  GRAPH (E/E,OV) TIME (AX=OMIT),RK(SC=2000.0,LO=0.0)
C  GRAPH (F/E,DE=TEK618) TIME,RDDOTM(SC=500.0)
C  GRAPH (F/E,OV) TIME(AX=OMIT),RDDK(AX=OMIT)
C  GRAPH (G/F,DE=TEK618) TIME,U
C  GRAPH (H/G,DE=TEK618) TIME,GS1
C  GRAPH (I/G,DE=TEK618) TIME,GS2
C  GRAPH (J/G,DE=TEK618) TIME,GS3
C  GRAPH (K/H,DE=TEK618) TIME,GR11
C  GRAPH (L/H,DE=TEK618) TIME,GR12
C  GRAPH (M/H,DE=TEK618) TIME,GR21
C  GRAPH (N/H,DE=TEK618) TIME,GR22
C  GRAPH (O/F,DE=TEK618) TIME,BDDOT
END
STOP
FORTRAN

```



```

SUBROUTINE KALMAN(RNG, RM, RDOTM, RDDOTM, RK, RDK, RDDK,
RKP1, RDKP1, RDDKP1, K, DELR, PR, RMCOV, S, LOS, LOSD, LOSDD,
SK, SDK, SDDK, TIME, SKP1, SDKP1, SDDKP1, SDEL, SMCOV,
PS, TK, RG, SG, HH)
C SUBROUTINE TO ITERATE A KALMAN FILTER FOR RANGE
C VARIABLES
C GIVEN THE COVARIANCE MATRIX AND OBSERVATIONS
REAL*8 RNG(3), RM, RDOTM, RDDOTM, RK, RDK, RDDK, RKP1,
* RDKP1, RDDKP1, DELR(3), PR(3,3), RMCOV(3,3), S(3),
* LOS, LOSD, LOSDD, SK, SDK, SDDK, SKP1, SDKP1, SDDKP1, SDEL,
* SMCOV, TIME, PS(3,3), TK, TKSQ, A, B, C, D,
*
TEMP1(3),
TEMP2(2,2), TEMP3(3,3), RPHI(3,3), COVR(3,3),
* DET, SCOV, SPHI(3,3), RG(3,3), SG(3), QR(3,3), QS(3,3)
* TKSQ = TK*TK

C FIND THE NEW VALUES OF RPHI FROM THE PREVIOUS VALUES
C OF SIGMA
C MATRIX
A = -3*SDKP1*SDDKP1
B = -3*SDKP1*SDKP1
RPHI(1,1) = 1
RPHI(1,2) = TK
RPHI(1,3) = .5*TKSQ
RPHI(2,1) = .5*A*TKSQ
RPHI(2,2) = 1 + .5*B*TKSQ
RPHI(2,3) = TK
RPHI(3,1) = A*TK
RPHI(3,2) = B*TK + .5*A*TKSQ
RPHI(3,3) = 1 + .5*B*TKSQ

C FIND THE PROJECTED COVARIANCE PR(K/K-1) =
RPHI*PR(K-1/K-1)*RPHI
CALL ZERO(TEMP3,3)

C DO 104 L=1,3
DO 103 M=1,3
DO 102 N=1,3
TEMP3(L,M) = TEMP3(L,M) + RPHI(L,N)*PR(N,M)
102 CONTINUE
103 CONTINUE
104 CONTINUE
C CLEAR THE OLD COVARIANCE MATRIX
CALL ZERO(PR,3)
C MULTIPLY BY RPHI TRANSPOSE
DO 107 L=1,3
DO 106 M=1,3
DO 105 N=1,3
PR(L,M) = PR(L,M) + TEMP3(L,N)*RPHI(M,N)
105 CONTINUE
106 CONTINUE
107 CONTINUE
C DEFINE THE Q MATRIX OF MANEUVER COVARIANCE
C
QR(1,1) = 500
QR(1,2) = 0.0
QR(1,3) = 0.0
QR(2,1) = 0.0
QR(2,2) = 500
QR(2,3) = 0.0
QR(3,1) = QR(1,3)
QR(3,2) = QR(2,3)
QR(3,3) = 500
C NOW ADD TO THE COVARIANCE MATRIX
DO 111 L=1,3
DO 110 M=1,3
PR(L,M) = PR(L,M) + QR(L,M)
110 CONTINUE
111 CONTINUE

```

```

C      NOW PR IS THE COVARIANCE OF THE PREDICTED ESTIMATE
PR(K/K-1)
C      FIND THE ESTIMATE OF RANGE MATRIX AT STEP K
C
C      ZERO A TEMPORARY MATRIX
      CALL ZERO (TEMP2,2)
      DO 121 L=1,2
      DO 120 M=1,2
        TEMP2(L,M) = PR(L,M) + RMCOV(L,M)
120      CONTINUE
121      CONTINUE
      DET = TEMP2(1,1)*TEMP2(2,2) - TEMP2(1,2)*TEMP2(2,1)

      COVR(1,1) = TEMP2(2,2)/DET
      COVR(1,2) = {-1}*TEMP2(1,2)/DET
      COVR(2,1) = {-1}*TEMP2(2,1)/DET
      COVR(2,2) = TEMP2(1,1)/DET
C      HERE COVR = (HPH + R) INVERSE
C      ZERO A TEMPORARY MATRIX
      CALL ZERO (RG,3)
      DO 132 L=1,3
      DO 131 M=1,2
      DO 130 N=1,2
        RG(L,M)=RG(L,M) + PR(L,N) * COVR(N,M)
130      CONTINUE
131      CONTINUE
      RG(L,3) = 0
132      CONTINUE
C      RG = PH(HPH + R) (INVERSED) H
C      ZERO A TEMP MATRIX FOR THE RNG MATRIX
      DO 140 L=1,3
        TEMP1(L)=0
140      CONTINUE
C
      DO 142 L=1,3
      DO 141 M=1,2
        TEMP1(L) = TEMP1(L) + RG(L,M) * DELR(M)
141      CONTINUE
142      CONTINUE
      DO 143 N=1,3
        RNG(N) = TEMP1(N) + RNG(N)
143      CONTINUE
C      SAVE THE VALUES OF RANGE MATRIX AT STEP K
      RK = RNG(1)
      RDK = RNG(2)
      RDDK = RNG(3)
C
C      ZERO THE OLD RANGE TEMPORARY MATRIX
      DO 150 N = 1,3
        TEMP1(N) = 0
150      CONTINUE
C      FIND THE ESTIMATE OF THE STEP K+1 FOR THE RANGE MATRIX

      DO 152 L = 1,3
      DO 151 M = 1,3
        TEMP1(L) = TEMP1(L) + RPHI(L,M) * RNG(M)
151      CONTINUE
152      CONTINUE
C
C      SAVE THE VALUES OF RNG(K+1/K)
      DO 153 N=1,3
        RNG(N) = TEMP1(N)
153      CONTINUE
C
      RKP1 = RNG(1)
      RDKP1 = RNG(2)
      RDDKP1 = RNG(3)
C      FIND THE COVARIANCE OF FILTERED ESTIMATE
C      RG = PH(HPH+R)INVERSED H
C      THEREFORE P(K/K) = P(K/K-1) + RG*P(K/K-1)

```



```

211      CONTINUE
C      T
C      CALCULATE (HPH + R) INVERSE
C
C      SCOV = PS(1,1) + SMCOV
C
C      SG(1) = PS(1,1)/SCOV
C      SG(2) = PS(2,1)/SCOV
C      SG(3) = PS(3,1)/SCOV
C      NOW FIND THE CURRENT VALUES OF THE SIGMA MATRIX
C      S(1) = S(1) + SG(1)*SDEL
C      S(2) = S(2) + SG(2)*SDEL
C      S(3) = S(3) + SG(3)*SDEL
C
C      STORE THE SIGMA MATRIX FOR USE IN THE PROGRAM
C      SK = S(1)
C      SDK = S(2)
C      SDDK = S(3)
C      FIND THE NEXT VALUES OF THE SIGMA MATRIX
C      S(K+1) = SPHI * S(K)
C
C      ZERO A TEMPORARY MATRIX
C
C      DO 220 L=1,3
C      TEMP1(L) = 0
220      CONTINUE
C      DO 222 L=1,3
C      DO 221 M=1,3
C      TEMP1(L)=TEMP1(L) + SPHI(L,M) * S(M)
221      CONTINUE
222      CONTINUE
C
C      INPUT BACK INTO SIGMA MATRIX
C      DO 223 N = 1,3
C      S(N) = TEMP1(N)
223      CONTINUE
C
C      STORE THE VALUE OF THE S MATRIX
C      SKP1 = S(1)
C      SDKP1 = S(2)
C      SDDKP1 = S(3)
C
C
C      NOW FIND THE P MATRIX AT STEP K
C      PS(3,3)=PS(3,3) - PS(1,3)*SG(3)
C      PS(3,2)=PS(3,2) - PS(1,2)*SG(3)
C      PS(3,1)=PS(3,1) - PS(1,1)*SG(3)
C      PS(2,3)=PS(2,3) - PS(1,3)*SG(2)
C      PS(2,2)=PS(2,2) - PS(1,2)*SG(2)
C      PS(2,1)=PS(2,1) - PS(1,1)*SG(2)
C      PS(1,3)=PS(1,3) - PS(1,3)*SG(1)
C      PS(1,2)=PS(1,2) - PS(1,2)*SG(1)
C      PS(1,1)=PS(1,1) - PS(1,1)*SG(1)
C      IF (HH .LE. 0.0) THEN
C      HH=50
C      WRITE (9,*) 'TIME IS ',TIME
C      WRITE (9,*) 'A,B,C,D,'
C      WRITE (9,*) A,B
C      WRITE (9,*) C,D
C      WRITE (9,*) 'RANGE PHI MATRIX'
C      DO 450 L=1,3
C      WRITE (9,*) (RPHI(L,M), M=1,3)
450      CONTINUE
C      WRITE (9,*) 'SIGMA PHI MATRIX'
C      DO 451 L=1,3
C      WRITE (9,*) (SPHI(L,M), M=1,3)
451      CONTINUE
C      OUTPUT THE COVARIANCE MATRICES AT STEP K

```

```

        WRITE (9,*) 'THE RANGE COVARIANCE MATRIX IS:'
        DO 401 M=1,3
            WRITE (9,*) (PR(M,N) , N=1,3)
401      CONTINUE
        WRITE (9,*) 'THE BEARING COVARIANCE MATRIX IS:'
        DO 402 M=1,3
            WRITE (9,*) (PS(M,N) , N=1,3)
402      CONTINUE
    ENDIF
    HH=HH-1
    RETURN
  END
  SUBROUTINE ZERO(A,N)
  C    CLEAR A TEMPORARY MATRIX
  C
    REAL*8 A(3,3)
    DO 301 L=1,N
        DO 300 M=1,N
            A(L,M)=0
300      CONTINUE
301      CONTINUE
    RETURN
  END

```

```

C      THIRD ORDER MISSILE SIMULATION USING CONSTANT GAINS
FOR
C      THE KALMAN FILTER.  A SECOND ORDER PROP NAV REFERENCE
C      MODEL IS SIMULATED FOR PLOTTING AND PARAMETER
COMPARISONS.
INITIAL
D      RNG(3),S(3),DELR(2),GS(3),GR(3,3),RPHI(3,3),SPHI(3,3)  DIMENSION
      K=0
      NN=0

C
C
C
METHOD RKSFX
CONST  G=32.2,D2R=.0175,K2F=1.66667
      TK = 0.01
      MISSX0=0.0
      MISSY0=0.0
      VM = 2500.0
      AM0 = 0.0
10     READ (2,10) VT,AT,THDG,TGTX0,TGTYO
      FORMAT (F6.1,2X,F5.1,2X,F6.1,2(2X,F10.2))
      TGTV=VT*K2F
      TGTA=-AT*G
      THDG=THDG*D2R
      TGTVX0=TGTV*SIN(THDG)
      TGTVY0=TGTV*COS(THDG)

C
C      INITIALIZE THE RANGE PHI MATRIX
      RPHI(1,1) = 1
      RPHI(1,2) = TK
      RPHI(1,3) = .5*TK*TK
      RPHI(2,1) = 0
      RPHI(2,2) = 1
      RPHI(2,3) = TK
      RPHI(3,1) = 0
      RPHI(3,2) = 0
      RPHI(3,3) = 1

C
C      INITIALIZE THE BEARING PHI MATRIX
      SPHI(1,1) = 1
      SPHI(1,2) = TK
      SPHI(1,3) = .5*TK*TK
      SPHI(2,1) = 0
      SPHI(2,2) = 1
      SPHI(2,3) = TK
      SPHI(3,1) = 0
      SPHI(3,2) = 0
      SPHI(3,3) = 1

C
C      CONSTANT STEADY STATE GAIN VALUES RANGE
      GR(1,1) = .5
      GR(1,2) = 0.0125
      GR(1,3) = 0
      GR(2,1) = 0.0025
      GR(2,2) = 1.0
      GR(2,3) = 0
      GR(3,1) = 0.1250
      GR(3,2) = 24.9991
      GR(3,3) = 0

C
C      CONSTANT STEADY STATE GAIN VALUES BEARING
      GS(1) = 1.5
      GS(2) = 12.5
      GS(3) = 1250.0

C
C      INITIALIZATION OF PROP NAV MISSILE CONSTANT VELOCITY,
ZERO ACCEL
      LOS = ATAN2(TGTYO - MISSYO, TGTX0 - MISSX0)
      R=((TGTX0 - MISSX0)**2 + (TGTYO - MISSYO)**2)**.5
      TTGO= R/VM

```

```

PHDG=ATAN2(TGTY0+TGTVY0*TTG0-MISSY0,TGTX0+TGTVX0*TTG0-MISS-
X0)
  VMX0 = VM*COS(PHDG)
  VMY0 = VM*SIN(PHDG)
  RKP1 = R
  RDKP1 = -VM*COS(PHDG-LOS) + TGTV*SIN(THDG)/COS(LOS)

  RDDKP1 = 0
  SKP1 = LOS
  SDKP1 = (TGTVY0/COS(LOS) - VM*SIN(PHDG-LOS))/R
  SDDKP1 = 0
  B0 = LOS
  BD0 = 0
C
  RNG(1) = RKP1
  RNG(2) = RDKP1
  RNG(3) = RDDKP1
  S(1) = SKP1
  S(2) = SDKP1
  S(3) = SDDKP1
C
C      INITIALIZATION OF SECOND ORDER PROP NAV REFERENCE
MODEL
  G0=LOS
  GD0 = 0
C
C      DERIVATIVE
C
C      TARGET POSITION UPDATING
  TGTHDG = ATAN2(TVELX,TVELY)
  TGTAX=TGTA*COS(TGTHDG)
  TGTAY=(-1*TGTA)*SIN(TGTHDG)
  TVELX=INTGRL(TGTVX0,TGTAX)
  TVELY=INTGRL(TGTVY0,TGTAY)
  XT=INTGRL(TGTX0,TVELX)
  YT=INTGRL(TGTY0,TVELY)
C
C
C      THIRD ORDER PROP NAV MISSILE POSITION UPDATING
  BDOT = INTGRL(B0,BDDOT)
  B = INTGRL(B0,BDOT)
  AM = U
  MVELX = INTGRL(VMX0,-AM*SIN(PNHDG))
  MVELY = INTGRL(VMY0,AM*COS(PNHDG))
  PNHDG = ATAN2(MVELY,MVELX)
  PXM=INTGRL(MISSX0,MVELX)
  PYM=INTGRL(MISSY0,MVELY)
C
C      SECOND ORDER PROP NAV MISSILE
  GDDOT = -20*GDOT + (SOLOS-GAMMA)*100
  GDOT = INTGRL(GD0,GDDOT)
  GAMMA = INTGRL(G0,GDOT)
  SOHDG = INTGRL(PHDG,4*GDOT)
  SOXM = INTGRL(MISSX0,VM*COS(SOHDG))
  SOYM = INTGRL(MISSY0,VM*SIN(SOHDG))
C
C      DYNAMIC
C
C      THIRD ORDER PROP NAV MISSILE GEOMETRY UPDATE
  RM = ((XT-PXM)**2 + (YT-PYM)**2)**.5
  LOS = ATAN2(YT-PYM,XT-PXM)
  RDOTM = TGTV*SIN(TGTHDG)/COS(LOS)
VM*COS(PNHDG-LOS)
C      COMPUTE THE ERROR TERMS
  DELR(1) = RM - RKP1
  DELR(2) = RDOTM - RDKP1
  SDEL = LOS - SKP1
C

```

```

CALL KALMAN(RNG, RM, RDOTM, RDDOTM, RK, RDK, RDDK, RKP1,
+RDKP1, RDDKP1, DELR, S, LOS, LOSD, LOSDD, SK, SDK,
+SDDK, TIME, SKP1, SDKP1, SDDKP1, SDEL, GS, GR, RPHI, SPHI)
C
      BDDOT=SDDKP1+10*(SDK-BDOT)+33.33333*(LOS-B)
      U = -4*BDOT*RDOTM
C
C      SECOND ORDER PROP NAV MISSILE GEOMETR. UPDATE
      SOR = ((XT-SOXM)**2 + (YT-SOYM)**2)**.5
      SOLOS = ATAN2(YT-SOYM, XT-SOXM)
      SOU = -4*GDOT*SORD
C
      IF (PXM.GT. XT) THEN
        CALL ENDRUN
      ENDIF
C
C      STATEMENTS TO SAVE DATA FOR PLOTTING WITH DISSPLA
      IF (K.LE. 0) THEN
        WRITE (39,20) PXM,PYM,SOXM,SOYM
        WRITE (47,30) TIME,LOS,U
        WRITE (48,30) TIME,SOLOS,SOU
        K=10
      IF (RM.LT. .1*R) THEN
        K=3
      ENDIF
      NN=NN+1
      ENDIF
      K=K-1
      FORMAT (4(2X,F10.2))
      FORMAT (F5.2,2X,E11.3,2X,E14.6)
20
30
SAMPLE
C      STATEMENTS TO SAVE DATA FOR GRAFAEL
C      SAVE (A) 0.1,XT,YT,PXM,PYM
C      SAVE (B) 0.1, LOS,B,SK
C      SAVE (C) 0.1,LOSD,BDOT,SDK
C      SAVE (D) 0.1,SDEL
C      SAVE (E) 0.1,RM,RK,RDDOTM,RDDK
C      SAVE (F) 0.1,U,BDDOT
C      SAVE (G) 0.1,GS1,GS2,GS3
C      SAVE (H) 0.1,GR11,GR12,GR21,GR22
C
C      0.1,RM,RKP1,RK,RDOTM,RDKP1,RDK,RDDOTM,RDDKP1,RDDK
C
C      0.1,PNHDG,LOS,B,SK,LOSD,BDOT,SDK,LOSDD,BDDOT,SDDK
C      CONTROL FINTIM=10.0,DELT=.01
C
C      TERMINAL
      READ (1,40) MM
      WRITE (1,40) NN
40
      FORMAT (F6.1)
C      STATEMENTS FOR PLOTTING USING GRAFAEL
C      GRAPH (A/A,DE=TEK618) (A/A,DE=TEK618) XT
C      (SC=1600,LO=0.0),YT(SC=500,PO=16000)
C      GRAPH (A/A,OV) PXM (SC=1600,AX=OMIT),PYM(SC=500)
C      GRAPH (B/B,DE=TEK618) TIME,LOS(SC=.025,LO=-.1)
C      GRAPH (B/B,OV) TIME(AX=OMIT),B(PO=7.5,SC=.025,LO=-.1)
C      GRAPH (B/B,OV) TIME(AX=OMIT),SK(AX=OMIT,SC=.025,LO=-.1)
C      GRAPH (C/C,DE=TEK618) TIME,LOSD
C      GRAPH (C/C,OV) TIME(AX=OMIT),BDOT(PO=7.5)
C      GRAPH (C/C,OV) TIME(AX=OMIT),SDK(AX=OMIT)
C      GRAPH (D/D,DE=TEK618) TIME,SDEL
C      GRAPH (E/E,DE=TEK618) TIME,RM(SC=2000.0,LO=0.0)
C      GRAPH (E/E,OV) TIME (AX=OMIT),RK(SC=2000.0,LO=0.0)
C      GRAPH (F/E,DE=TEK618) TIME,RDDOTM(SC=500.0)
C      GRAPH (F/E,OV) TIME(AX=OMIT),RDDK(AX=OMIT)
C      GRAPH (G/F,DE=TEK618) TIME,U
C      GRAPH (H/G,DE=TEK618) TIME,GS1
C      GRAPH (I/G,DE=TEK618) TIME,GS2
C      GRAPH (J/G,DE=TEK618) TIME,GS3
C      GRAPH (K/H,DE=TEK618) TIME,GR11

```



```

C GRAPH (L/H,DE=TEK618) TIME,GR12
C GRAPH (M/H,DE=TEK618) TIME,GR21
C GRAPH (N/H,DE=TEK618) TIME,GR22
C GRAPH (O/F,DE=TEK618) TIME,BDDOT
END
STOP
FORTRAN
SUBROUTINE
KALMAN(RNG,RM,RDOTM,RDDOTM,RK,RDK,RDDK,RKP1,RDKP1,
*
RDDKP1,DELR,S,LOS,LOSD,LOSDD,SK,SDK,SDDK,TIME,SKP1,SDKP1,
* SDDKP1,SDEL,GS,GR,RPHI,SPHI)
C SUBROUTINE TO ITERATE A KALMAN FILTER FOR RANGE
VARIABLES
C GIVEN THE COVARIANCE MATRIX, OBSERVATIONS
REAL*8
RNG(3),RM,RDOTM,RDDOTM,RK,RDK,RDDK,RKP1,RDKP1,RDDKP1,
*
DELR(2),S(3),LOS,LOSD,RPHI(3,3),A,B,C,D,TEMP1(3),SPHI(3,3),
* GR(3,3),GS(3)
C
C FIND THE NEW VALUES OF RPHI FROM THE PREVIOUS VALUES
OF SIGMA
C MATRIX
C
DO 110 N = 1,3
TEMP1(N) = 0.0
110 CONTINUE
C CONSTANT GAIN INPUTS
DO 121 L=1,3
DO 120 M=1,2
TEMP1(L) = TEMP1(L) + GR(L,M) * DELR(M)
120 CONTINUE
121 CONTINUE
DO 125 N=1,3
RNG(N) = TEMP1(N) + RNG(N)
125 CONTINUE
C SAVE THE VALUES OF RANGE MATRIX AT STEP K
RK = RNG(1)
RDK = RNG(2)
RDDK = RNG(3)
C
C ZERO THE OLD RANGE TEMPORARY MATRIX
C FIND THE ESTIMATE OF THE STEP K+1 FOR THE RANGE MATRIX
DO 131 L = 1,3
DO 130 M = 1,3
TEMP1(L) = TEMP1(L) + RPHI(L,M) * RNG(M)
130 CONTINUE
131 CONTINUE
C
C SAVE THE VALUES OF RNG(K+1/K)
DO 132 N=1,3
RNG(N) = TEMP1(N)
132 CONTINUE
C
RKP1 = RNG(1)
RDKP1 = RNG(2)
RDDKP1 = RNG(3)
C
C SUBROUTINE TO ITERATE A KALMAN FILTER FOR SIGMA
VARIABLES
C GIVEN THE COVARIANCE MATRIX, OBSERVATION.
C WHERE H= (1 0 0)
C
C NOW FIND THE CURRENT VALUES OF THE SIGMA MATRIX
S(1) = S(1) + GS(1)*SDEL
S(2) = S(2) + GS(2)*SDEL
S(3) = S(3) + GS(3)*SDEL
C

```

```

C      STORE THE SIGMA MATRIX FOR USE IN THE PROGRAM
      SK      = S(1)
      SDK      = S(2)
      SDDK     = S(3)
C      FIND THE NEXT VALUES OF THE SIGMA MATRIX
      S(K+1) = SPHI * S(K)
C      ZERO A TEMPORARY MATRIX
      DO 140 L=1,3
      TEMP1(L) = 0
140    CONTINUE
      DO 142 L=1,3
      DO 141 M=1,3
      TEMP1(L)=TEMP1(L) + SPHI(L,M) * S(M)
141    CONTINUE
142    CONTINUE
C      INPUT BACK INTO SIGMA MATRIX
      DO 143 N = 1,3
      S(N) = TEMP1(N)
143    CONTINUE
C      STORE THE VALUE OF THE S MATRIX
      SKP1     = S(1)
      SDKP1    = S(2)
      SDDKP1   = S(3)
C
      RETURN
      END
C      SUBROUTINE ZERO(A,N)
C      CLEAR A TEMPORARY MATRIX
      REAL*8 A(3,3)
      DO 201 L=1,N
      DO 200 M=1,N
      A(L,M)=0
200    CONTINUE
201    CONTINUE
      RETURN
      END

```

# INITIAL DISTRIBUTION LIST

	No. Copies
1. Defense Technical Information Center Cameron Station Alexandria, Virginia 22304-6145	2
2. Superintendent Attn: Library, Code 1424 Naval Postgraduate School Monterey, California 93943-5100	2
3. Department Chairman, Code 62 Department of Electrical Engineering Naval Postgraduate School Monterey, California 93943-5100	1
4. Professor H. A. Titus, Code 62TS Department of Electrical Engineering Naval Postgraduate School Monterey, California 93943-5100	1
5. Professor M. A. Morgan, Code 62MW Department of Electrical Engineering Naval Postgraduate School Monterey, California 93943-5100	1
6. Commandant of the Marine Corps Code TE 06 Headquarters, U.S. Marine Corps Washington, District of Columbia 203660-0001	1
7. Commander Naval Weapons Center Attn: Code 35405 (Mr. Conaway) China Lake, California 93555-6004	1
8. Dr. James Hilkert Texas Instruments Inc. P.O. Box 660246 (stop 3647) Dallas, Texas 75266	1
9. Captain J. W. Williams 1015 Mt. Holly Rd. Annapolis, Maryland 21401	2